REGULATORY INFORMATION DISTRIBUTION SYSTEM (RIDS)

ACCESSION NBR:8312200339 DOC.DATE: 83/12/14 NOTARIZED: NO DOCKET #
FACIL:50-335 St. Lucie Plant, Unit 1, Florida Power & Light Co. 05000335
AUTH.NAME AUTHOR AFFILIATION
WILLIAMS,J.W. Florida Power & Light Co.
RECIP.NAME RECIPIENT AFFILIATION
EISENHUT,D.G. Division of Licensing

SUBJECT: Forwards "Evaluation of Irradiated Capsule W-97:Reactor Vessel Matls Irradiated Surveillance Program."
SEE REPTS.

DISTRIBUTION CODE: A001S COPIES RECEIVED:LTR 1 ENCL 1 SIZE: 1+125
TITLE: OR Submittal: General Distribution

NOTES:

	RECIPIENT ID CODE/NAME		COPIES LTTR	COPIES ENCL	RECIPIENT ID CODE/NAME		COPIES LTTR	COPIES ENCL
	NRR ORB3 BC	01	7	7				
INTERNAL:	ELD/HDS2		1	0	NRR/DE/MTEB		1	1
	NRR/DL DIR		1	1	NRR/DL/ORAB		1	0
	NRR/DSI/METB		1	1	NRR/DSI/RAB		1	1
	REG FILE	04	1	1	RGN2		1	1
EXTERNAL:	ACRS	09	6	6	LPDR	03	1	1
	NRC PDR	02	1	1	NSIC	05	1	1
	NTIS		1	1				

TOTAL NUMBER OF COPIES REQUIRED: LTTR 25 ENCL 23

[illegible]

[illegible]

[illegible]

[illegible]

[illegible]	[illegible]	[illegible]	[illegible]
[illegible]	[illegible]	[illegible]	[illegible]

BOX 14000, JUNO BEACH, FL 33408

FLORIDA POWER & LIGHT COMPANY

December 14, 1983
L-83-583

Office of Nuclear Reactor Regulation
Attention: Mr. Darrell G. Eisenhut, Director
Division of Licensing
U. S. Nuclear Regulatory Commission
Washington, D.C. 20555

Dear Mr. Eisenhut:

Re: St. Lucie Unit I
Docket Nos. 50-335
Reactor Vessel Surveillance Specimen
Capsule W-97

Our letter L-83-316, dated May 20, 1983, as supplemented by L-83-538, dated October 31, 1983, committed to providing a final report summarizing the test results obtained from the first reactor vessel material irradiation surveillance specimen.

Please find attached the evaluation of irradiated capsule W-97.

Very truly yours,

for
J. W. Williams, Jr.
Vice President
Nuclear Energy

JWW/JEM/DAC/cab

Attachment

cc: Mr. James P. O'Reilly, Region II
Harold F. Reis, Esquire
PNS-LI-83-732

A001
1/1

TR-F-MCM-004

FLORIDA POWER
& LIGHT COMPANY
ST. LUCIE UNIT NO. 1

30

POST-IRRADIATION EVALUATION OF REACTOR VESSEL SURVEILLANCE CAPSULE W-97

December 1983

Prepared by: S. T. Byrne
S. T. Byrne, Cognizant Engineer
Date: 11-16-83

Approve by: S. M. Schloss
S. M. Schloss, Supervisor
Primary Boundary Materials
Date: 11-17-83

Approved by: John J Koziol
J. J. Koziol, Manager
Systems Materials
Date: 11.17.83

Approved by: WR Moran for T.P. Gates
T. P. Gates, St. Lucie Unit #1
Project Manager
Date: 11/17/83

Combustion Engineering, Inc.
Nuclear Power Systems
Windsor, Connecticut

TABLE OF CONTENTS

List of Tables

List of Tables (cont'd)

List of Figures

List of Figures (cont'd)

List of Figures (cont'd)

I. SUMMARY

The first surveillance wall capsule (W-97) was removed from the St. Lucie Unit 1 reactor vessel in May 1983 after 4.67 effective full power years of reactor operation. The surveillance test specimens and monitors were evaluated at C-E's Windsor, Connecticut laboratory facility.

Post-irradiation evaluation of the temperature monitors indicated that the irradiation temperature was between 536°F and 558°F. Analysis of the neutron threshold detectors provided a capsule fluence of 5.5×10^{18} n/cm^2 (E>1 MeV), which corresponded to a maximum fluence at the inside surface of the reactor vessel of 3.9×10^{18} n/cm^2.

Radiation induced changes in the uniaxial tension and impact properties were determined for the base metal, weld metal and heat-affected zone surveillance materials. Transition temperature shifts ranged from 68°F to 74°F for the base and weld metal, respectively. The upper shelf impact energy after irradiation was in excess of 75 ft-lb for each of the surveillance materials, ranging from 77.5 ft-lb for the base metal (transverse) to 106.5 ft-lb for the base metal (longitudinal).

Chemical analysis of the irradiated base and weld metal Charpy specimens was performed by X-ray fluorescence. The analysis confirmed that the chemistry of the irradiated materials was consistent with the chemistry originally reported for the surveillance materials.

The base metal, weld metal and HAZ exhibited similar changes in tensile properties after irradiation. The yield strength and ultimate strength increased approximately 14%, while total elongation and reduction in area decreased 2% to 3% (on average) after irradiation.

The NDTT shift prediction method from the St. Lucie Unit 1 Technical Specifications was found to be conservative by a factor of 90% for the base metal and 85% for the weld metal based on the W-97 surveillance capsule measurements. In contrast, shifts predicted using Regulatory Guide 1.99 were 115% higher than measured for the weld metal and 17% higher than measured for the base metal. The radiation resistance of the weld is attributed to the low nickel content (.11%). Based upon experimental data, the weld metal shift will continue to be similar to that of the plate, despite the difference in copper content (0.23 w/o for the weld and 0.15 w/o for the plate). Therefore, a more accurate shift prediction method was developed using the surveillance measurements and the slope of the Regulatory Guide 1.99 shift correlation. The predicted end-of-life (32EFPY) RTNDT shift for the surveillance plate and weld at the inside surface of the reactor vessel is 187^{O}F using the revised prediction method and the projected EOL fluence of 3.5×10^{19} n/cm^2 (based on operation without the thermal shield subsequent to Cycle 5).

The predicted decrease in upper shelf energy at end-of-life based on the method given in Regulatory Guide 1.99 is 41% for the weld and 37% for the plate at the one-quarter thickness location in the vessel. Using this conservative prediction, the upper shelf energy of the plates will remain above 70 ft-lb during the design life of the vessel, and the weld shelf energy will remain above 85 ft-lb. These projected values are well in excess of the 50 ft-lb value currently considered to be a reasonable lower limit for continued safe operation.

The projected changes in upper shelf energy and NDTT shift are based on the post-irradiation test measurements from the W-97 encapsulated materials, and projected EOL fluence values for operation without the thermal shield following Cycle 5 using planned power distributions for Cycle 6 to extrapolate beyond 4.67 EFPY. These surveillance results are representative of the six beltline plates, the closing girth seam weld (9-203), and the intermediate shell course longitudinal seam welds (2-203). The lower shell course longitudinal seam welds (3-203) and the upper to intermediate shell girth weld (8-203), because of their higher nickel content, are expected to be more sensitive to radiation than the surveillance weld, so an alternate shift prediction methodology should be used. (Further information concerning shift prediction methodology for these welds is addressed in a separate report[11].)

Recommended changes to the surveillance capsule withdrawal schedule were provided to meet the requirements of 10CFR50, Appendix H. If the proposed schedule is implemented, the next capsule will be withdrawn after 7 to 9 effective full power years of operation.

II. Introduction

The purpose of the St. Lucie Unit 1 surveillance program is to monitor the radiation induced changes in the mechanical properties of ferritic materials in the reactor vessel beltline during the operating lifetime of the reactor vessel. The surveillance program includes the determination of the pre-irradiation (baseline) strength and toughness properties and periodic determinations of the property changes following neutron irradiation. These property changes are used to verify and update the operating limits (heat-up and cool down pressure/temperature limit curves) for the primary system.

The St. Lucie Unit 1 Surveillance Program[1] is based upon ASTM E185-70, "Recommended Practice for Surveillance Tests for Nuclear Reactor Vessels". The pre-irradiation (baseline) evaluation results from the St. Lucie Unit 1 reactor vessel surveillance materials are described in C-E report TR-F-MCM-005.[2] This report describes the results obtained from evaluation of irradiated materials from capsule W-97 which was removed from the reactor in May 1983.

III. Surveillance Program Description

The St. Lucie Unit 1 reactor pressure vessel was designed and fabricated by Combustion Engineering, Inc. The reactor vessel beltline, as defined by 10CFR50, Appendix H, consists of the six plates used to form the lower and intermediate shell courses in the vessel, the included longitudinal seam welds and the lower to intermediate shell girth seam weld. The plates were manufactured from SA533 Grade B Class 1 quenched and tempered plate. The heat treatment consisted of austenization at 1600 ± 50F for four hours, water quenching and tempering at 1225 ± 25F for four hours. The ASME Code qualification test plates were stress relieved at 1150 ± 25F for forty hours, and furnace cooled to 600F. The longitudinal and girth seam welds were fabricated using E8018-C3 manual arc electrodes and Mil B-4 submerged arc weld wire with Linde 124, 0091 and 1092 flux. The post weld heat treatment consisted of a forty hour* 1150 ± 25F stress relief heat treatment followed by furnace cooling to 600F. The beltline materials are identified in Tables III-1 and III-2. The chemical analyses of the six beltline plates are given in Table III-3. The materials included in the surveillance program were obtained from the actual reactor vessel beltline materials. The base metal surveillance material, a section from plate C-8-2, was selected from the six beltline plates on the basis of the highest initial Charpy 30 ft-lb index temperature. The heat treatment of the surveillance plate duplicated that of the reactor vessel ASME Code qualification test plates. The surveillance weld material was fabricated by welding together sections of plates C-8-1 and C-8-3 using the same weld procedure and wire-flux combination used for the intermediate to lower shell girth seam weld (9-203). Mil B-4 submerged arc filler wire and Linde 0091 flux were used. The post-weld heat treatment consisted of a forty hour stress relief at 1125 ± 25F followed by furnace cooling to 600F. The surveillance heat-affected zone material was fabricated by welding together sections of plates C-8-2 and C-8-3 in the same manner as the surveillance weld material with the same post weld heat treatment. The chemical analyses of the surveillance plate and weld[2] is given in Table III-4.

*Eighteen hours for the closing girth seam weld.

TABLE III-1
REACTOR VESSEL
BELTLINE PLATES

Location	Piece Number	Code Number	Heat Number	Supplier
Intermediate Shell	215-02A	C-7-1	A-4567-1	Lukens
Intermediate Shell	215-02B	C-7-2	B-9427-1	Lukens
Intermediate Shell	215-02C	C-7-3	A-4567-2	Lukens
Lower Shell	215-03B	C-8-1	C-5935-1	Lukens
Lower Shell	215-03C	C-8-2	C-5935-2	Lukens
Lower Shell	215-03A	C-8-3	C-5935-3	Lukens

TABLE III-2

REACTOR VESSEL BELTLINE WELDS

Location	Weld Seam No.	Wire Heat No.	Flux Type	Flux Batch
Intermediate Shell Longitudinal Seam	2-203A	A-8746/34B009 M/A IAGI*	Linde 124	3878 & 3688
Intermediate Shell Longitudinal Seam	2-203B	A-8746/34B009 M/A IAGI* M/A CBBF*	Linde 124	3878 & 3688
Intermediate Shell Longitudinal Seam	2-203C	A-8746/34B009 M/A IAGI* M/A CBBF*	Linde 124	3878 & 3688
Lower Shell Longitudinal Seam	3-203A	34B009 M/A KBEJ*	Linde 1092	3889
Lower Shell Longitudinal Seam	3-203B	34B009 M/A KBEJ* M/A JACJ*	Linde 1092	3889
Lower Shell Longitudinal Seam	3-203C	34B009 M/A KBEJ*	Linde 1092	3889
Intermediate to Lower Girth Seam	9-203	90136 M/A ABEA* M/A FOAA*	Linde 0091	3999

*Manual shielded metal arc electrode (all others automatic submerged arc wire).

TABLE III-3
REACTOR VESSEL BELTLINE
PLATES CHEMICAL ANALYSIS
(WEIGHT PERCENT)

Element	C-7-1	C-7-2	C-7-3	C-8-1	C-8-2	C-8-3
Si	.17	.20	.20	.17	.17	.19
S	.013	.010	.012	.010	.010	.010
P	.004	.004	.004	.006	.006	.004
Mn	1.28	1.28	1.33	1.28	1.29	1.22
C	.24	.23	.21	.28	.28	.22
Cr	.03	.03	.06	.07	.07	.06
Ni	.64	.64	.58	.56	.57	.58
Mo	.60	.59	.58	.65	.66	.59
V	.003	.003	.003	.002	.002	.002
Cb	<.01	<.01	<.01	<.01	<.01	<.01
B	.0003	.0002	.0002	.0003	.0003	.0001
Co	.005	.006	.005	.007	.007	.006
Cu	.11	.11	.11	.15	.15	.12
Al	.018	.020	.020	.027	.025	.022
W	<.01	<.01	<.01	<.01	<.01	<.01
Ti	<.01	<.01	<.01	<.01	<.01	<.01
As	.015	.015	.010	.013	.014	.011
Sn	.006	.006	.006	.009	.010	.006
Zr	.002	.002	.002	.002	.002	.002
N_2	.006	.007	.007	.008	.009	.006

TABLE III-4

SURVEILLANCE PLATE AND WELD METAL CHEMICAL ANALYSIS

Element	Weight Percent: Plate C-8-2[a]	Weight Percent: Weld C-8-1/C-8-3[b]
Si	.17	.20
S	.010	.012
P	.006	.013
Mn	1.29	1.02
C	.28	.12
Cr	.07	.06
Ni	.57	.11
Mo	.66	.55
V	.002	.006
Cb	<.01	<.01
B	.0003	.0001
Co	.007	.004
Cu	.15	.23
Al	.025	.021
W	<.01	<.01
Ti	<.01	<.01
As	.014	.014
Sn	.010	.005
Zr	.002	.001
N_2	.004	.008

a - Heat C-5935-2

b - Mil B-4 wire heat 90136, Linde 0091 Flux lot 3999

Drop weight, Charpy impact and tension test specimens were machined from the surveillance materials as described in reference 1. In addition to the surveillance material specimens, Charpy impact specimens were machined from a section of plate 01 from the Heavy Section Steel Technology (HSST) program to serve as standard reference material (SRM).

The surveillance and SRM test specimens were enclosed in six capsules for irradiation in the St. Lucie Unit 1 reactor vessel. The surveillance capsule assembly is shown in Figure III-1. Each assembly consists of four compartments containing Charpy impact specimens (Figure III-2) and three compartments (Figure III-3) containing tension specimens and monitors (flux and temperture). Each capsule is positioned in a holder tube attached to the reactor vessel cladding to irradiate the specimens in an environment which duplicates as closely as possible that experienced by the reactor vessel. Capsule locations are shown in Figure III-4. The axial portion of each capsule is bisected by the midplane of the core. The circumferential locations were selected to coincide with the peak flux regions of the reactor vessel.

The existing Technical Specification withdrawal schedule for the surveillance capsules is given in Table III-5.

The type and quantity of test specimens contained in the W-97 capsule are given in Table III-6.

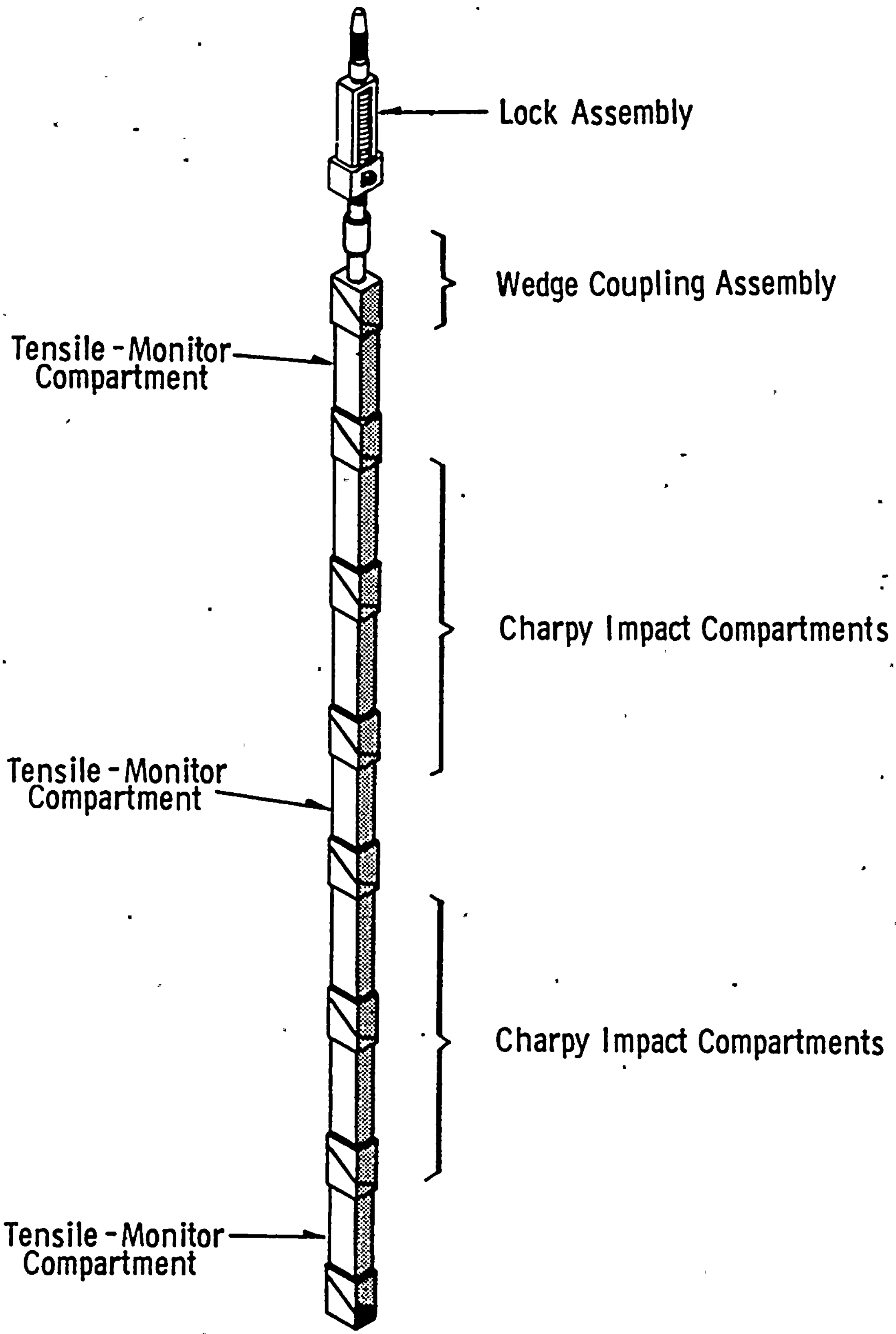

FLORIDA POWER & LIGHT CO. St. Lucie Unit 1	TYPICAL SURVEILLANCE CAPSULE ASSEMBLY	Figure III-1

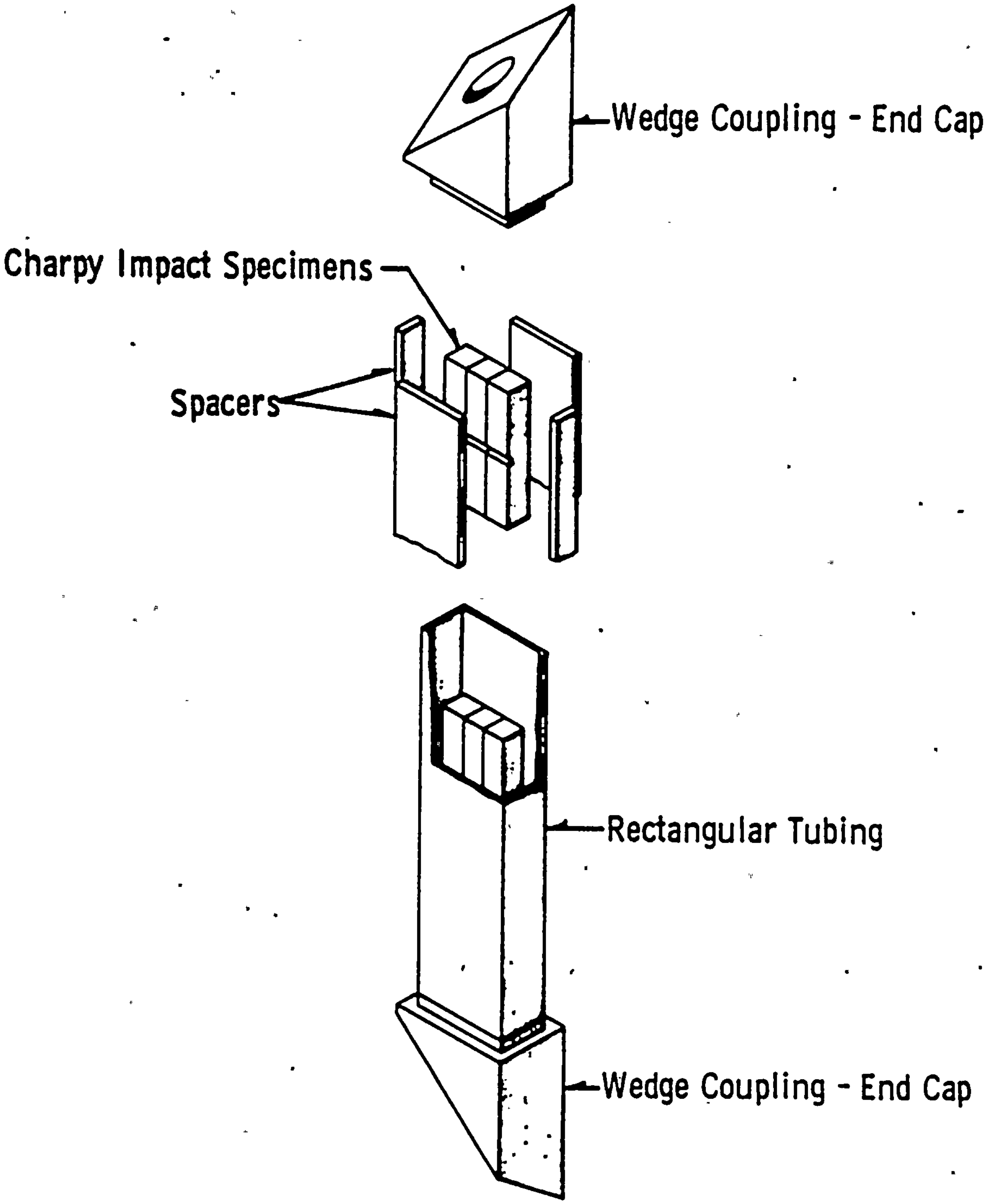

FLORIDA POWER & LIGHT CO. St. Lucie Unit 1	TYPICAL CHARPY IMPACT COMPARTMENT ASSEMBLY	Figure III-2

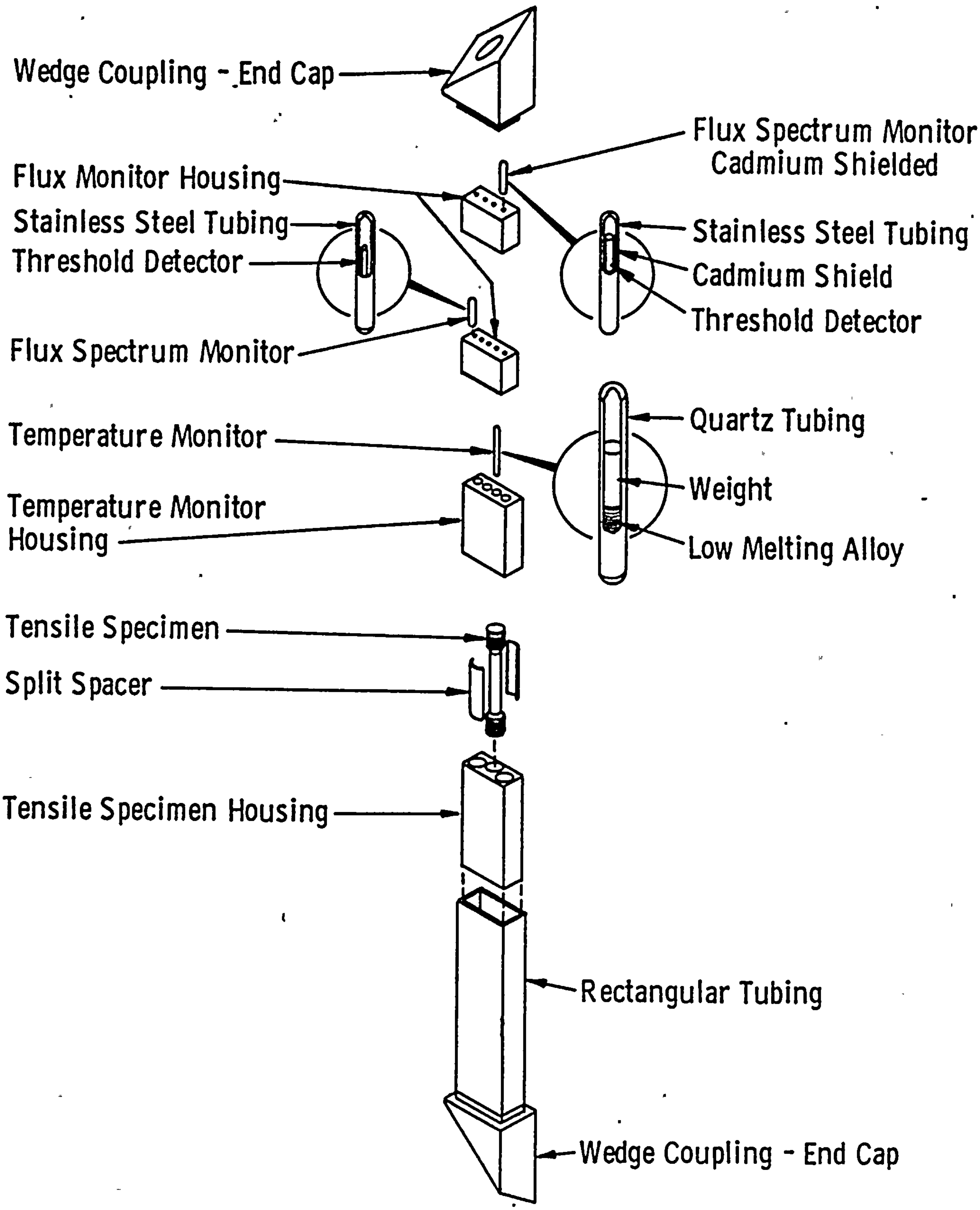

FLORIDA POWER & LIGHT CO. St. Lucie Unit 1.	TYPICAL TENSILE-MONITOR COMPARTMENT ASSEMBLY	Figure III-3

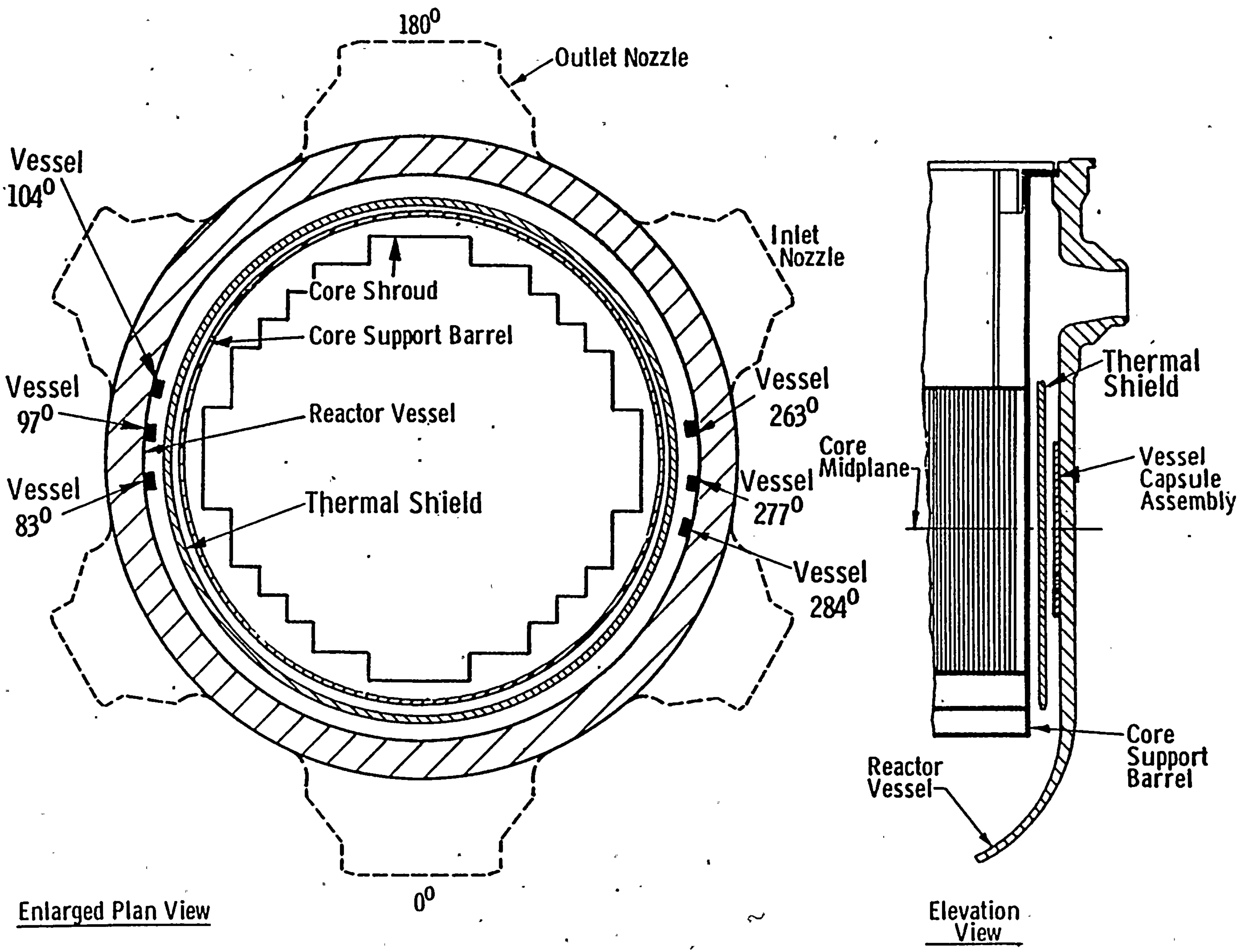

FLORIDA POWER & LIGHT CO.
St. Lucie Unit 1

LOCATIONS OF SURVEILLANCE CAPSULE ASSEMBLIES

Figure III-4

TABLE III-5

EXISTING TECHNICAL SPECIFICATION SCHEDULE FOR

ST. LUCIE UNIT 1 REACTOR VESSEL

SURVEILLANCE CAPSULE REMOVAL

Removal Sequence	Azimuthal Location	Approximate Removal Time (Years)	Target Fluence (n/cm^2)
1	97^o	8	3.2×10^{18}
2	104^o	16	5.7×10^{18}
3	284^o	23	8.3×10^{18}
4	263^o	30	1.2×10^{19}
5	277^o	35	1.4×10^{19}
6	83^o	40	1.7×10^{19}

TABLE III-6
TYPE AND QUANTITY OF
SPECIMENS IN W-97 CAPSULE

Material	Charpy Impact	Tension
Base Metal (Transverse)	12	-
Base Metal (Longitudinal)	12	3
Weld Metal	12	3
Heat-Affected Zone	12	3
Total	48	9

IV. CAPSULE WITHDRAWAL AND DISASSEMBLY

The St. Lucie Unit 1 reactor vessel was shut down for refueling on February 26, 1983. A special* retrieval tool was attached to the W-97 capsule adapter to disengage the latches, and the capsule was withdrawn from its holder and out of the reactor vessel. The W-97 capsule was transferred to the spent fuel pool where it was sectioned into lengths for insertion into a shipping cask. Sectioning was accomplished by drilling to separate the individual specimen compartments.

The surveillance capsule was shipped to Neutron Products, Inc. in Dickerson, Maryland, for inspection, disassembly and specimen removal in the hot cell facility. No unusual features or damage were revealed by visual inspection. An inventory of the mechanical test specimens removed from the W-97 capsule is given in Table IV-1.

*A special tool was used since the lock assembly adapter (ACME threaded nose cone which normally serves as the point of attachment for the retrieval tool) had previously disengaged from the assembly and was removed from the reactor vessel.

TABLE IV-1

MECHANICAL TEST SPECIMENS

REMOVED FROM W-97 CAPSULE

Compartment Number	Material and Specimen Type	Specimen Identification
7214	HAZ Tension	4JC, 4JP, 4J5
7224	HAZ Charpy	42C, 425, 41U 42T, 42B, 427 42D, 42A, 42P 42E, 426, 41Y
7232	Base Metal Charpy (Transverse)	232, 231, 22D 23A, 22B, 22A 22E, 227, 237 23K, 23L, 22J
7241	Base Metal Tension	1JY, 1KB, 1KC
7251	Base Metal Charpy (Longitudinal)	131, 12T, 114, 12L, 12U, 127 116, 12A, 134 132, 113, 115
7263	Weld Metal Charpy	36P, 323, 34C, 35P, 347, 334 341, 35B, 31A 33E, 36E, 371
7273	Weld Metal Tension	3KC, 3L3, 3JT

V. TEST RESULTS

A. Irradiation Environment

1. Temperature Monitors

Each Tensile-Monitor Compartment (Figures III-1 and III-3) in the capsule assembly contained a set of four temperature monitors to provide an indication of the maximum temperature in the capsule during irradiation. The composition and melting point of each eutectic alloy monitor are given in Table V-1. Each monitor consisted of a helix of the eutectic alloy and a stainless steel weight encapsulated in a quartz tube. Each set of four temperature monitors was inserted into a stainless steel housing, and the temperature monitors were irradiated in the top, middle and bottom surveillance compartments.

Post-irradiation examination of the temperature monitors was performed at C-E's Windsor, Connecticut facility. Each temperature monitor was identified by length, photographed, and inspected to determine whether the eutectic alloy helix had melted and been crushed by the weight. Photographs of the three sets of monitors at 5X are shown in Figures V-1 through V-3. The 536^{O}F monitors (80% Au - 20% Sn) were completely melted. The 558^{O}F monitor (90% Pb - 5% Sn - 5% Ag) helices were distorted but exhibited no melting. Each set of monitors exhibited similar features, indicating that the maximum irradiation temperature was in the 550^{O}F - 558^{O}F range and uniform along the length of the surveillance capsule.

TABLE V-1

COMPOSITION AND MELTING POINTS OF TEMPERATURE MONITOR MATERIALS

Composition (Weight %)	Melting Temperature ^{o}F
80 Au, 20 Sn	536
90 Pb, 5 Sn, 5 Ag	558
97.5 Pb, 2.5 Ag	580
97.5 Pb, 0.75 Sn, 1.75 Ag	590

FIGURE V-1 TEMPERATURE MONITORS COMPARTMENT 7214 (5x)

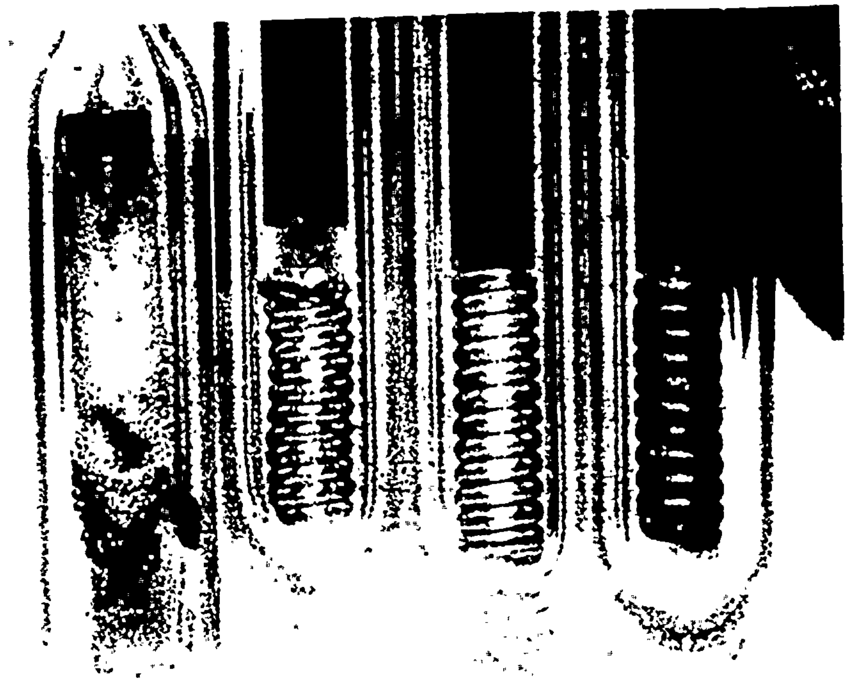

536F 558F 580F 590F

FIGURE V-2 TEMPERATURE MONITORS COMPARTMENT 7241 (5x)

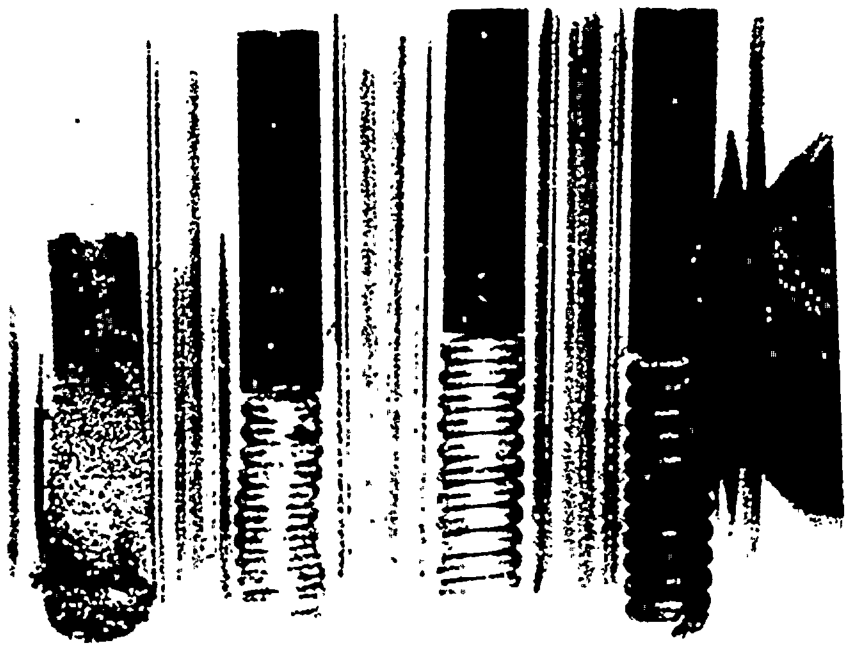

536F 558F 580F 590F

FIGURE V-3

TEMPERATURE MONITORS
COMPARTMENT 7273 (5x)

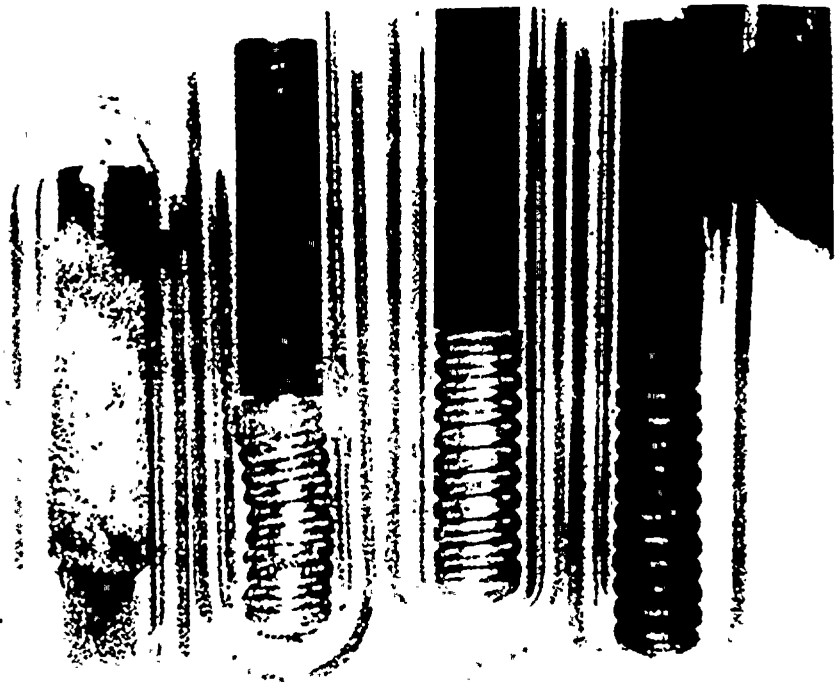

536F 558F 580F 590F

2. Neutron Dosimetry

Each Tensile-Monitor compartment (Figures III-1 and III-3) in the capsule assembly contained two sets of neutron flux monitors as described in Table V-2. Each flux monitor was encapsulated in a stainless steel sheath (except for the sulfur which had a quartz sheath); in addition, cadmium covers were placed around the uranium, cobalt, nickel and copper monitors which have competing thermal activities. Each set of nine flux monitors was inserted into two stainless steel housings, one set for each of the top, middle and bottom surveillance capsule compartments.

The flux monitors were removed from the capsule compartments in the hot cell. Each monitor was inspected and its position in the housing verified by the number of grooves in the stainless steel sheath. The monitors were then repackaged and shipped to C-E's Windsor, Connecticut facility for radiochemical analysis. The identity of individual monitors to their originating compartments was lost because of an error in packaging at the hot cell.

a. Radiochemical Analysis

Radiochemical analysis of the flux monitors was performed in accordance with C-E Procedure 00000-FMD-401, Rev. 0, November 1, 1978 ("Standard Method for the Analysis of Radioisotopes in Reactor Irradiation Surveillance Detectors and Flux Distribution Monitors"). The samples were prepared for radiochemical analysis using standard methods. Atomic absorption spectroscopy was used for the uranium, copper and nickel monitors to establish the amount of monitor material recovered. Simple gravimetric methods were used for the remaining monitors.

TABLE V-2

NEUTRON FLUX MONITORS

Monitor	Material	Reaction	Threshold Energy (MeV)	Half-Life
1	Cobalt (Cadmium Shielded)	$Co^{59}(n,\gamma)Co^{60}$	Thermal	5.27 years
2	Uranium*	$U^{238}(n,f)Cs^{137}$	1.2	30.2 years
3	Titanium	$Ti^{46}(n,p)Sc^{46}$	8.0	65 days
4	Iron	$Fe^{54}(n,p)Mn^{54}$	4.0	312.5 days
5	Cobalt	$Co^{59}(n,\gamma)Co^{60}$	Thermal	5.27 years
6	Uranium* (Cadmium Shielded)	$U^{238}(n,f)Cs^{137}$	1.2	30.2 years
7	Nickel (Cadmium Shielded)	$Ni^{58}(n,p)Co^{58}$	3.5	70.8 days
8	Copper (Cadmium Shielded)	$Cu^{63}(n,\alpha)Co^{60}$	7.0	5.27 years
9	Sulfur	$S^{32}(n,p)P^{32}$	2.9	14.3 days

*U-238 foil depleted in U-235 to .05 w/o

Gamma counting was performed with a 4096 channel gamma spectrometer system coupled with a hyperpure germanium detector. The system was calibrated at 0.5 Kev per channel to span the gamma energy range from 0.05 to 2 Mev. Efficiency calibration was performed using eight (8) gamma energies emitted from a mixed isotope standard traceable to the National Bureau of Standards. Phosphorus-32 beta activity was measured on a gas flow proportional counter which was calibrated with NBS traceable beta standards.

Physical constants used in the calculation of radioisotope activity levels are as follows:

Isotope	Half-Life	Gamma Energy (MeV)	Intensity[a]
Cobalt-58	70.8 days	0.8105	0.99
Cobalt-60	5.27 years	1.3325	1.00
Cesium-137	30.2 years	0.6616	0.85
Manganese-54	312.5 days	0.8347	1.00
Scandium-46	65 days	0.8892	1.00
Phosphorus-32	14.3 days	(b)	1.00

a - Intensity is branching ratio (gamma rays or beta particles per disintegration).

b - Decays by beta only.

Flux spectrum monitor activity levels are presented in Table V-3. All values are decay corrected to the time of reactor shutdown, February 26, 1983. The uncertainty listed with each result is the 2-sigma counting error only. An additional error of $\pm 20\%$ for uranium monitors, $\pm 12\%$ for copper and nickel monitors and $\pm 7\%$ for all other metal monitors is estimated from volumetric and gravimetric operations and from the stated uncertainties of calibration isotopes. An additional error associated with the sulfur monitor results is $\pm 8\%$.

The shutdown activities determined from gamma ray emission rates were calculated as follows:

$$A = \frac{N_p}{EWBC\ (e^{-\lambda t})}$$

where: A = shutdown activity in disintergrations per minute per milligram of material (dpm/mg)

Np = radioisotope net counts per minute

E = full energy peak efficiency (counts per gamma ray emitted)

W = weight of monitor sample (milligrams)

B = radioisotope gamma ray branching ratio (gamma rays per disintegration)

C = correction for coincident or random summing

λ = radioisotope decay constant

t = elapsed time between plant shutdown and counting

TABLE V-3

ST. LUCIE UNIT 1 FLUX

SPECTRUM MONITOR ACTIVITIES

Monitor Material	Number of Grooves	Measured Isotope	Weight (mg)	Activity at End of Irradiation (dmp/mg)
(1) Cobalt (shielded)	0	Co-60	7.8	$2.75 \pm 0.04 \times 10^5$
			7.6	$2.78 \pm 0.04 \times 10^5$
			7.6	$2.76 \pm 0.04 \times 10^5$
(2) Uranium	1	Cs-137	24.6	$3.66 \pm 0.09 \times 10^4$
			24.7	$4.96 \pm 0.11 \times 10^4$
			36.9	$4.30 \pm 0.09 \times 10^4$
(3) Titanium	2	Sc-46	13.0	$3.52 \pm 0.20 \times 10^4$
			12.9	$3.78 \pm 0.20 \times 10^4$
			13.0	$3.96 \pm 0.21 \times 10^4$
(4) Iron	3	Mn-54	23.8	$1.09 \pm 0.02 \times 10^5$
			23.9	$1.18 \pm 0.02 \times 10^5$
			23.6	$1.16 \pm 0.02 \times 10^5$
(5) Cobalt	4	Co-60	8.0	$1.83 \pm 0.01 \times 10^6$
			7.7	$1.32 \pm 0.01 \times 10^6$
			7.4	$1.80 \pm 0.01 \times 10^6$
(6) Uranium (shielded)	5	Cs-137	12.4	$1.49 \pm 0.09 \times 10^4$
			10.1	$2.01 \pm 0.11 \times 10^4$
			11.2	$2.30 \pm 0.12 \times 10^4$
(7) Nickel (shielded)	6	Co-58	22.3	$1.95 \pm 0.01 \times 10^6$
			19.6	$2.07 \pm 0.01 \times 10^6$
			21.1	$1.74 \pm 0.01 \times 10^6$
(8) Copper (shielded)	7	Co-60	17.5	$8.58 \pm 0.19 \times 10^3$
			21.5	$8.28 \pm 0.17 \times 10^3$
			20.9	$9.09 \pm 0.39 \times 10^3$
(9) Sulfur	-	P-32	8.4	$3.72 \pm 0.03 \times 10^5$
			19.4	$4.17 \pm 0.03 \times 10^5$
			17.1	$1.19 \pm 0.01 \times 10^6$

b. Threshold Detector Analysis

The SAND-II[3] and DOT IV version 4.3[4] computer codes were used to calculate the fast flux and fluence at the surveillance capsule assembly location and at the reactor vessel.

The DOT IV neutron transport code was used in order to determine the spatial distribution of the neutron flux and the spectrum associated with it within the St. Lucie 1 vessel. The St. Lucie 1 geometry was modelled in the DOT calculation using Rθ coordinates and octant symmetry as shown in Figure V-4. The DOT calculations used a source distribution deduced from pinwise PDQ power distributions. Figures V-5 and V-6 show assembly average power distributions for Cycles 1 through 5 and the planned distributions for Cycle 6, respectively, which were deduced from the PDQ results. A major difference which is evident in these two power distributions is the change from an out-in to a low-leakage fuel management for Cycles 5 and 6. For extrapolation to future cycles, the Cycle 6 fast fluxes were used. The removal of the St. Lucie 1 thermal shield after Cycle 5 contributed the only change to the physical geometry of St. Lucie 1. The DLC-23E CASK, 40 group neutron and gamma ray cross section library was used in the DOT calculation. A representation of the surveillance capsule detail, as used in the DOT model, is shown in Figure V-7.

The SAND II code which was used in the analysis of dosimeter activation requires, as input, saturated dosimeter activities (A_{sat}). These saturated activities are deduced from the operating history and the decay constants for the various dosimeters. In order to obtain the saturated activities, equation 1 is used to convert the measured (unsaturated) activities to saturation in units of (dps/a).

$$(1) \quad A_{sat} = \frac{A_{unsat} * A_W}{N_a * I * S} * \; 16.67 \, \frac{\text{mg. min}}{\text{g. sec}}$$

where: A_{sat} = saturated activity (dps/a)
Aunsat = measured activity (dpm/mg) from Table V-3
A_W = atomic weight (g/mole)
N_A = Avogadros number (atoms/mole)
I = isotopic abundance of target isotope
S = saturation factor (see below)

In order to determine the saturation factor(s) for equation 1, the operating history of St. Lucie 1 was modelled by intervals of constant power (P_i) relative to a full power operation (P_o) for Cycles 1-5. Hence the saturation factor for each isotope may be given as:

$$(2) \quad S = \sum_i \left(\frac{P_i}{P_o}\right) f_i \, e^{-\lambda T_i} \left[1-e^{-\lambda t_i}\right]$$

where: P_i = power of the i^{th} time interval.
P_o = full power level
T_i = time from end of interval i to reactor shutdown
t_i = length of time interval i
f_i = radial power distribution adjustment factor
λ = decay constant

The activity for the short-lived isotopes ($t_{1/2}$ < cycle length) in the St. Lucie 1 dosimeters is indicative of the leakage flux for Cycle 5 and, therefore, in this case where the peripheral assembly powers decreased in the fifth cycle relative to the first 4 cycles, the monitor activity for the short lived isotopes underestimates the leakage flux relative to the average leakage over the five cycles. For very long-lived isotopes, the saturation factor builds up to a steady rate through all five cycles. As a first order correction, the short-lived saturation factor was adjusted by setting f_i equal to the ratio of the weighted assembly average power level factor for the surveillance capsule position during Cycle 5 to the average over Cycles 1 to 5. For the long lived isotopes, f_i is approximately 1 as the average power distribution through Cycles 1 to 5 is seen by these isotopes. This correction is somewhat approximate due to the fact that the power distribution within the cycle is changing relative to the cycle average. Once again, this has the greatest effect on the short-lived isotopes.

Using the DOT flux spectrum at the surveillance capsule as input, the SAND code was used in the activity mode to calculate saturated activities relative to the normalized DOT spectrum. From this, an effective cross section ($\bar{\sigma}$) is obtained as shown in equation 3. These $\bar{\sigma}$'s are based on the ENDF/B-V dosimetry cross section library, DOSCROS81, Reference 5.

$$(3) \qquad \bar{\sigma} = \frac{A_{sat}\text{ (calculated)}}{\int_{1.0}^{\infty} \phi(E)\,dE}$$

From this effective $\bar{\sigma}$, the fast neutron flux (ϕ) above 1 MeV is found by:

$$(4) \qquad \phi(>1\text{ MeV}) = \frac{A_{sat}\text{ (measured)}}{\bar{\sigma}}$$

Using this method, an inferred flux is obtained for each monitor material.

The dosimeters from the three separate flux monitor compartments were mixed when shipped from the hot cell and, therefore, individual monitors were not identified as to their originating compartments. The activity levels of a given dosimeter type were

pooled as one set for the SAND analysis, and the compartment specific results were obtained by using axial factors at the capsule compartment elevations derived from an axial RZ DOT calculation. Table V-4 shows the results of the analysis of the axial variation in the surveillance capsule fast neutron flux.

Tables V-2 and V-3 summarize the flux monitors used and their measured activities. Table V-5 shows the saturated activity in units of disintegrations per second per atom (dps/a) calculated using Equation 1, the correction factors discussed above, and as used in the SAND analysis. The uranium fission monitor activities were also corrected for the thermal and epithermal fission of the U-235 impurities (350 ppm). The resulting correction factor (0.935) was applied to the measured fission product activity to obtain the activity due to U-238 fissions. The U-238 fission product activities were input to the SAND analysis in terms of fissions per second per U-238 atom (fps/a). This value was obtained by dividing the saturated activity (A_{sat}) by the fission yield for U-238 of the fission product being analyzed. The fission yields were obtained from ASTM E704-79 and give a fission yield of 5.99% for Cs-137. No correction has been included for photofission yield of U-238. Neglect of the photofission correction provides a conservative (higher) result for the fast neutron flux.

Figures V-8 and V-9 show the fast neutron flux azimuthal distribution at the vessel/clad interface for Cycles 1 to 5 and for Cycle 6 normalized to their respective peak azimuthal values as given in Table V-6.

The average axial power distribution for Cycles 1 to 5 and for Cycle 6 are shown in Figures V-10 and V-11. The axial peak for Cycles 1 to 5 is 1.18 and 1.11 for Cycle 6. These source distributions were used in RZ DOT calculations to obtain the axial fast flux distributions for BOC to EOC5 and Cycle 6 at the vessel clad interface as shown in Figures V-12 and V-13, respectively.

The fluence values in Table V-7 were based on the average flux values in Table V-6. For the extrapolation to end of life (EOL), Cycle 6 values were used for operation beyond Cycle 5. This extrapolation is based on the assumption of a uniformly thick core support barrel.*

Reference 3 states that the SAND code will give fluxes that are accurate to within ± 10% to ± 30% if the errors in the measured activities are within similar limits. In Table V-3, the quoted uncertainties are at a 2-Sigma level and are determined from counting statistics. An additional error of ± 20% for uranium monitors, ± 12% for copper and nickel monitors, and ± 7% for all other metal monitors is estimated from volumetric and gravimetric operations and from the stated uncertainties of calibration isotopes.

Taking into account the adjustments used in the saturation factor correction and in the use of pooled data from different capsule locations, an estimated ± 35% uncertainty should be used for the measured flux at the surveillance capsule. This uncertainty does not include variations that may occur in the Lead Factor due to changes in the azimuthal distributions which could result from different fuel management strategies.

* The repaired core support barrel (CSB) will contain holes of various sizes that are filled with water and covered on one end by 1/4 to 1/2 inch thick stainless steel plugs. These non-uniformities will cause neutron streaming at these locations and hence higher flux and fluence values at the corresponding vessel locations. These hole effects are treated in a separate report[11].

Figure V-4
GEOMETRY USED IN DOT MODEL

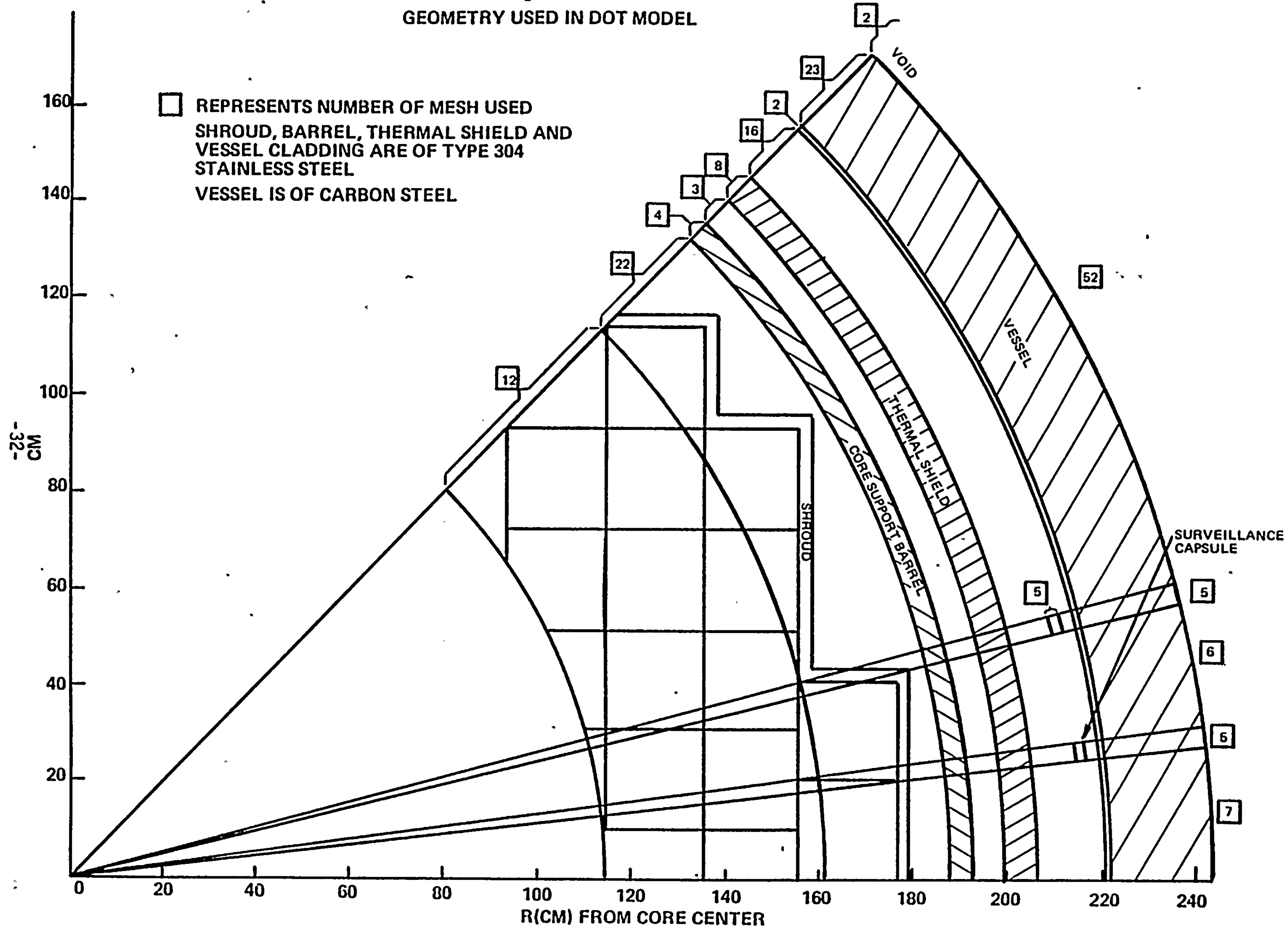

Figure V-5
POWER DISTRIBUTIONS USED IN DOT CYCLES 1-5

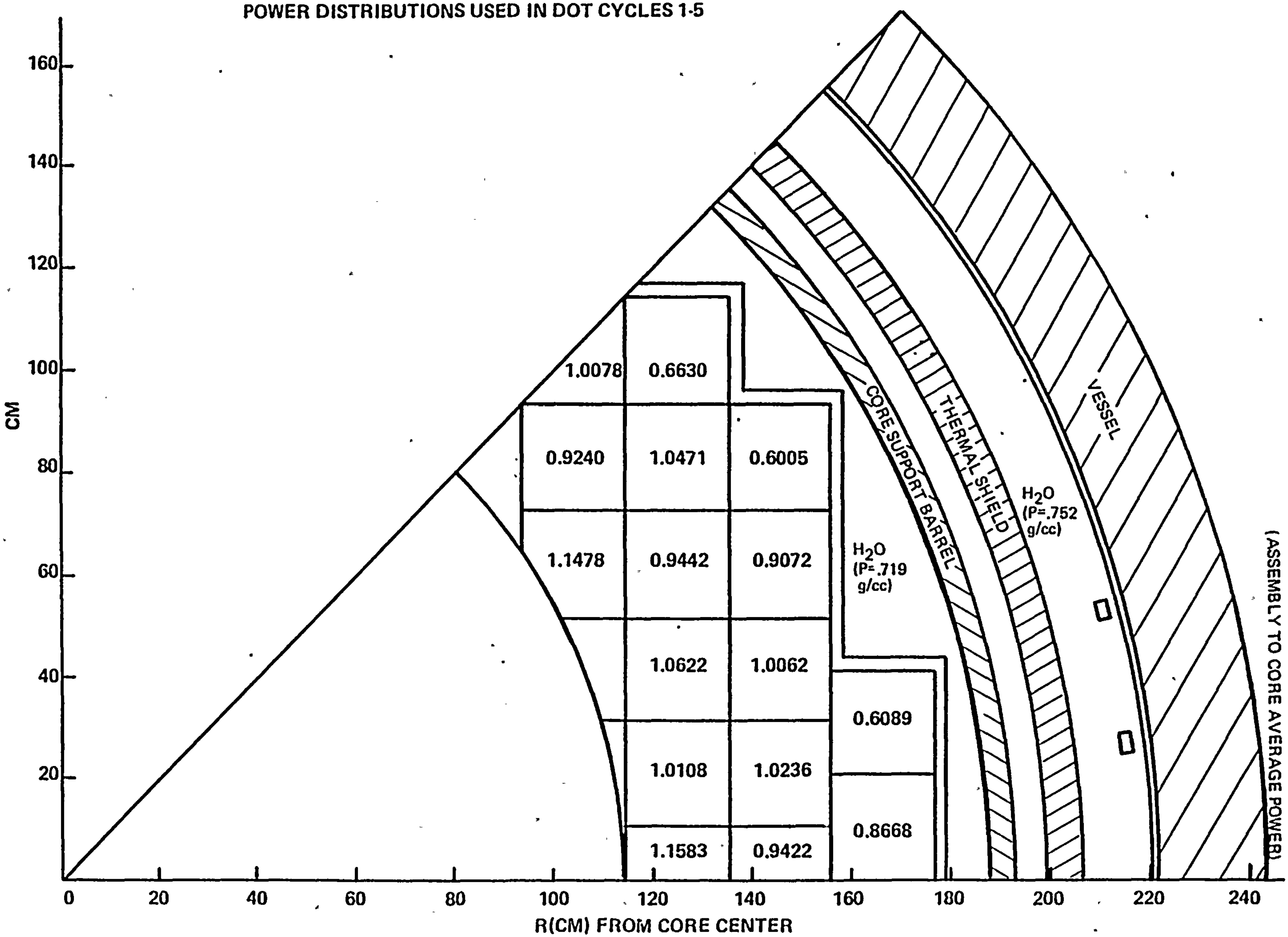

Figure V-6

POWER DISTRIBUTION USED IN DOT CYCLE 6

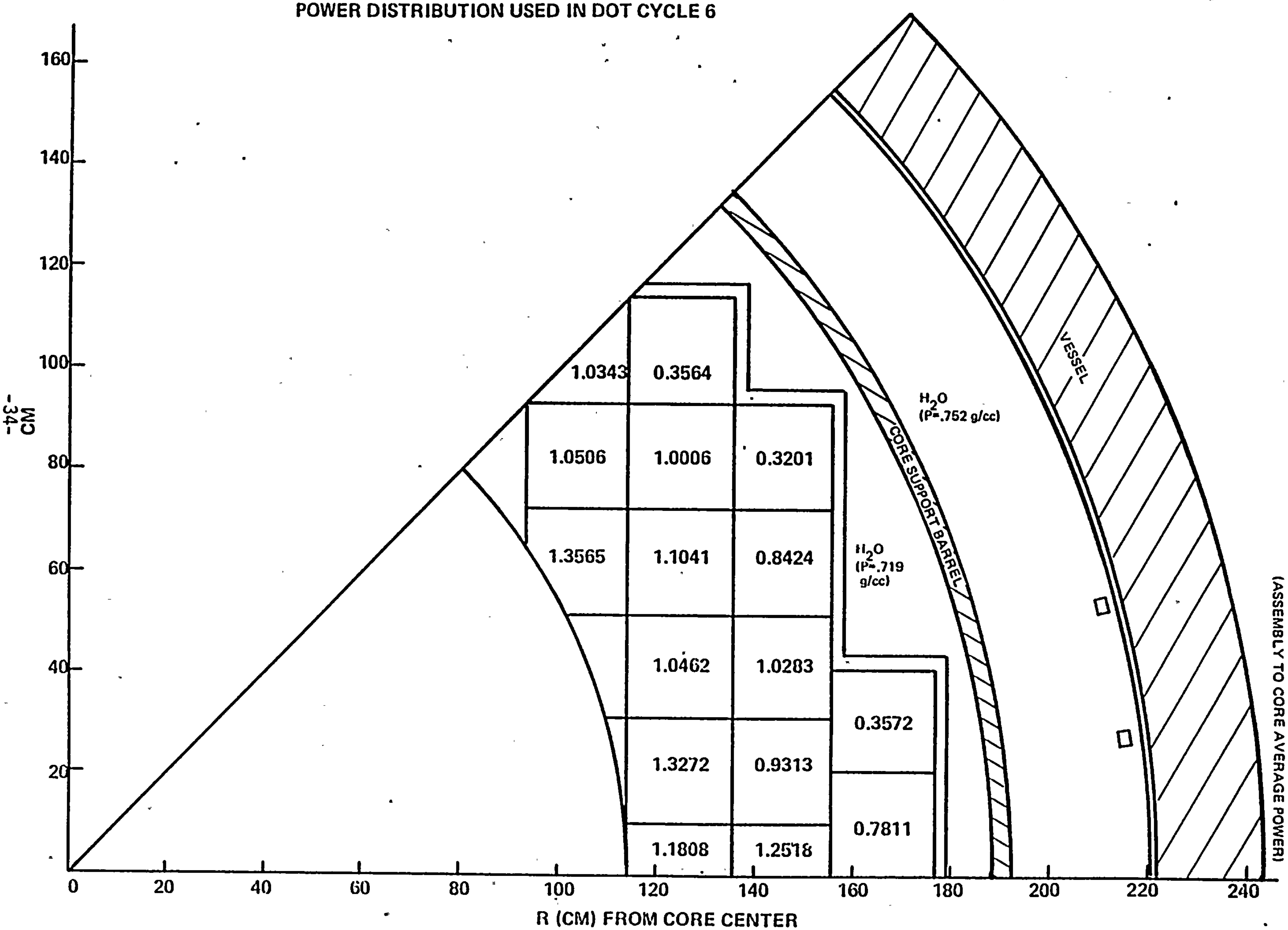

Figure V-7
DOT MODEL OF W-97 SURVEILLANCE CAPSULE

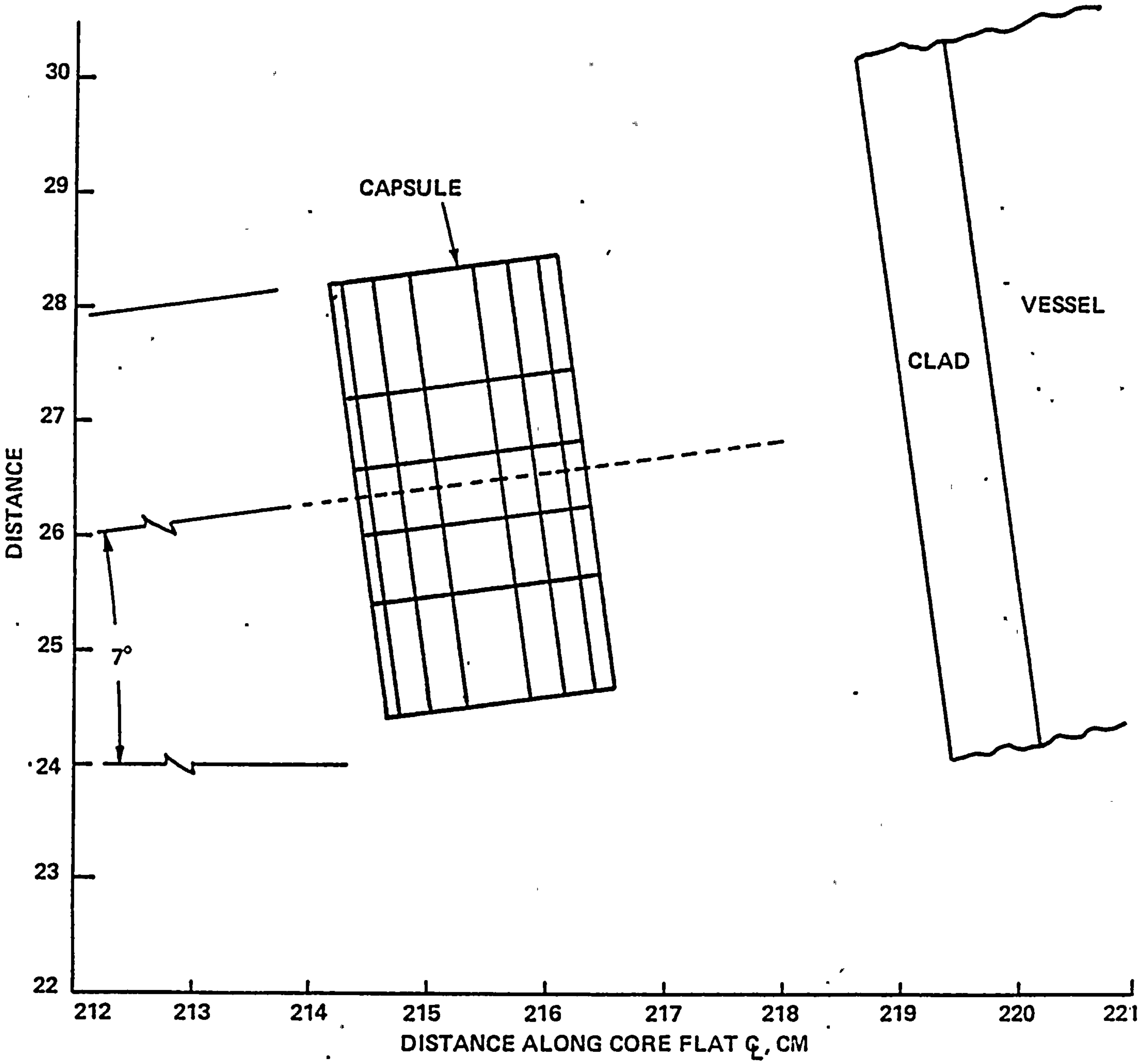

TABLE V-4

Axial Variation in Surveillance Capsule Fast Flux

Surveillance Capsule Axial Compartment	Axial Position Relative to Core Midplane (CM)	Fast Neutron ($E_n > 1$ Mev) Flux ($n/cm^2.s$)
7214	+89.6	3.6 + 10
7241	+ 2.9	3.7 + 10
7273	-83.8	3.5 + 10

TABLE V-5

Flux Monitor Saturated Activities

Flux Monitor Type	Measured Activity (dpm/mg)	Saturated Activity (dps/a)
1	2.75+5	6.16-13
1	2.78+5	6.25-13
1	2.76+5	6.21-13
2 (Cs)*	3.66+4	2.09-14**
2 (Cs)	4.96+4	2.83-14**
2 (Cs)	4.30+4	2.46-14**
3	3.52+4	6.33-16
3	3.78+4	6.80-16
3	3.96+4	7.12-16
4	1.09+5	3.49-15
4	1.18+5	3.78-15
4	1.16+5	3.71-15
5	1.83+6	4.11-12
5	1.32+6	2.97-12
5	1.80+6	4.05-12
6 (Cs)	1.49+4	1.53-14
6 (Cs)	2.01+4	2.06-14
6 (Cs)	2.30+4	2.36-14
7	1.95+6	5.04-15
7	2.07+6	5.34-15
7	1.74+6	4.49-15
8	8.58+3	5.12-17
8	8.28+3	4.94-17
8	9.09+3	5.42-17
9	3.72+5	3.84-16**
9	4.17+5	4.31-16**
9	1.19+6	1.23-15**

*Fission Yield of Cs-137 is 5.99%
**These monitors were not used in the SAND analysis

Figure V-8
ST. LUCIE I BOL TO EOC5
AVERAGE AZIMUTHAL FAST NEUTRON ($E_n > 1$ MeV) FLUX
DISTRIBUTION AT VESSEL/CLAD INTERFACE

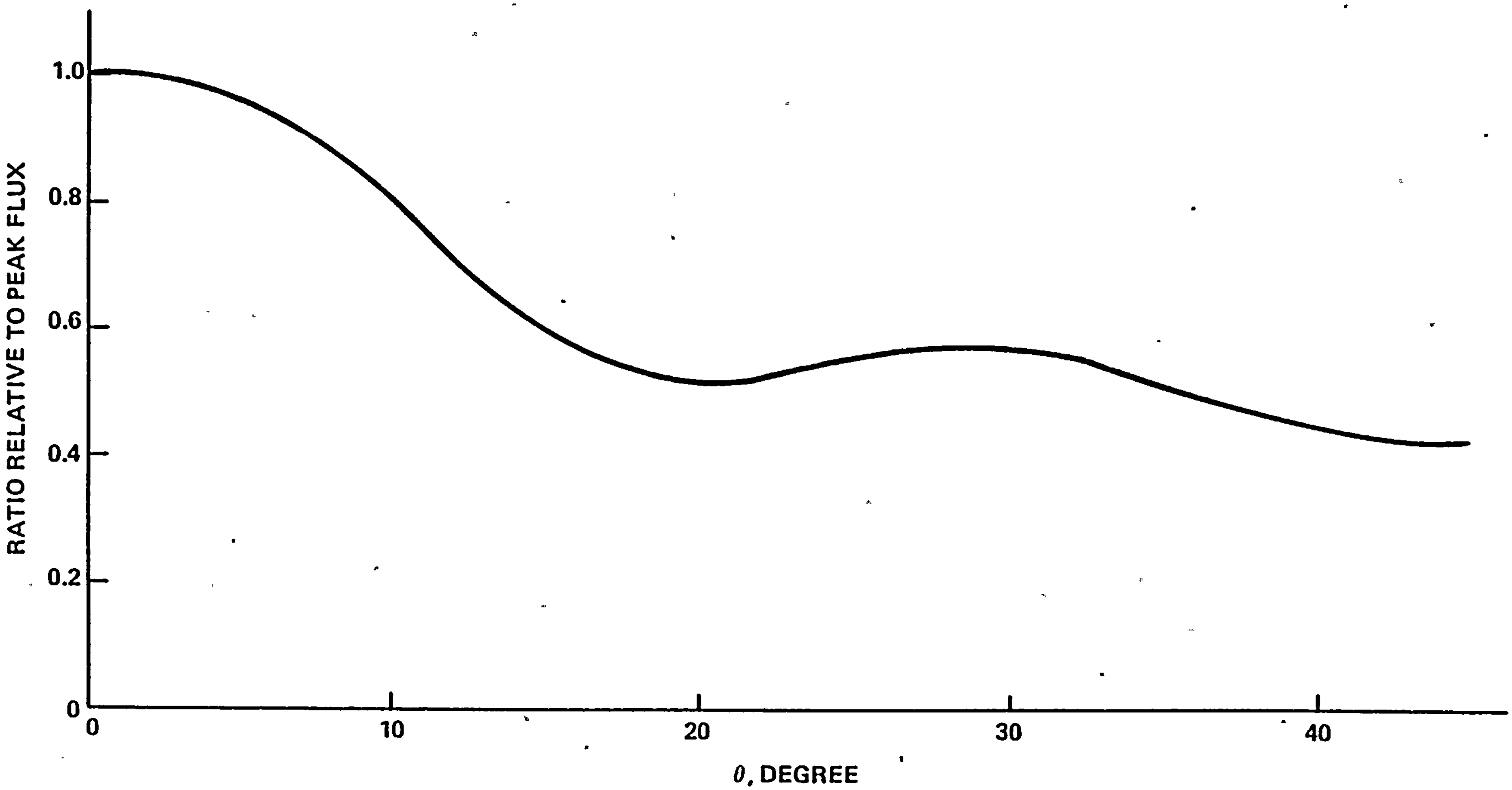

Figure V-9
ST. LUCIE I CYCLE 6
AVERAGE AZIMUTHAL FAST NEUTRON ($E_n > 1$ MeV) FLUX
DISTRIBUTION AT VESSEL/CLAD INTERFACE

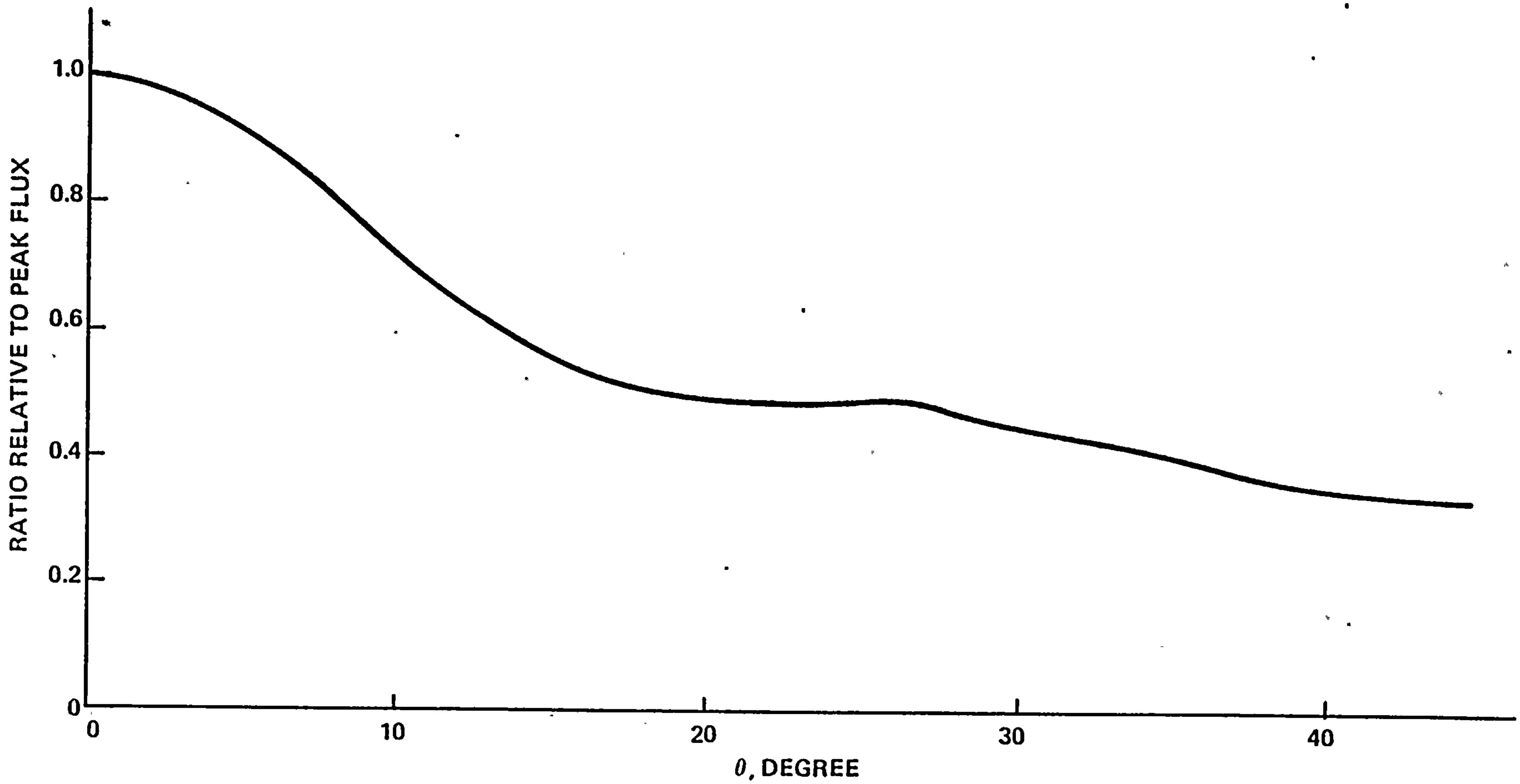

TABLE V-6

St. Lucie 1
Average Fast Neutron Flux (E_n>1 MeV) (n/cm^2.s)
(At Peak Axial and Azimuthal Location)

	BOL to EOC5 Actual	Cycle 6 Average (Without Thermal Shield)
Surveillance Capsule	3.7+10[1]	4.4+10
Vessel/Clad Interface	2.7+10	3.7+10
1/4 Thru Vessel	1.4+10	2.0+10
1/2 Thru Vessel	6.6+9	9.3+9
3/4 Thru Vessel	2.9+9	4.1+9

TABLE V-7

Fast Neutron Fluence (E_n>1 MeV) (n/cm^2)
(At Peak Axial and Azimuthal Location)

	BOL to EOC5[2] (Actual)	BOL TO EOL[3] (Without Thermal Shield)
Surveillance Capsule	5.5+18	4.3+19
Vessel/Clad Interface	3.9+18	3.5+19
1/4 Thru Vessel	2.1+18	1.9+19
1/2 Thru Vessel	9.8+17	9.0+18
3/4 Thru Vessel	4.3+17	3.9+18

[1] Numbers shown as 3.7+10 are to be interpreted as 3.7×10^{10}.

[2] 4.67 EFPY (1.473+8s) @ 2700 Mwt.

[3] EOL corresponding to 32 EFPY (1.009+9s) @ 2700 Mwt; extrapolation based on planned Cycle 6 operating characteristics.

Figure V-10
ST. LUCIE I
PERIPHERAL ASSEMBLY NORMALIZED AXIAL POWER
AVERAGED OVER CYCLES 1 TO 5

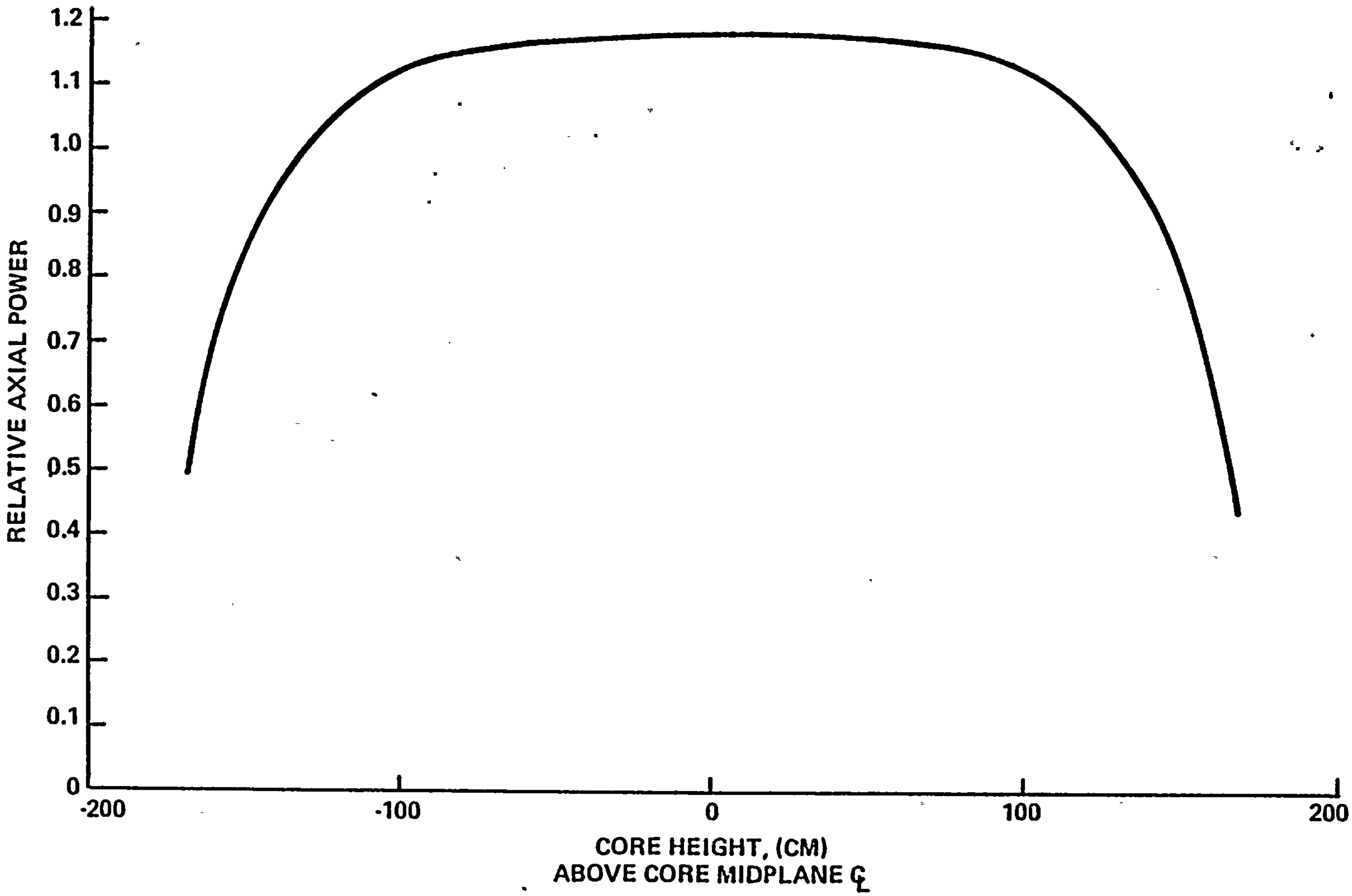

Figure V-11
ST. LUCIE I
PERIPHERAL ASSEMBLY NORMALIZED AXIAL POWER
AVERAGED OVER CYCLE 6

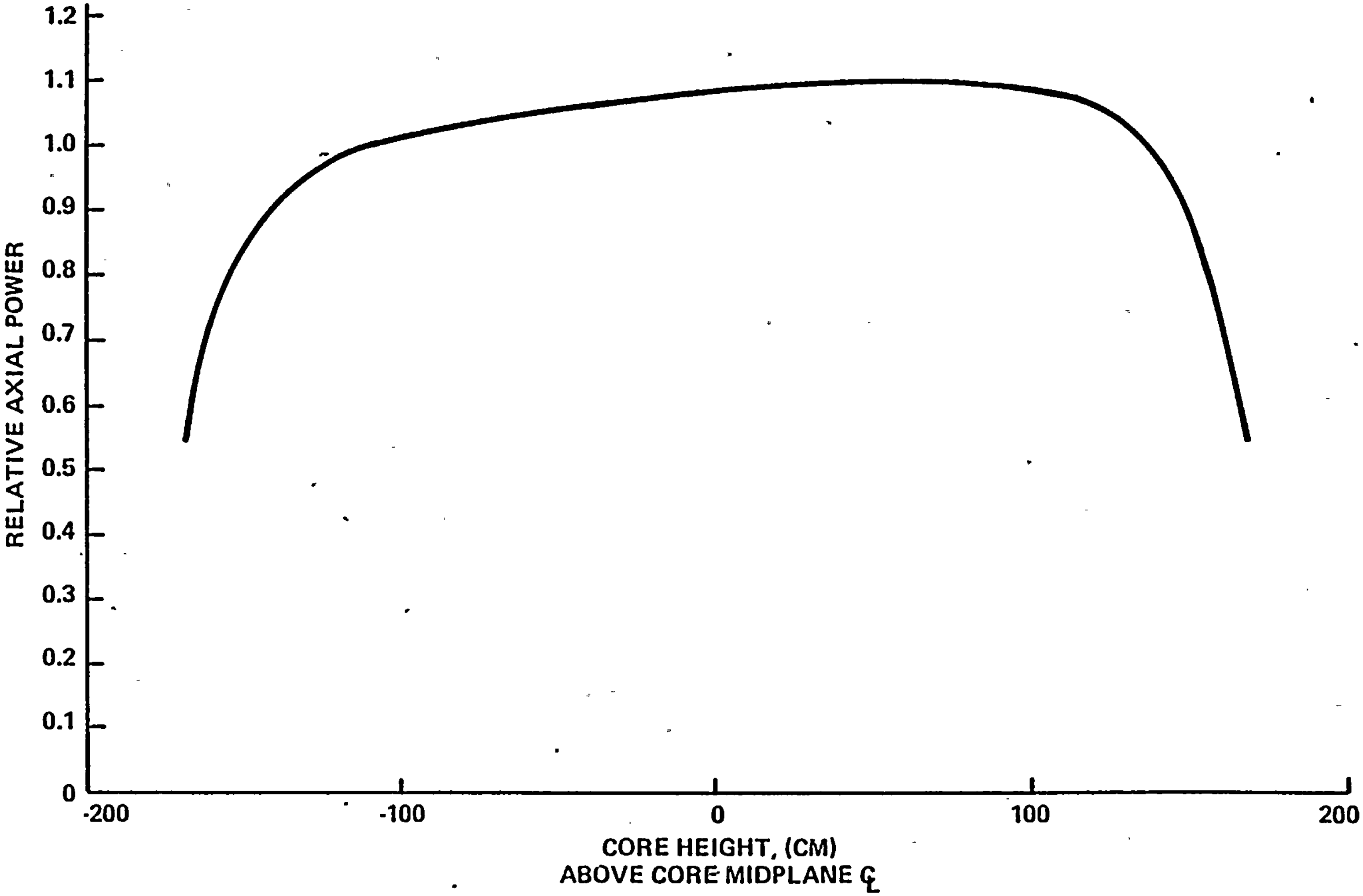

Figure V-12
ST. LUCIE I
AXIAL FAST NEUTRON FLUX AT VESSEL/CLAD INTERFACE
BOL-EOC5 (NORMALIZED TO PEAK VALUE AT 1.18 AXIAL PEAK)

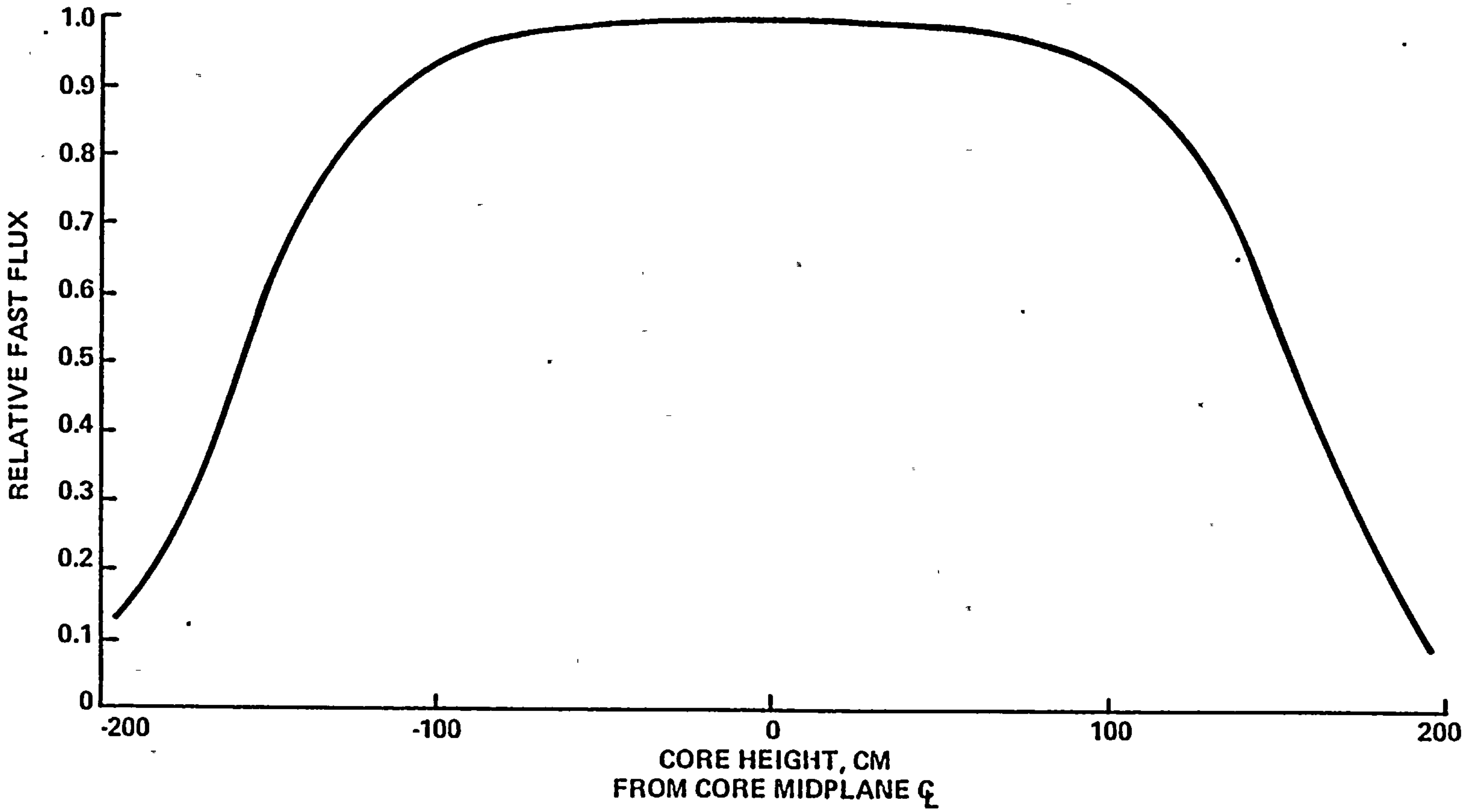

Figure V-13
ST. LUCIE I
AXIAL FAST NEUTRON FLUX AT VESSEL/CLAD INTERFACE
CYCLE 6 (NORMALIZED TO PEAK VALUE AT 1.11 AXIAL PEAK)

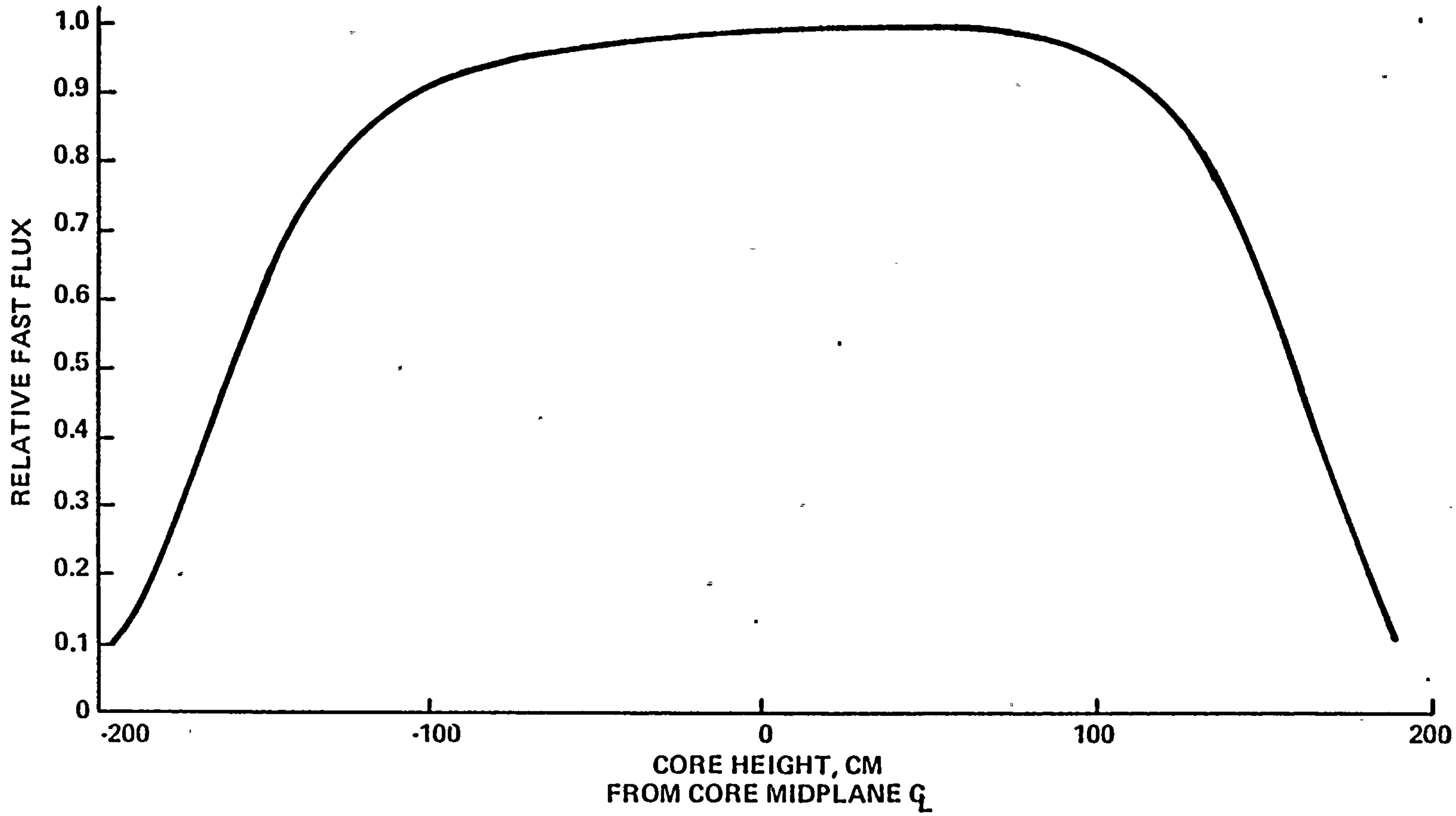

B. Chemical Analysis

Six Charpy specimens each of the base metal (transverse orientation) and weld metal were chemically analyzed by X-ray fluorescence for molybdenum, copper, nickel, manganese, silicon, sulfur and phosphorus content. Each Charpy specimen was placed in a carrier with a graphite mask for analysis. Calibration curves were initially established for the seven elements using nine plate and weld specimens with a known chemical content. One of these specimens (11E) was used to check for reproducibility with copper and phosphorus as the selected elements. Twelve separate measurements yielded a copper reproducibility of $\pm$ 1% and a phosphorus reproducibility of $\pm$ 7% at one standard deviation. Specimen 11E was also used as a control for irradiated specimen measurements.

Results of the analysis of the irradiated specimens and the control specimen are given in Table V-8. (Results for the unirradiated specimens are also included.) The base metal specimens represent three different sections of the surveillance plate at the 1/4 and 3/4 thickness locations. The weld metal specimens represent six separate regions through the thickness of the weld as shown in Figure V-14, which was based on the weld metal specimen layout drawing.[6]

C. Strength and Toughness Properties

1. Tension Tests

Tension tests were conducted in accordance with applicable ASTM standards and C-E laboratory procedures. The test method and equipment are described in Appendix A.

The three irradiated specimens from each material (base metal, weld metal and heat-affected zone) were tested at room tempera-

TABLE V-8

IRRADIATED PLATE AND WELD
MATERIAL CHEMICAL ANALYSIS

Specimen ID	Lab Number	Material	Chemical Content (Weight Percent) Mo	Cu	Ni	Mn	Si	S	P
227	2220	Plate(WR)	0.62	0.14	0.57	1.26	0.21	0.018	0.007
232	2223	Plate(WR)	0.61	0.13	0.57	1.28	0.21	0.018	0.007
23L	2226	Plate(WR)	0.62	0.14	0.58	1.29	0.20	0.018	0.007
132	2222	Plate(RW)	0.62	0.14	0.57	1.28	0.20	0.018	0.008
113	2224	Plate(RW)	0.62	0.14	0.56	1.26	0.20	0.018	0.006
12A	2225	Plate(RW)	0.63	0.14	0.57	1.29	0.20	0.018	0.009
371	2215	Weld	0.53	0.22	0.05	1.07	0.20	0.012	0.014
36P	2216	Weld	0.53	0.22	0.05	1.06	0.21	0.012	0.016
323	2217	Weld	0.53	0.32	0.06	1.04	0.20	0.012	0.015
31A	2218	Weld	0.53	0.32	0.06	1.05	0.20	0.012	0.018
341	2219	Weld	0.52	0.22	0.06	1.07	0.20	0.012	0.016
36E	2221	Weld	0.53	0.22	0.06	1.07	0.20	0.012	0.016
11E	#1	Control	0.56	0.15	0.54	1.24	0.21	0.014	0.009
11E	#2	Control	0.56	0.15	0.53	1.23	0.21	0.014	0.010
11E	#3	Control	0.55	0.15	0.54	1.22	0.20	0.014	0.009
Unirradiated Data									
23C	1978	Plate(WR)	0.63	0.14	0.58	1.32	0.21	0.018	0.007
25K	1979	Plate(WR)	0.63	0.14	0.59	1.33	0.21	0.018	0.007
216	1980	Plate(WR)	0.62	0.14	0.58	1.33	0.21	0.017	0.006
221	1981	Plate(WR)	0.63	0.14	0.58	1.32	0.21	0.018	0.007
233	1982	Plate(WR)	0.62	0.14	0.58	1.33	0.21	0.017	0.007
235	1983	Plate(WR)	0.63	0.14	0.58	1.33	0.21	0.018	0.007
32L	1984	Weld	0.53	0.21	0.06	1.09	0.21	0.012	0.014
34T	1985	Weld	0.53	0.20	0.05	1.07	0.21	0.012	0.013
333	1986	Weld	0.53	0.44	0.06	1.08	0.21	0.011	0.013
356	1987	Weld	0.53	0.20	0.05	1.07	0.21	0.012	0.014
36C	1988	Weld	0.52	0.20	0.05	1.10	0.21	0.011	0.014
362	1989	Weld	0.53	0.21	0.05	1.11	0.21	0.012	0.013

FIGURE V-14
LOCATION OF WELD METAL
CHEMICAL ANALYSIS SPECIMENS
(COPPER CONTENT IN PARENTHESES)

		323[a] (.32)					34T[b] (.20)				TOP
			32L[b] (.21)							36E[a] (.22)	
									362[b] (.21)		
					341[a] (.22)						
										36P[a] (.22)	
31A[a] (.32)											
							356[b] (.20)				
			333[b] (.44)								
									36C[b] (.20)	371[a] (.22)	BOTTOM

SIDE VIEW

← WELDING DIRECTION →

a Irradiated specimens

b Baseline specimens

ture, 250°F and 550°F. The tensile properties are listed in Table V-9, and the stress-strain curves are shown in Figure V-15 through V-23. The pre-irradiation tensile properties[2] are summarized in Table V-10 (each value average of three tests). Photographs of the broken irradiated specimens are shown in Figure V-24.

2. Charpy V-Notch Impact Tests

Charpy V-notch impact tests were conducted in accordance with applicable ASTM standards and C-E laboratory procedures. The test method and equipment are described in Appendix B.

Twelve irradiated specimens from each material (transverse and longitudinal base metal, weld metal and heat-affected zone) were tested at a series of temperatures to establish the transition temperature behavior. The impact data (impact energy, lateral expansion and fracture appearance as a function of test temperature) are shown in Tables V-11 through V-14 and Figures V-25 through V-36. (Also shown in each of the figures is the unirradiated transition temperature curve from the baseline evaluation.[2]) Fracture surface photographs of the broken irradiated specimens are shown in Figures V-37 through V-40.

Each impact test was instrumented. Additional data related to instrumented impact testing are presented in Appendix C.

TABLE V-9

POST-IRRADIATION TENSION TEST PROPERTIES

Material	Specimen Code	Test Temp. (°F)	Yield Strength 0.2% Offset (ksi)	Ultimate Tensile Strength (ksi)	Fracture Load (lb)	Fracture Strength[a] (ksi)	Fracture Stress[b] (ksi)	Reduction of Area (%)	Elongation (1-inch gage) TE/UE[d] (%)
Base Metal	1KB	72	80.6	103.0	3240	65.5	201.7	67.5	26/9.7
	1JY	250	76.4	96.9	3240	66.0	190.9	65.4	24/8.8
	1KC	550	71.5	98.4	3270	66.6	177.9	62.5	23/8.1
Weld Metal	3KC	72	84.9	98.0	2970	60.0	198.6	69.8	28/12.2
	3JT	250	79.5	91.6	2940	59.9	191.0	69.1	25/11.1
	3L3	550	75.2	94.4	3370	68.7	165.5	58.5	26/8.6
HAZ	4J5	72	78.2	98.6	3018	61.5	187.9	67.3	27/8.3
	4JC	250	75.2	94.7	2986	60.8	196.8	69.1	(c) /7.5
	4JP	550	75.2	95.6	3192	65.0	158.8	59.0	24/9.1

a - Fracture strength is the fracture load divided by initial cross sectional area

b - Fracture stress is the fracture load divided by final cross sectional area

c - Not determined; specimen broke outside gauge length

d - TE = total elongation, UE = uniform elongation

TABLE V-10

PRE-IRRADIATION TENSION TEST PROPERTIES

Material	Test Temp. (°F)	Yield Strength 0.2% Offset (ksi)	Ultimate Tensile Strength (ksi)	Fracture Load (lb)	Fracture Strength[a] (ksi)	Fracture Stress[b] (ksi)	Reduction of Area (%)	Elongation (1-inch gage) TE/UE[c] (%)
Base Metal	72	71.4	92.3	2720	56.8	207	73	27/10.3
	250	66.8	86.2	2640	53.9	186	71	23/8.1
	550	63.9	90.1	2940	61.0	182	67	25/8.9
Weld Metal	72	71.9	84.7	2300	46.9	186	75	30/11.1
	250	69.0	79.0	2400	48.9	180	73	26/9.5
	550	65.9	84.6	2760	56.2	175	64	26/9.9
HAZ	72	66.8	86.0	2580	52.6	204	52	27/10.0
	250	66.2	80.8	2640	53.8	179	69	23/8.0
	550	62.4	84.4	2730	55.0	178	69	24/8.5

a - Fracture strength is the Fracture Load divided by initial cross sectional area

b - Fracture stress is the Fracture Load divided by final cross sectional area

c - TE = total elongation, UE = uniform elongation

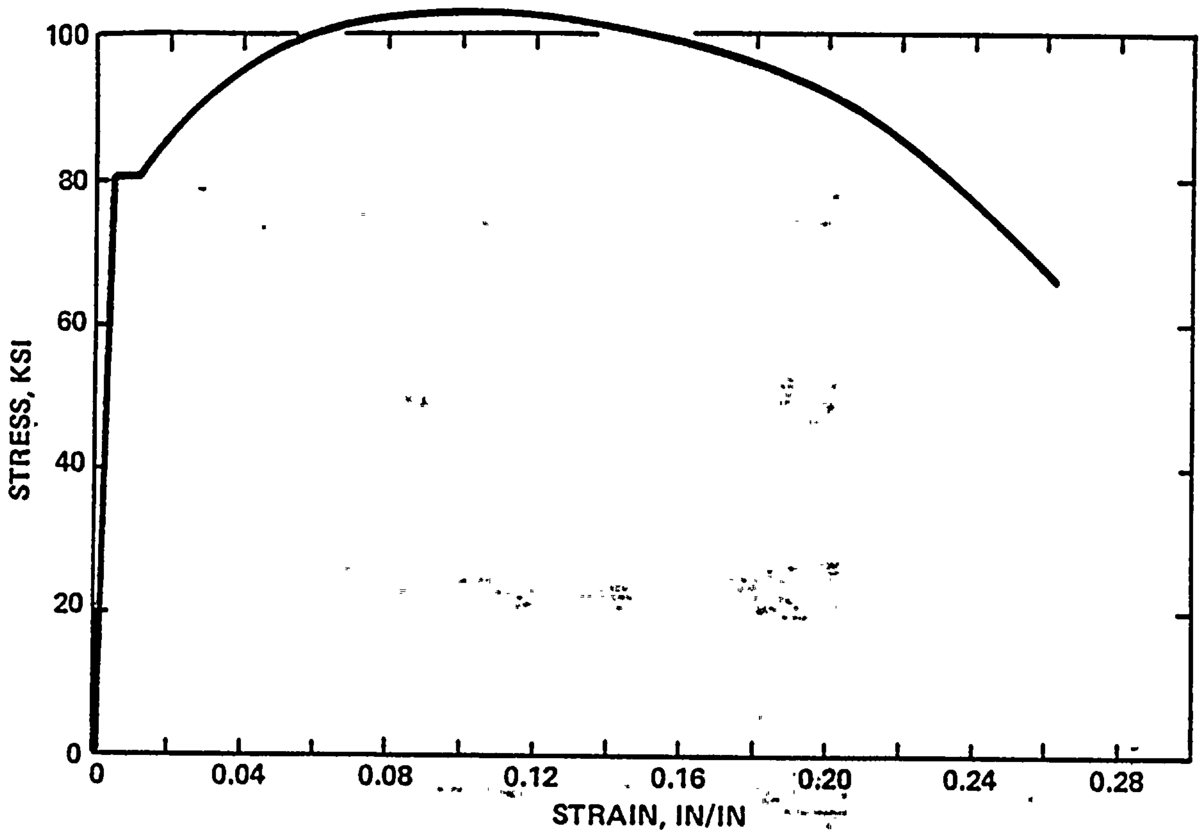

Figure V-15 STRESS-STRAIN RECORD, BASE METAL PLATE C-8-2 SPECIMEN No. 1KB, TEST TEMPERATURE 72°F

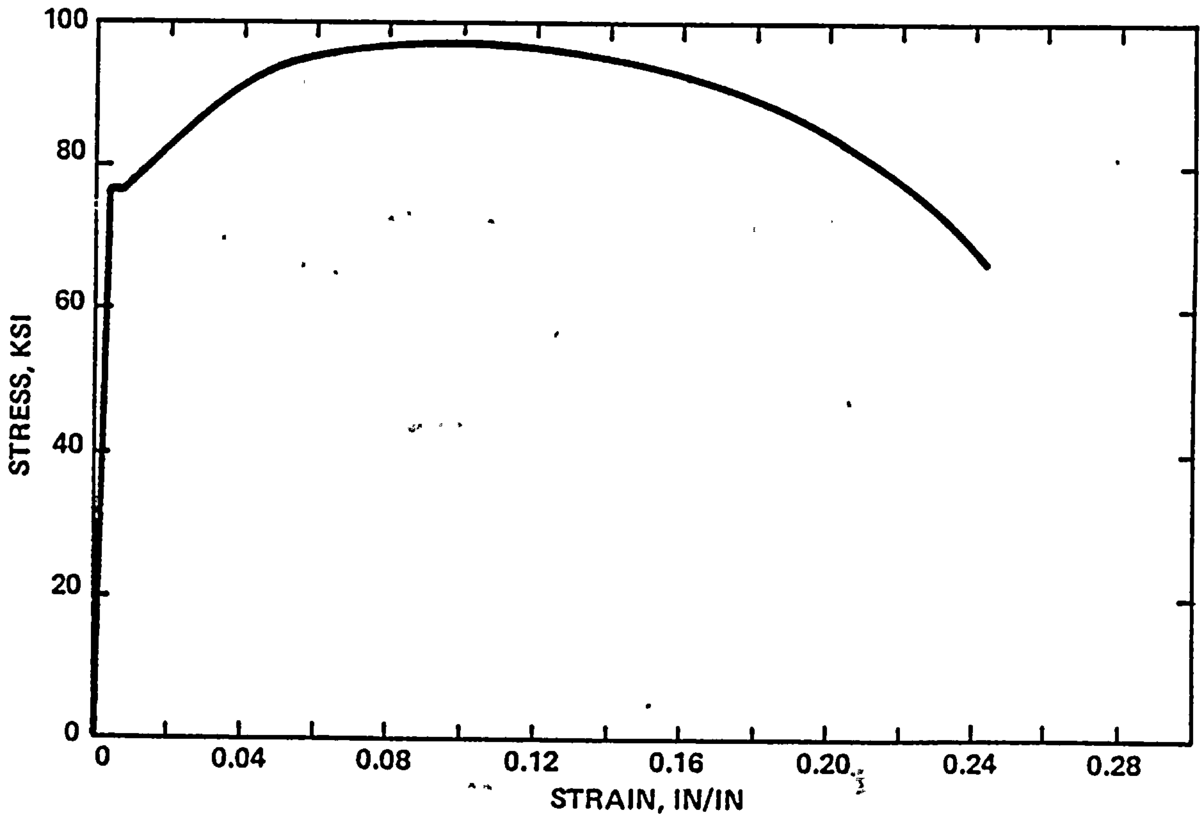

Figure V-16 STRESS-STRAIN RECORD, BASE METAL PLATE C-8-2 SPECIMEN No. 1JY, TEST TEMPERATURE 250°F

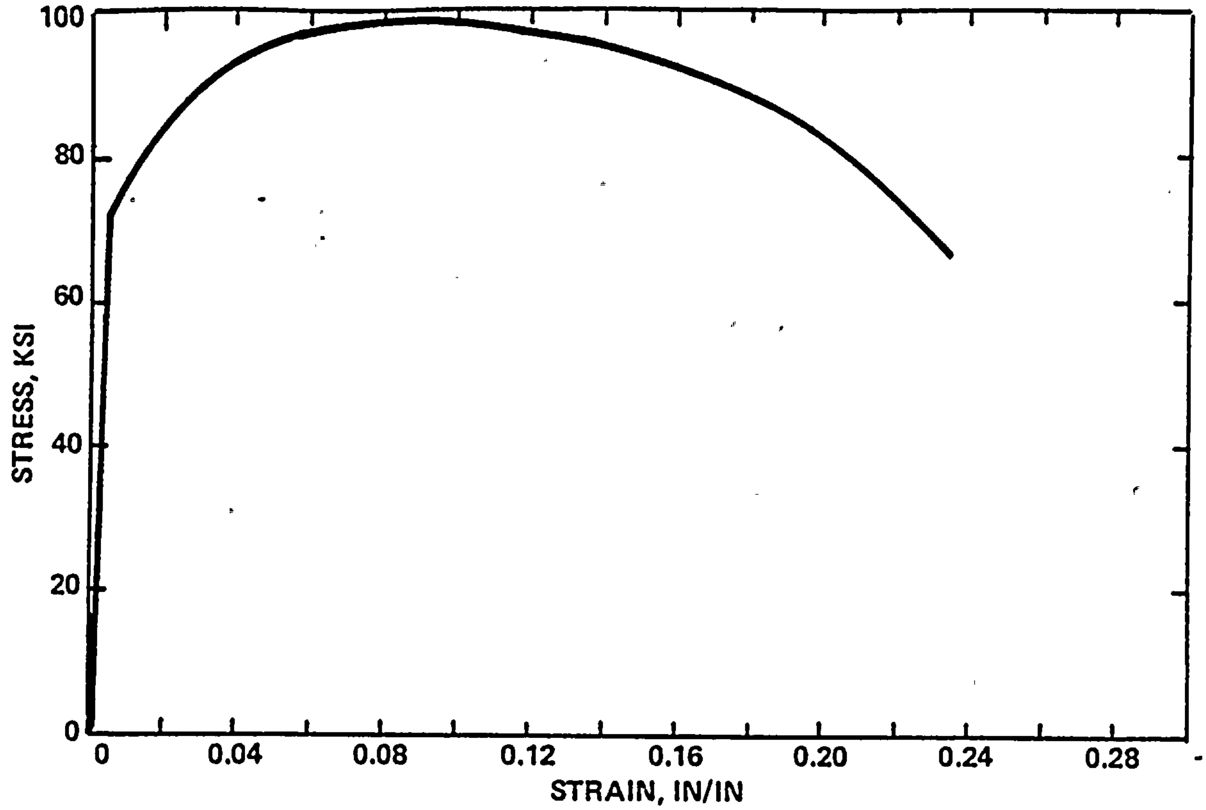

Figure V-17 STRESS-STRAIN RECORD, BASE METAL PLATE C-8-2
SPECIMEN No. 1KC, TEST TEMPERATURE 550° F

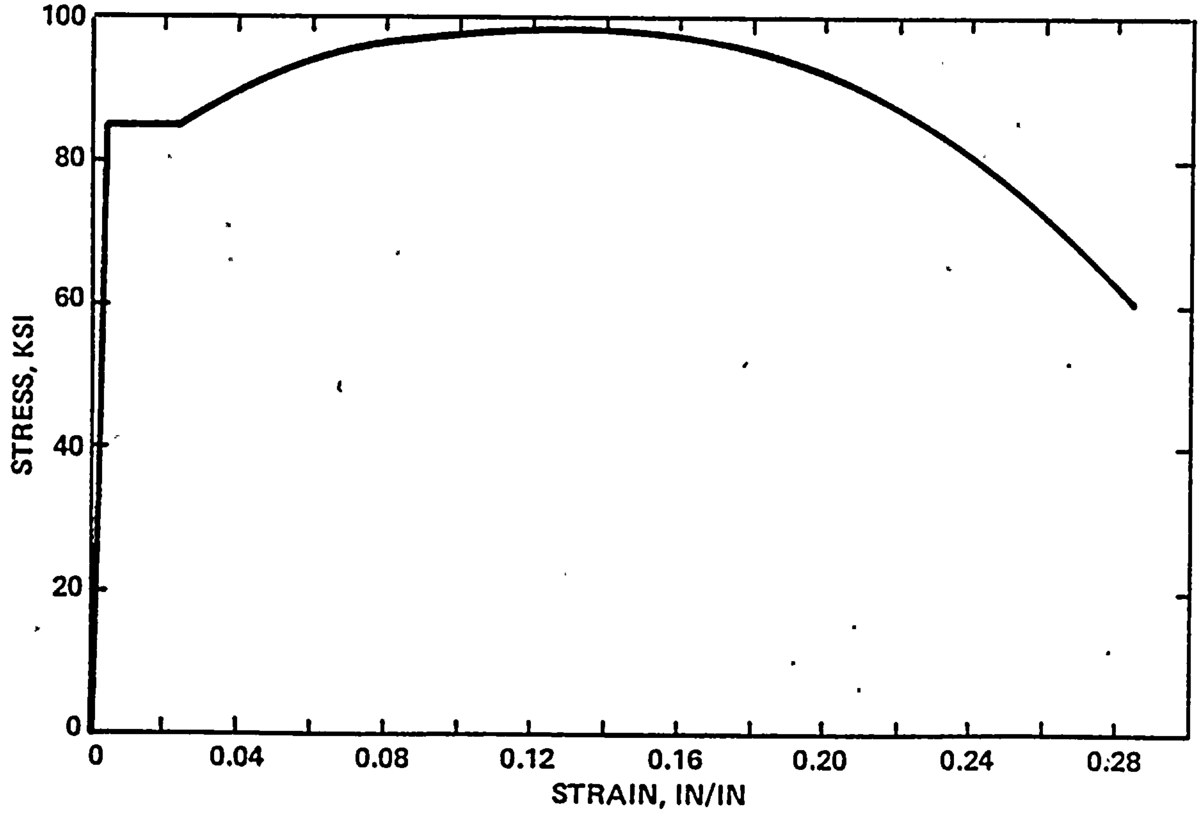

Figure V-18 STRESS-STRAIN RECORD, WELD METAL
SPECIMEN No. 3KC, TEST TEMPERATURE 72° F

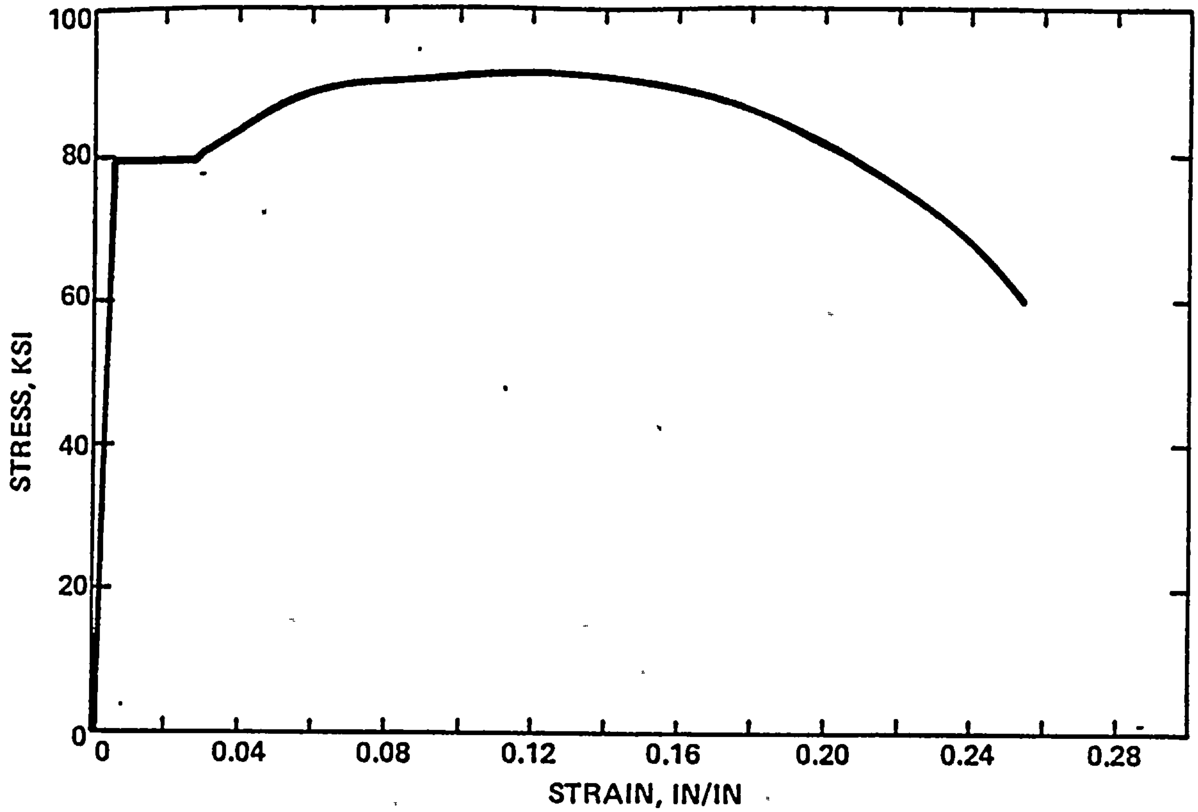

Figure V-19 STRESS-STRAIN RECORD, WELD METAL SPECIMEN No. 3JT, TEST TEMPERATURE 250° F

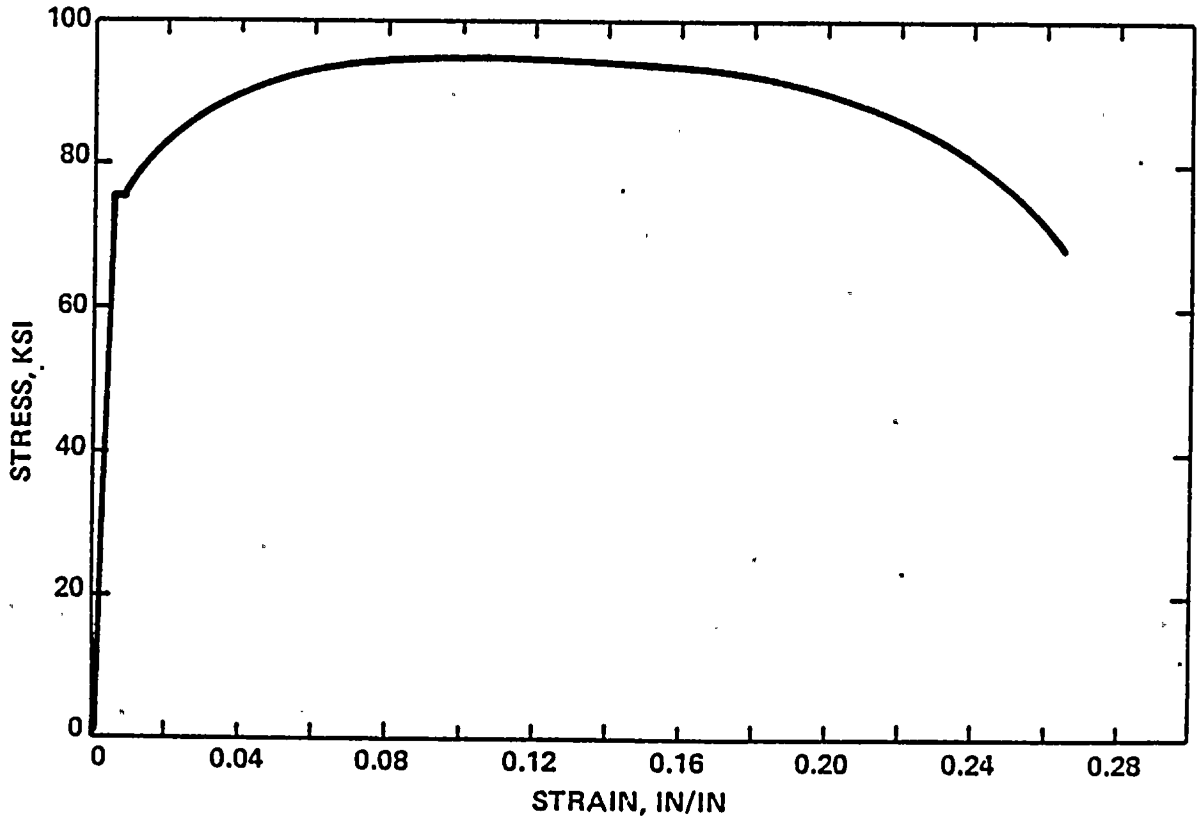

Figure V-20 STRESS-STRAIN RECORD, WELD METAL SPECIMEN No. 3L3, TEST TEMPERATURE 550° F

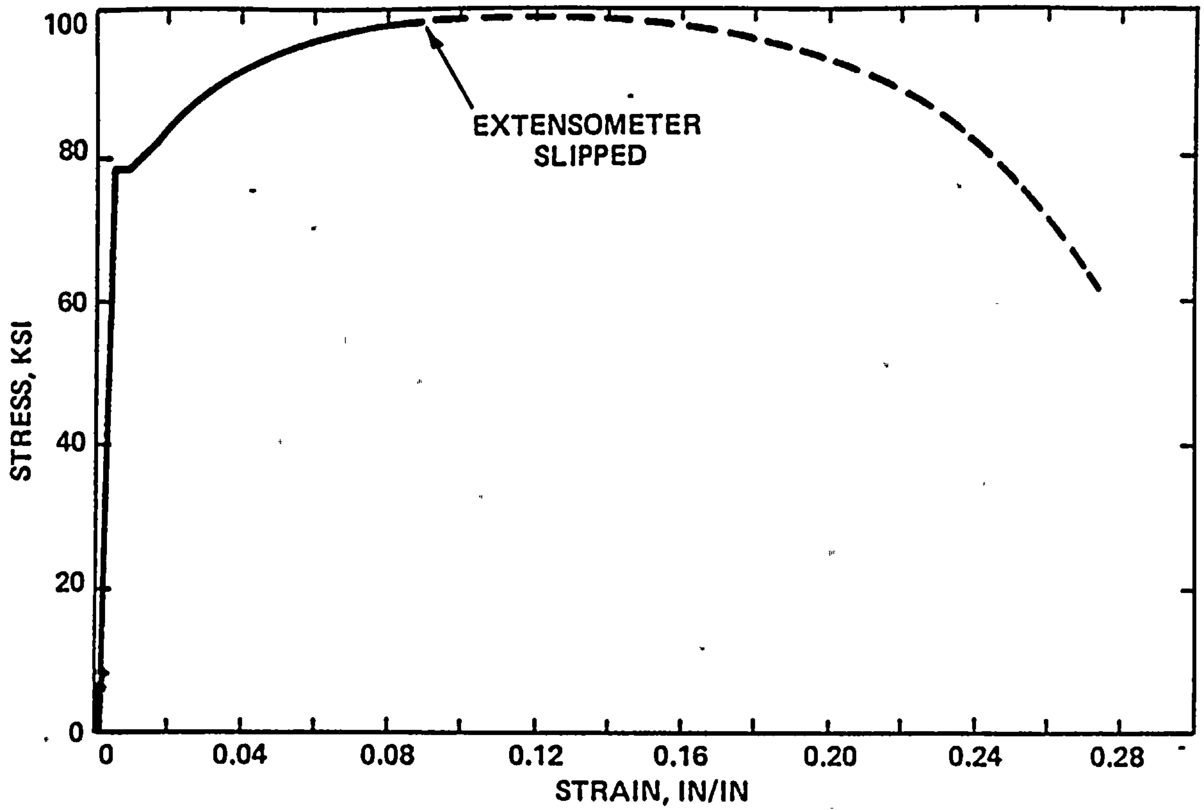

Figure V-21 STRESS-STRAIN RECORD, HEAT-AFFECTED ZONE SPECIMEN No. 4J5, TEST TEMPERATURE 72° F

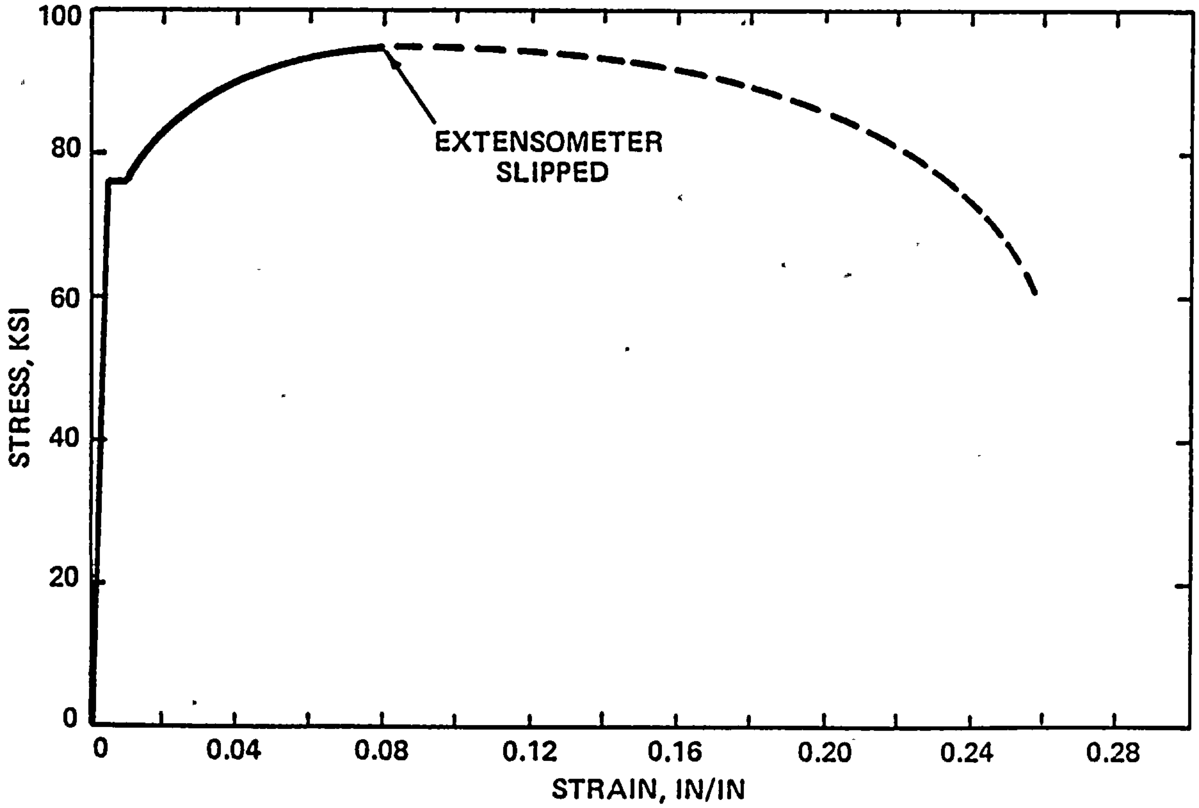

Figure V-22 STRESS-STRAIN RECORD, HEAT-AFFECTED ZONE SPECIMEN No. 4JC, TEST TEMPERATURE 250° F

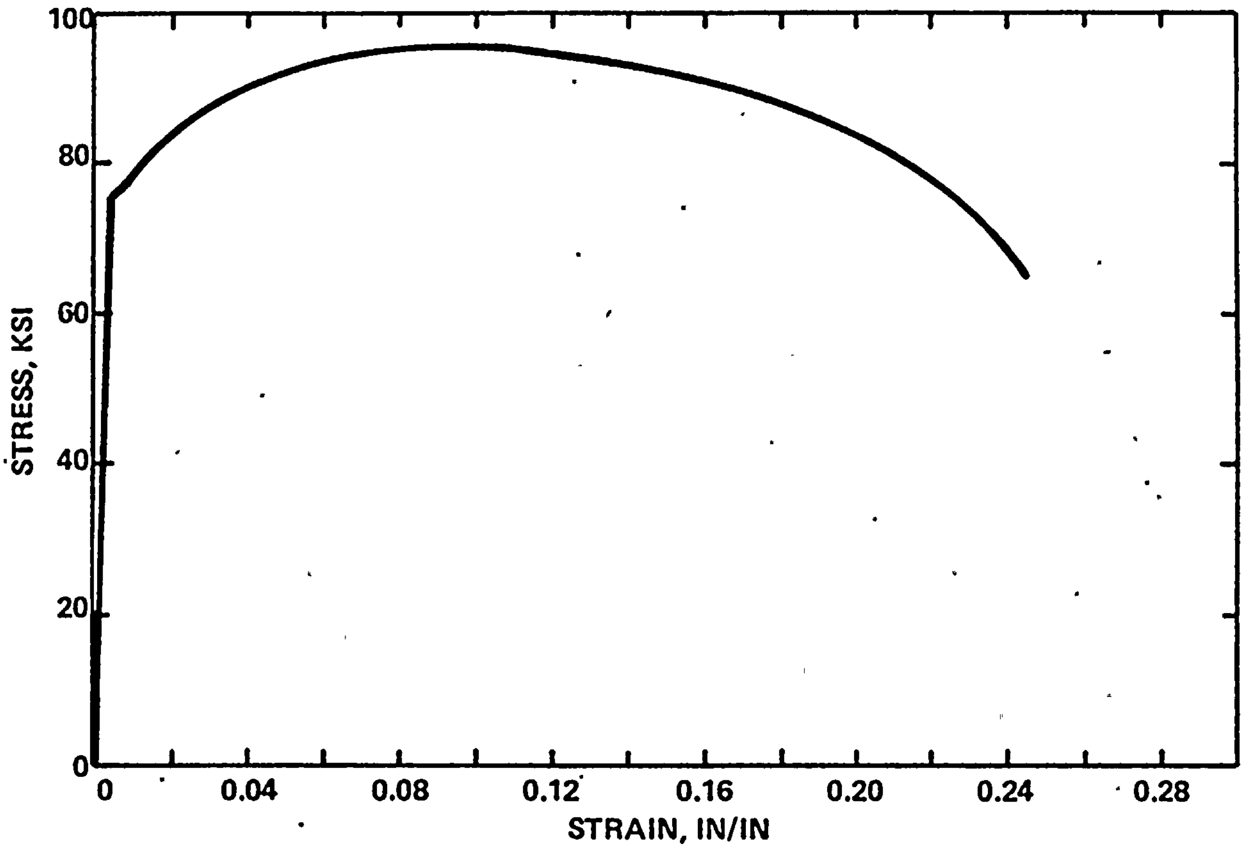

Figure V-23 STRESS-STRAIN RECORD, HEAT-AFFECTED ZONE SPECIMEN No. 4JP, TEST TEMPERATURE 550°F

FIGURE V-24

IRRADIATED TENSION SPECIMENS

Base Metal
Spec. 1KB, 72°F

Base Metal
Spec. 1JY, 250°F

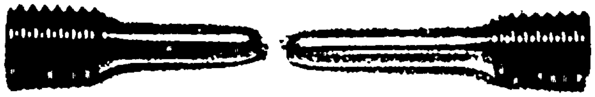

Base Metal
Spec. 1KC, 550°F

Weld Metal
Apec. 3KC, 72°F

Weld Metal
Spec. 3JT, 250°F

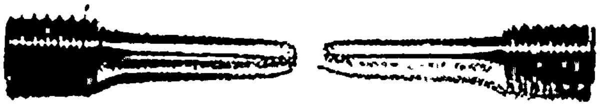

Weld Metal
Spec. 3L3, 550°F

HAZ
Spec. 4J5, 72°F

HAZ
Spec. 4JC, 250°F

HAZ
Spec. 4JP, 550°F

TABLE V-11
CHARPY V-NOTCH IMPACT RESULTS
IRRADIATED BASE METAL (TRANSVERSE)
(PLATE C-8-2)

Specimen Identification Number	Test Temperature (^{o}F)	Impact Energy (Ft-lbs.)	Lateral Expansion (mils)	Fracture Appearance (% Shear)
22A	0	5.5	0	0
23A	40	22.5	13	0
22D	60	19.5	17	10
237	60	27	19	10
232	80	34.5	29	20
22J	80	35	26	10
23L	120	38	32	20
227	160	52	40	30
23K	160	54.5	44	40
22B	210	76	56	80
22E	250	67	56	70
231	250	77.5	66	100

TABLE V-12

CHARPY V-NOTCH IMPACT RESULTS

IRRADIATED BASE METAL (LONGITUDINAL)

(PLATE C-8-2)

Specimen Identification Number	Test Temperature (^{o}F)	Impact Energy (Ft-lbs.)	Lateral Expansion (mils)	Fracture Appearance (% Shear)
12T	0	6	1	0
12A	40	23	16	0
114	60	25	20	10
131	60	25.5	17	10
113	80	32.5	23	10
134	80	33	22	10
116	120	44	35	30
132	160	69	52	40
127	200	107.5	77	100
12U	250	87	66	80
115	250	110	85	100
12L	300	102	76	100

TABLE V-13

CHARPY V-NOTCH IMPACT RESULTS

IRRADIATED WELD METAL

Specimen Identification Number	Test Temperature (^{o}F)	Impact Energy (Ft-lbs.)	Lateral Expansion (mils)	Fracture Appearance (% Shear)
34C	-40	6.5	0	0
36E	0	15	11	10
35B	20	55	28	30
33E	40	28.5	23	20
347	40	51	37	20
371	60	61	51	60
36P	60	62.5	50	50
35P	80	82	63	70
341	120	89	70	80
31A	160	102.5	81	100
323	200	95	72	100
33Y	200	102.5	77	100

TABLE V-14
CHARPY V-NOTCH IMPACT RESULTS
IRRADIATED HAZ METAL
(BASE METAL PLATE C-8-2)

Specimen Identification Number	Test Temperature (^oF)	Impact Energy (Ft-lbs.)	Lateral Expansion (mils)	Fracture Appearance (% Shear)
42D	-40	25	15	10
42E	-20	38.5	25	30
42B	-20	41	39	40
426	0	61	38	40
41Y	40	68	42	50
42P	40	72.5	48	70
42A	80	48	34	30
425	100	90	66	80
427	120	94	66	80
42C	160	72.5	49	70
41U	210	109	76	100
42T	210	118.5	72	100

Figure V-25
CHARPY IMPACT ENERGY, BASE METAL PLATE C-8-2 (TRANSVERSE)

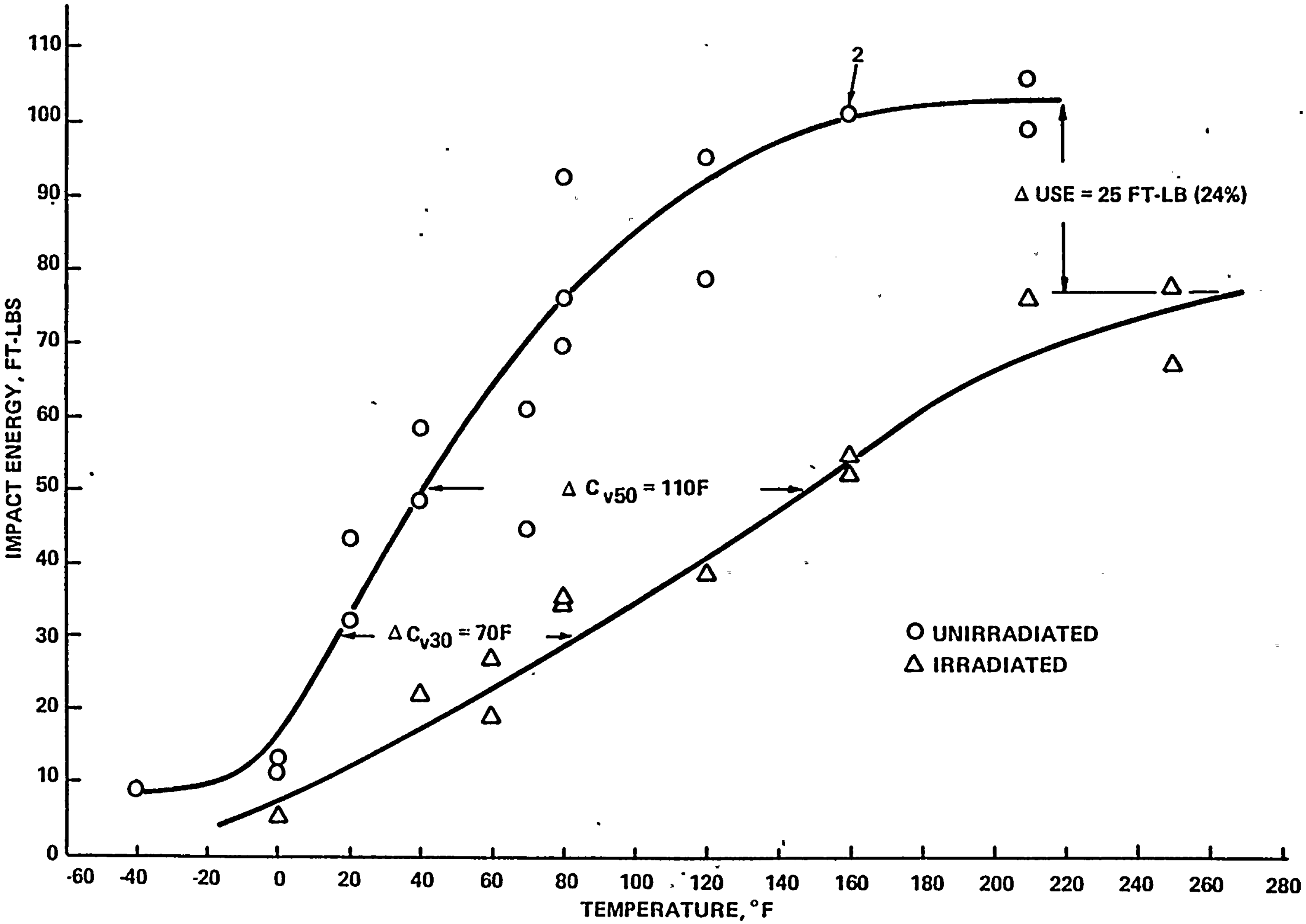

Figure V-26
CHARPY LATERAL EXPANSION, BASE METAL PLATE C-8-2 (TRANSVERSE)

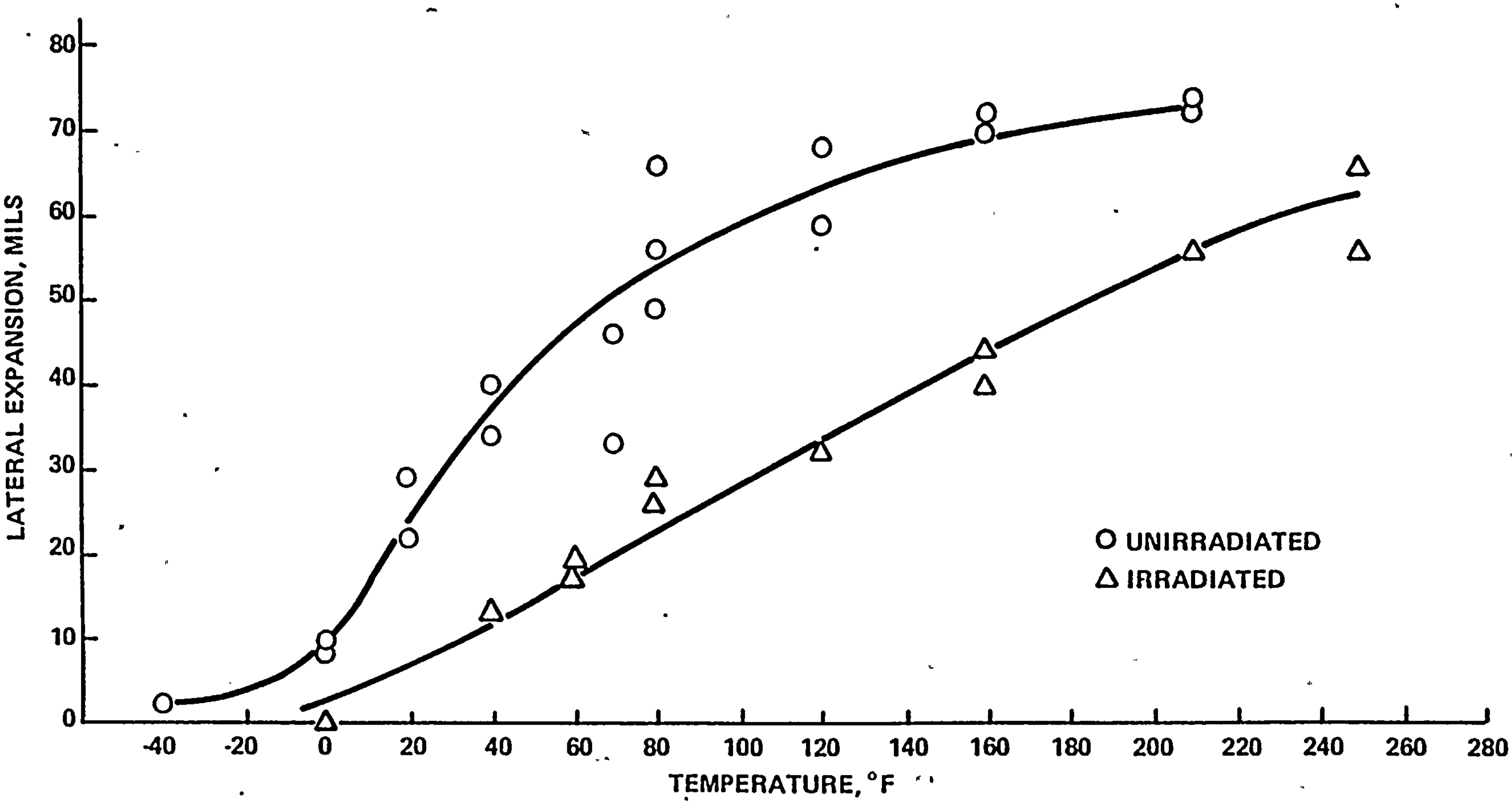

Figure V-27
CHARPY SHEAR FRACTURE, BASE METAL PLATE C-8-2 (TRANSVERSE)

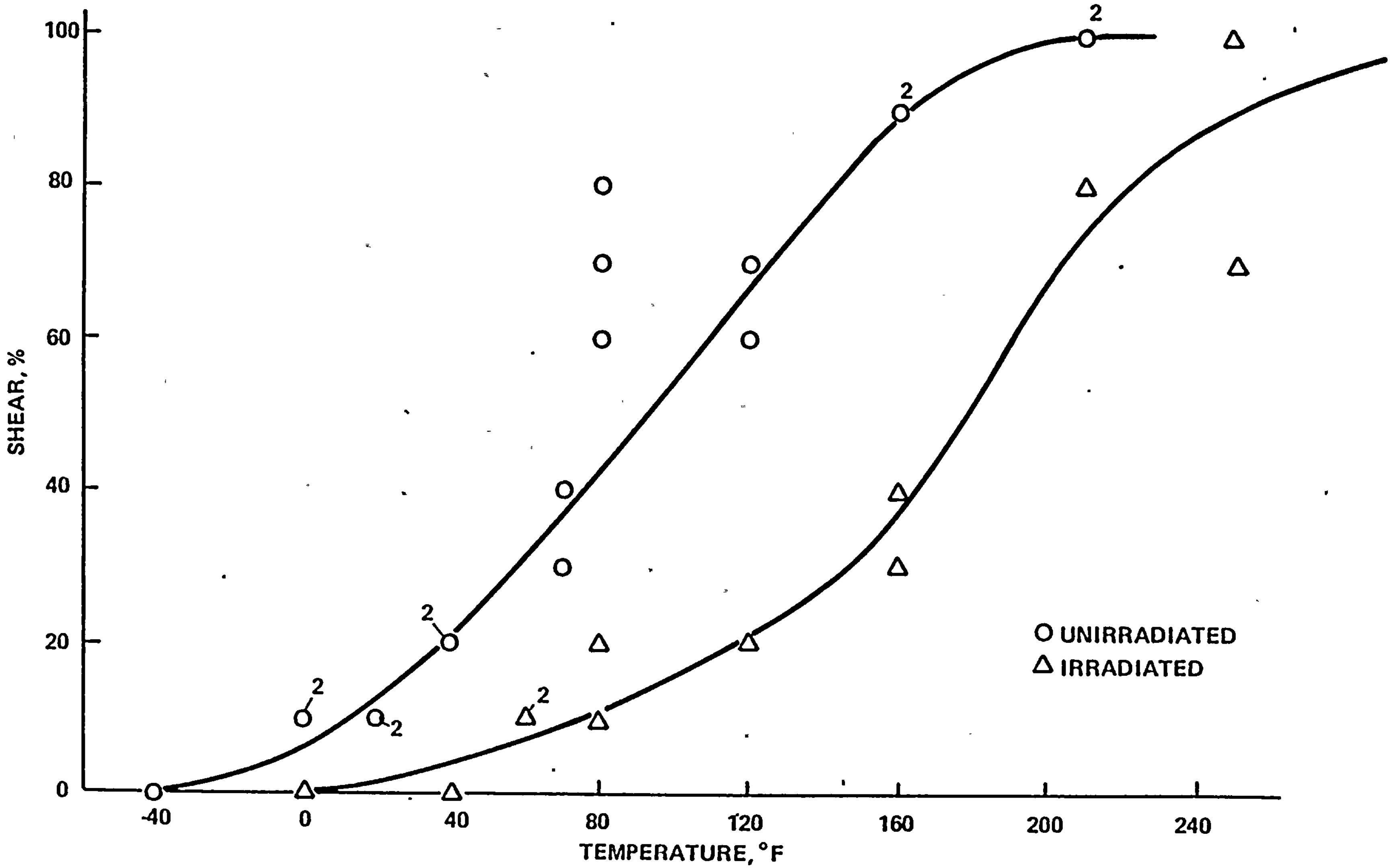

Figure V-28
CHARPY IMPACT ENERGY, BASE METAL PLATE C-8-2 (LONGITUDINAL)

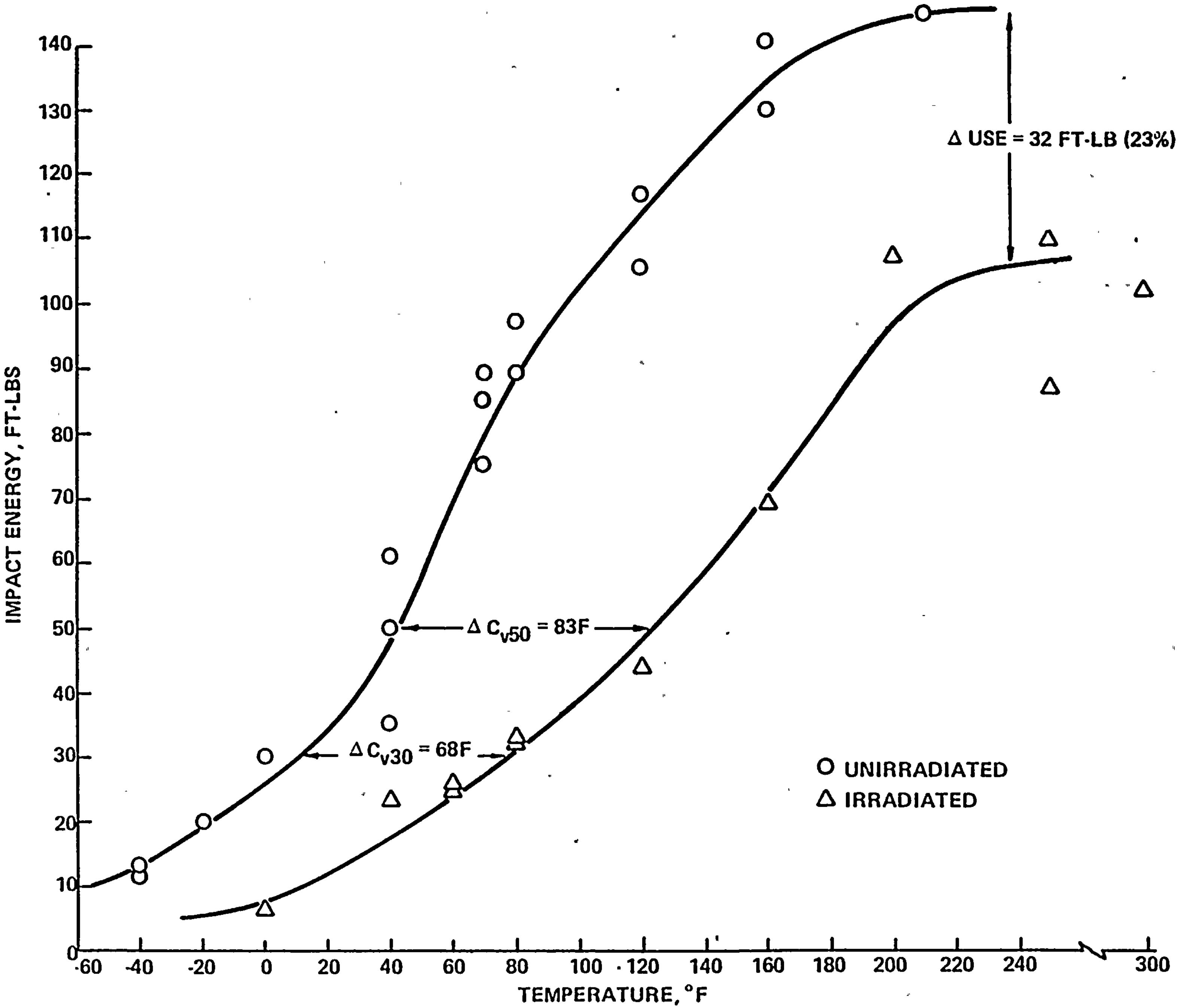

Figure V-29
CHARPY LATERAL EXPANSION, BASE METAL PLATE C-8-2 (LONGITUDINAL)

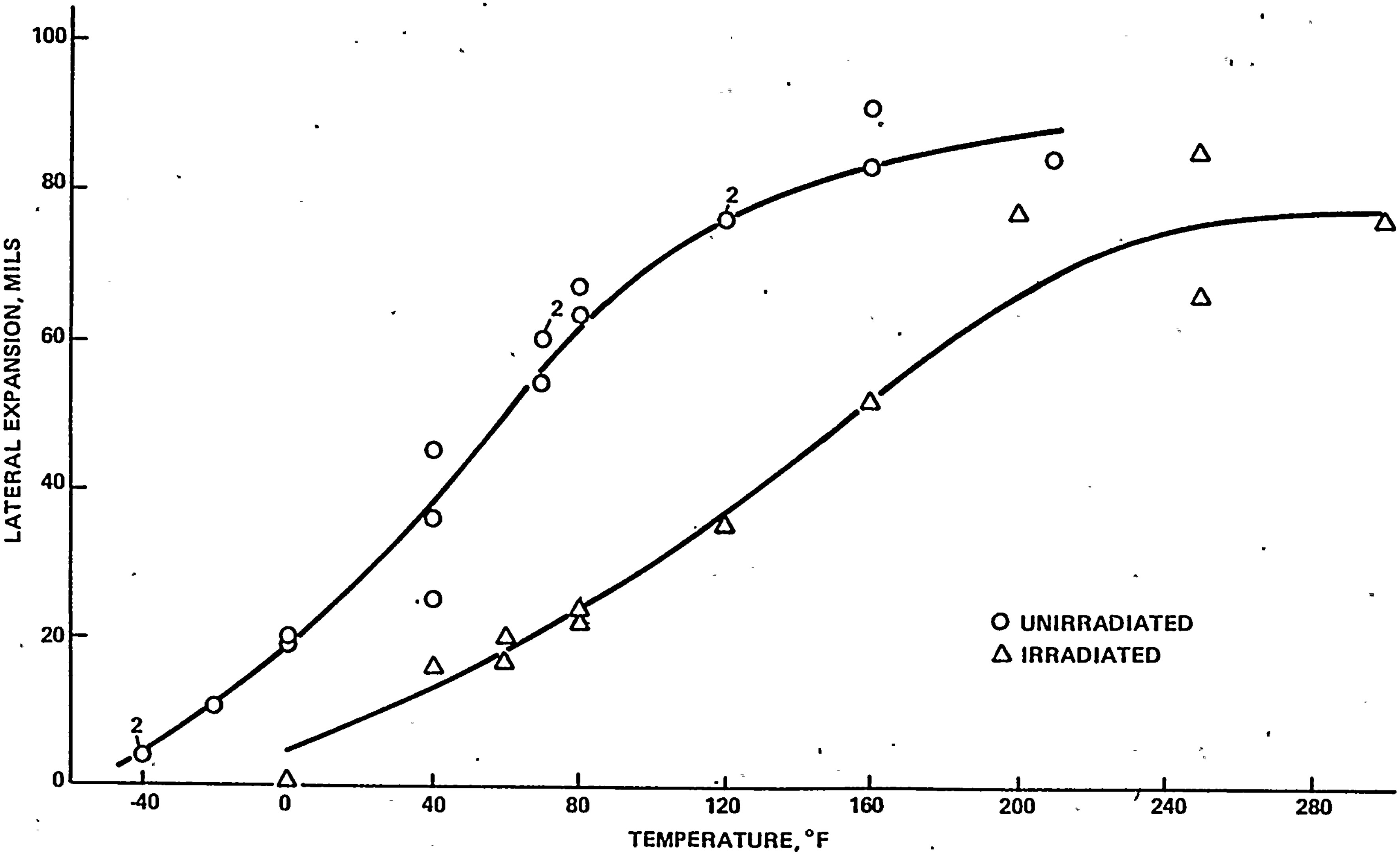

Figure V-30
CHARPY SHEAR FRACTURE, BASE METAL PLATE C-8-2 (LONGITUDINAL)

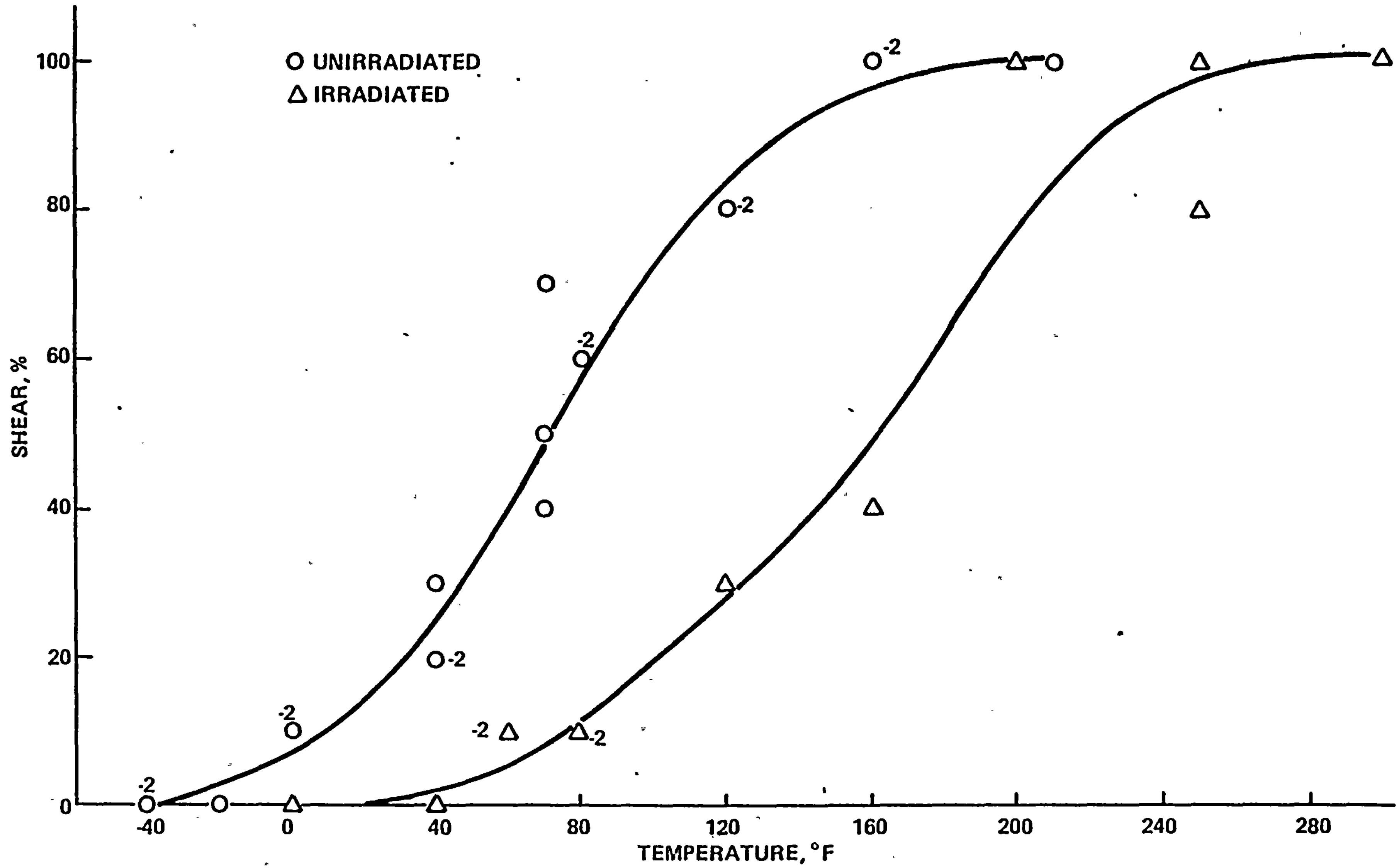

Figure V-31
CHARPY IMPACT ENERGY, WELD METAL

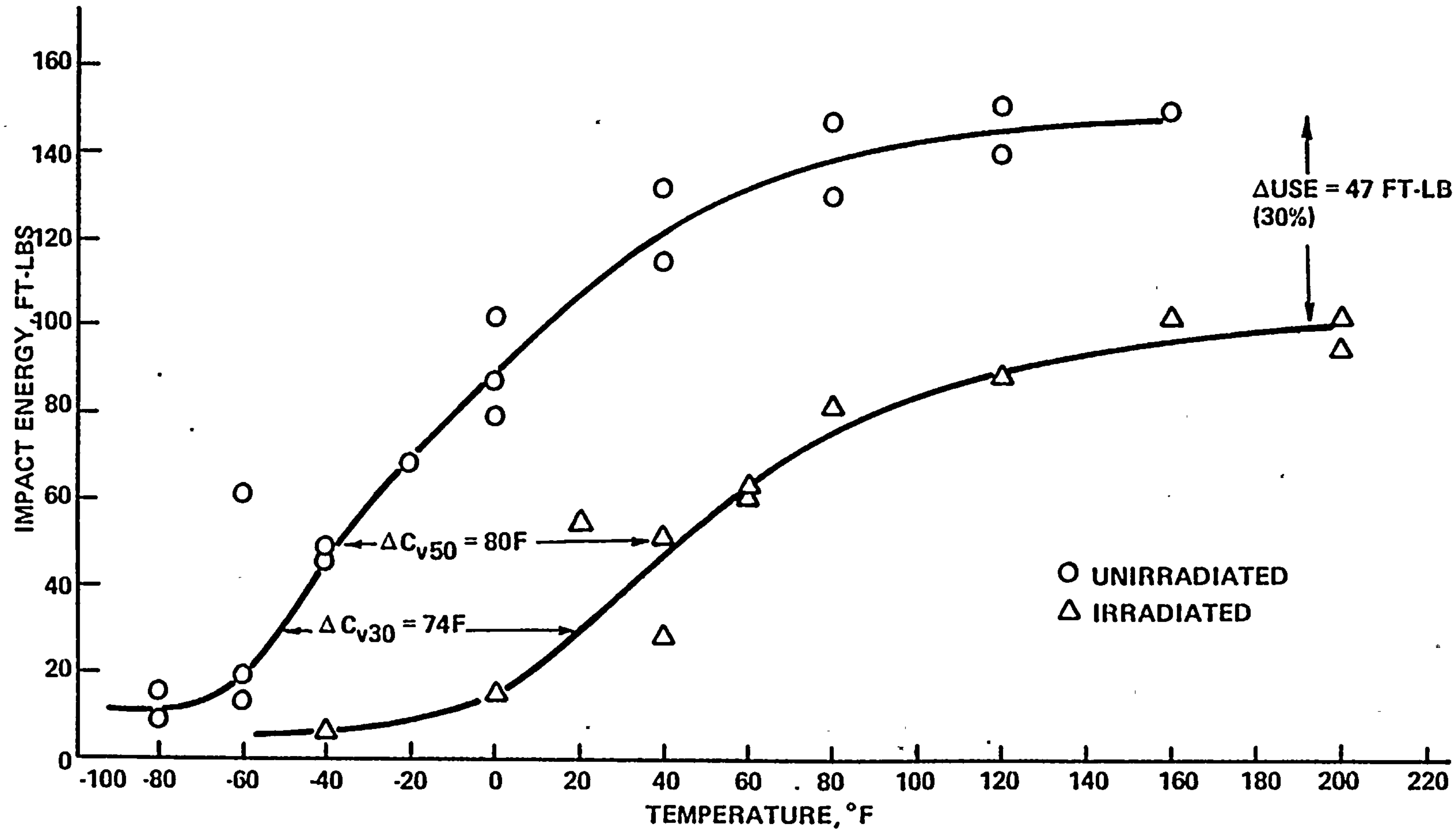

Figure V-32
CHARPY LATERAL EXPANSION, WELD METAL

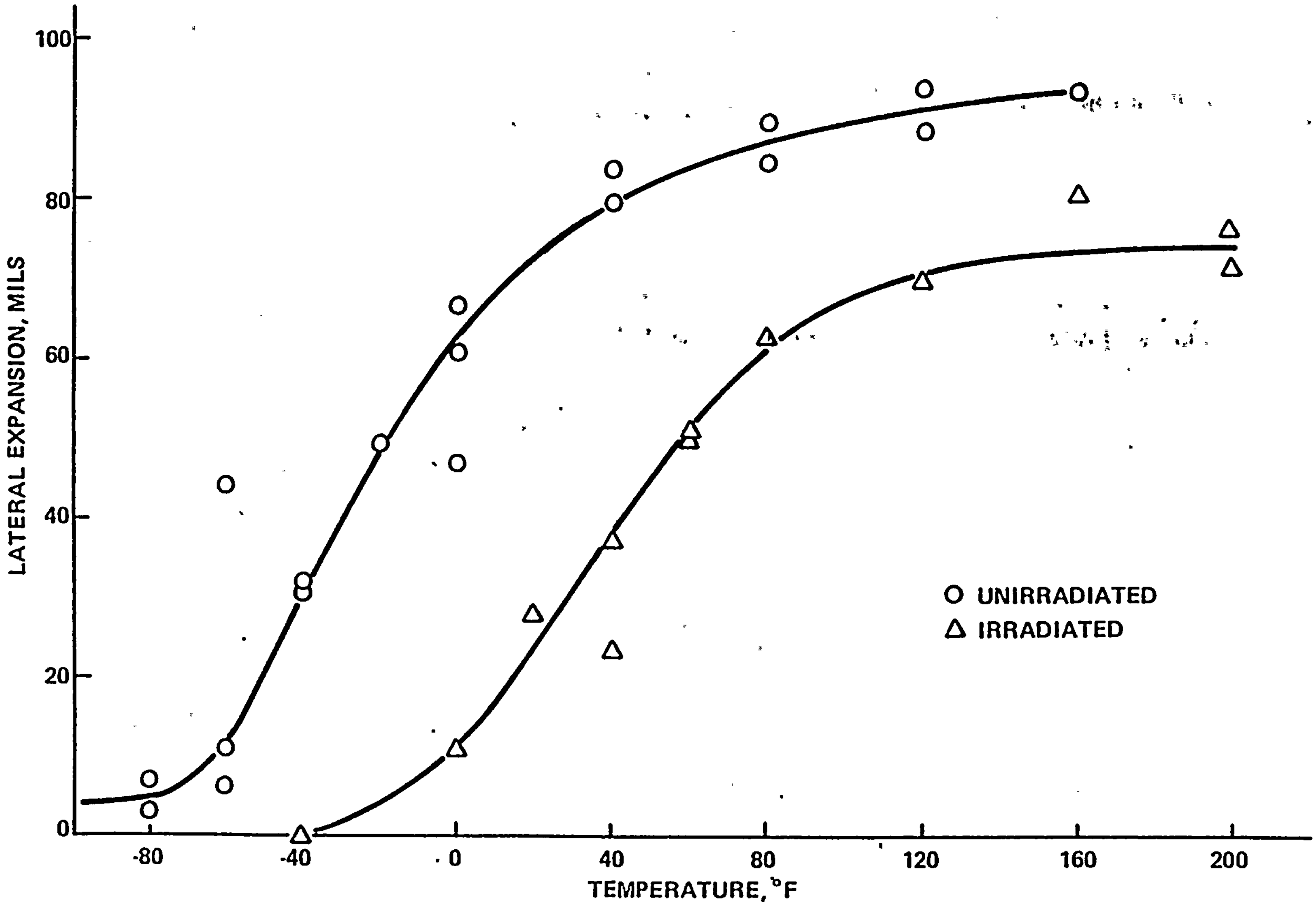

Figure V-33
CHARPY SHEAR FRACTURE, WELD METAL

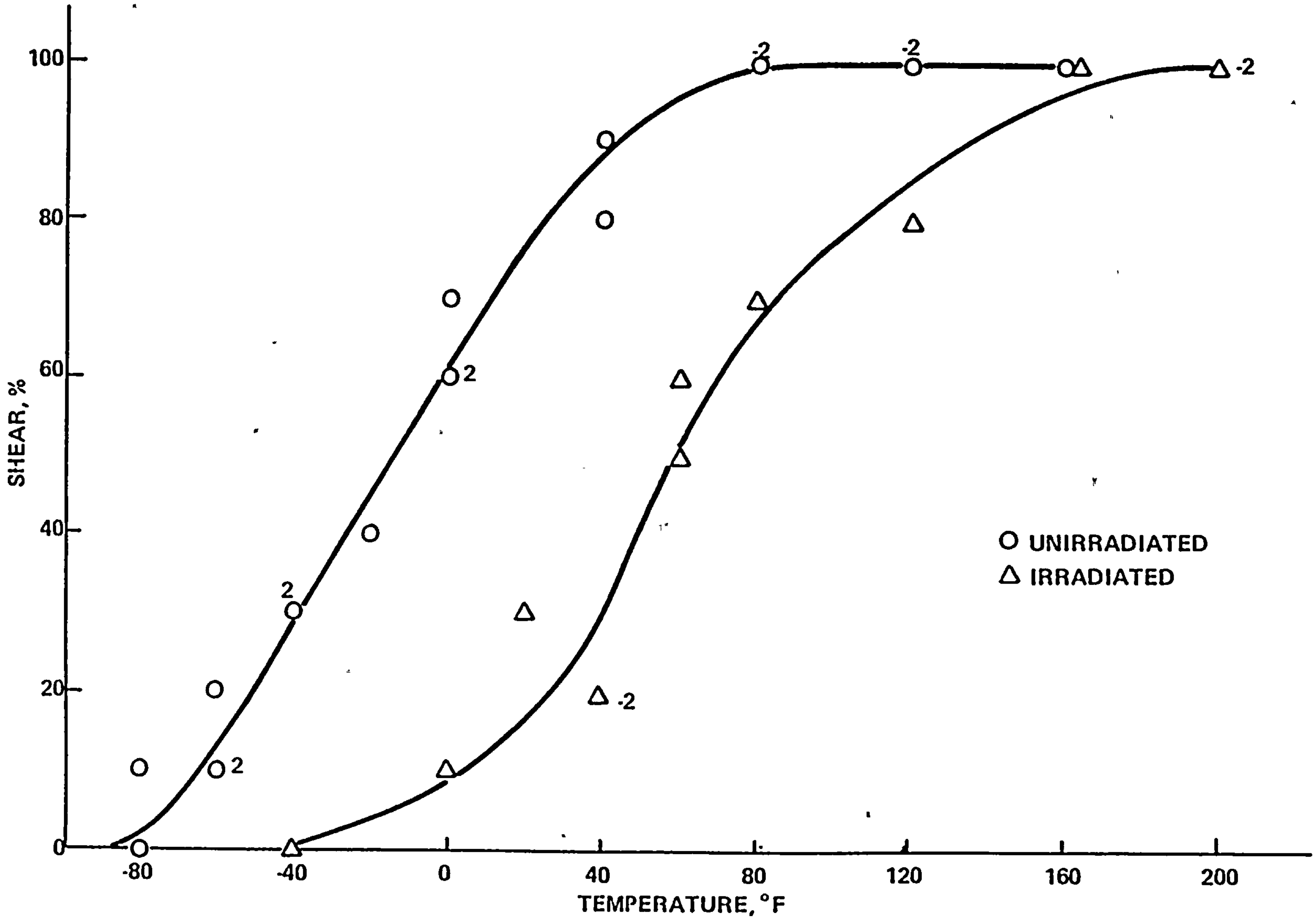

Figure V-34
CHARPY IMPACT ENERGY, HEAT-AFFECTED ZONE

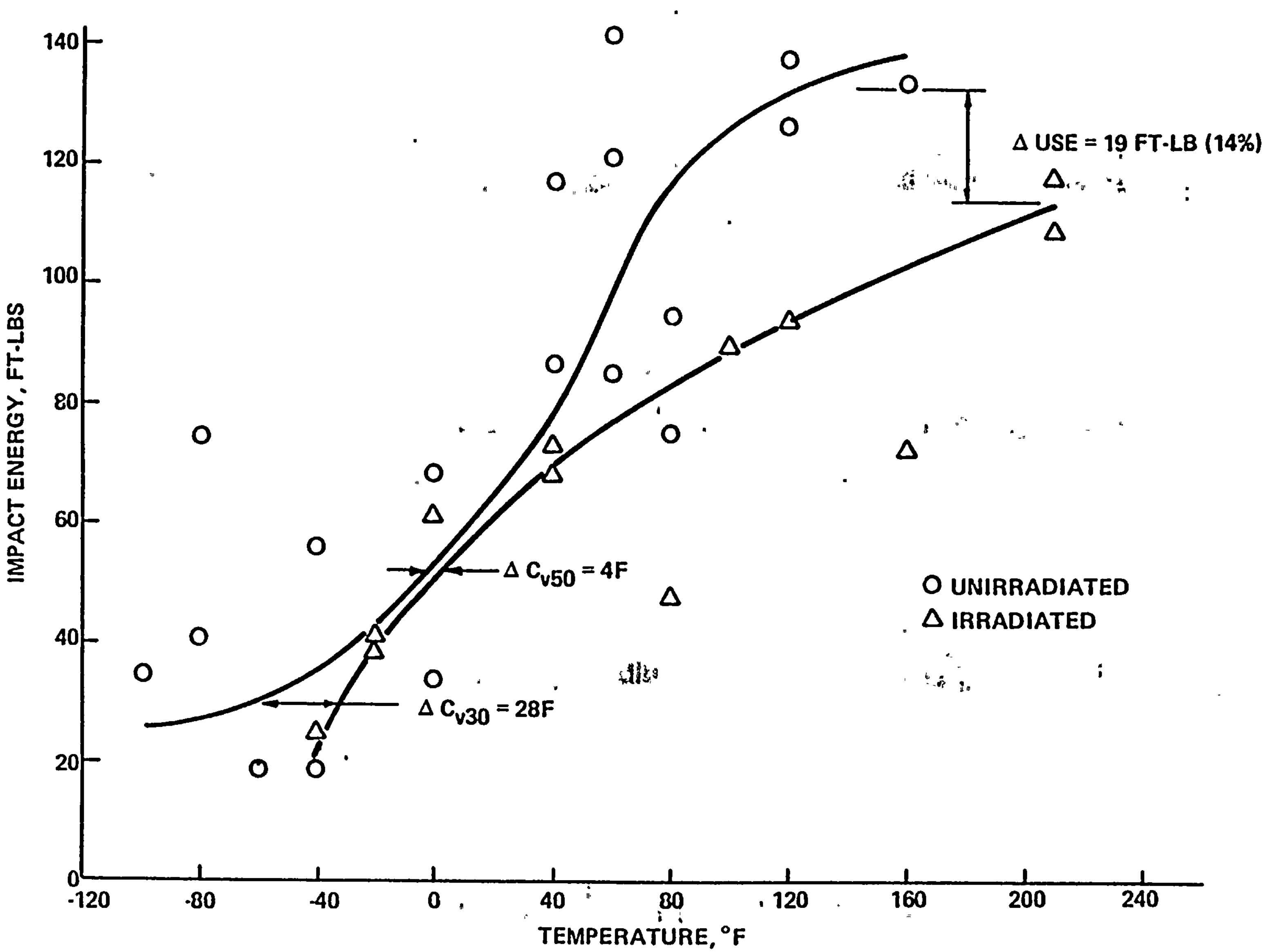

Figure V-35
CHARPY LATERAL EXPANSION, HEAT-AFFECTED ZONE

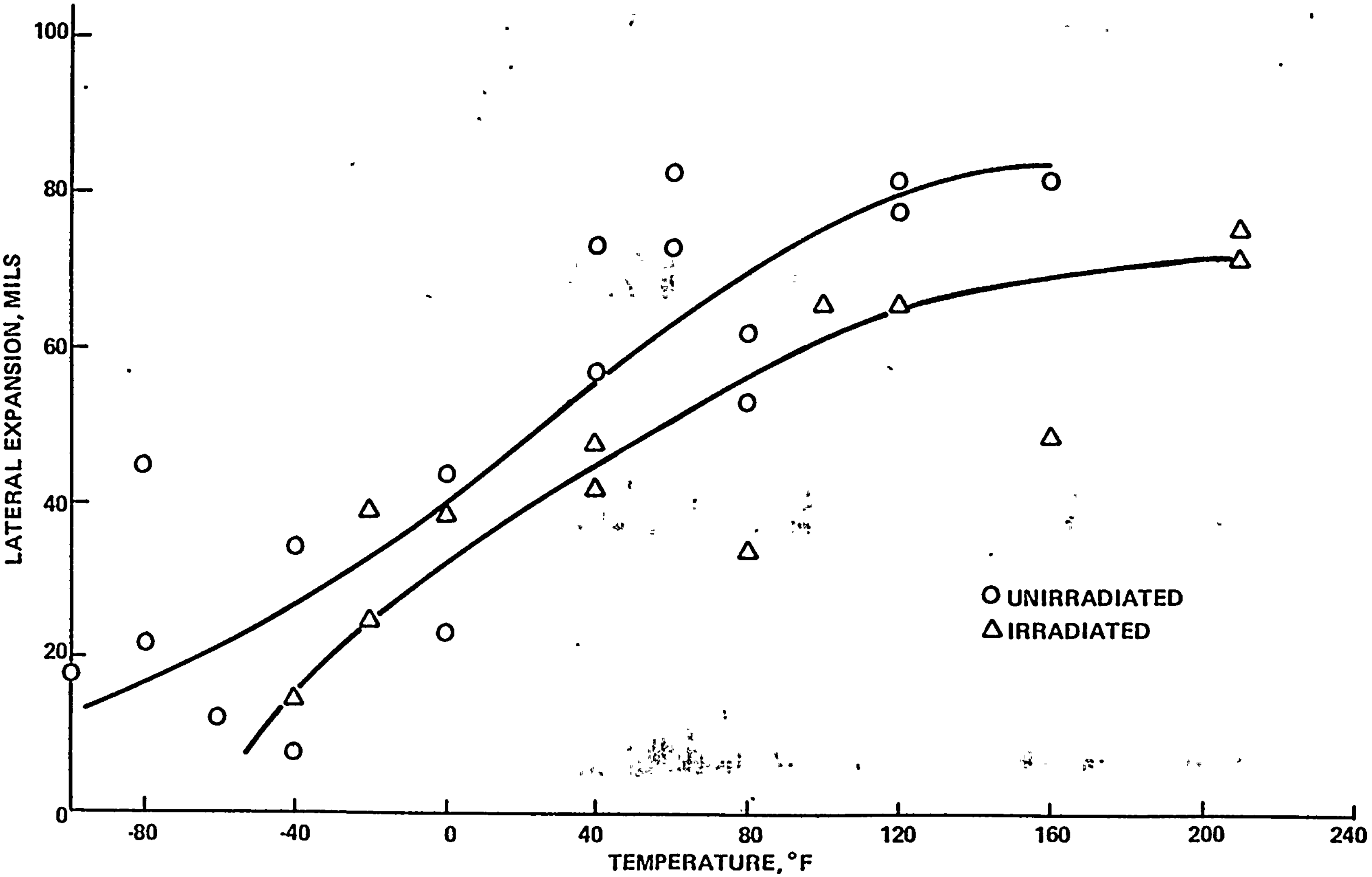

Figure V-36
CHARPY SHEAR FRACTURE, HEAT-AFFECTED ZONE

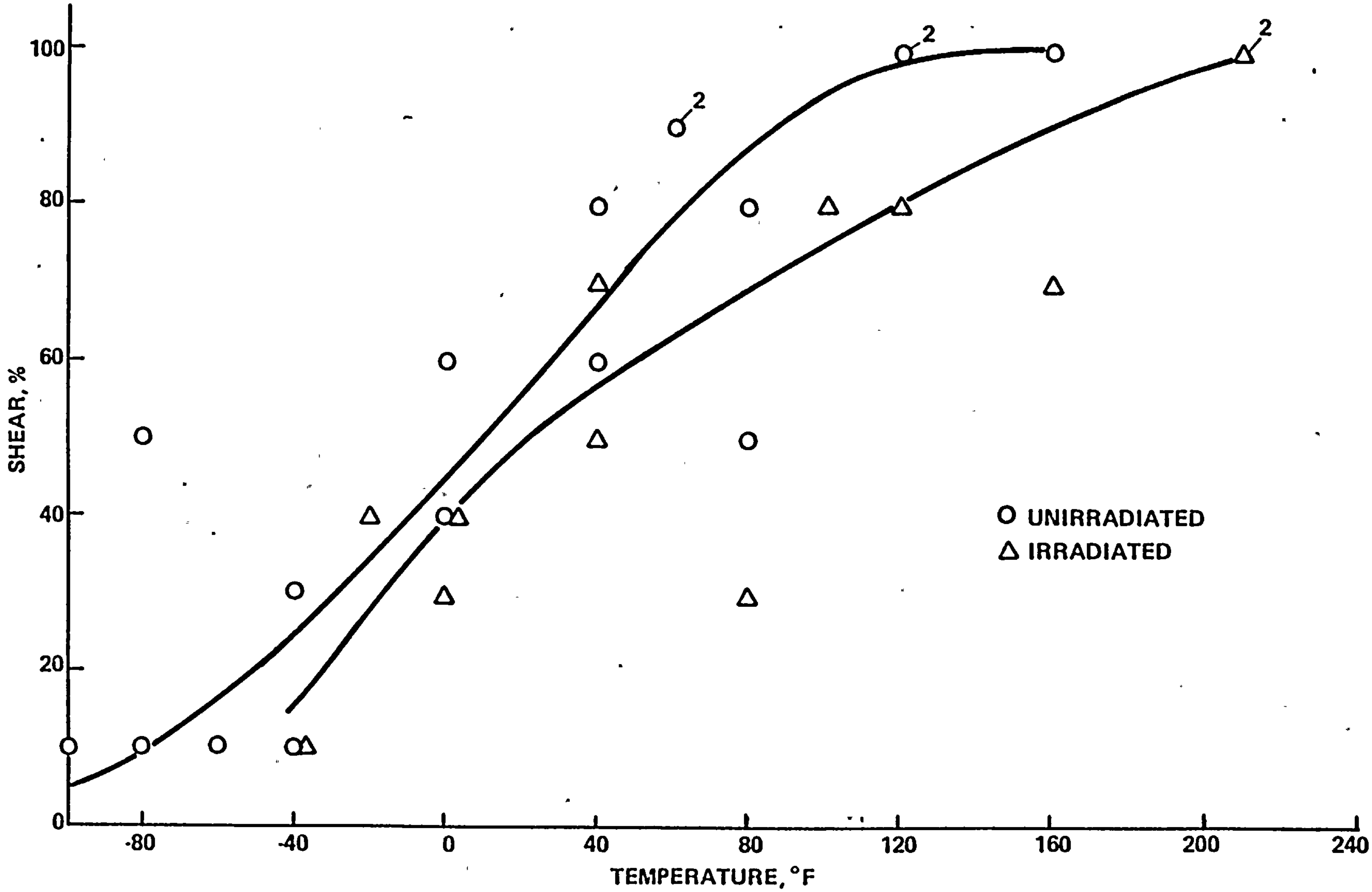

FIGURE V-37

FRACTURE SURFACES OF
CHARPY V-NOTCH IMPACT TEST SPECIMENS
BASE METAL (TRANSVERSE)

 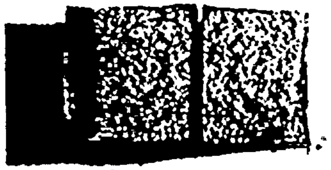 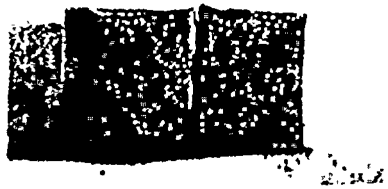

Specimen No.:	22A	23A	22D
Test Temperature.:	0°F	40°F	60°F

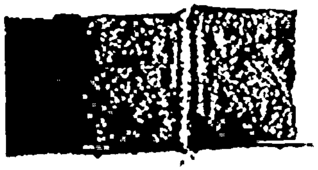 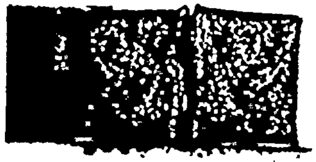 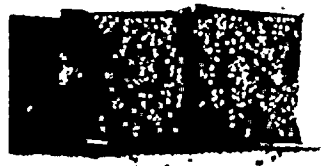

Specimen No.:	237	232	22J
Test Temperature:	60°F	80°F	80°F

  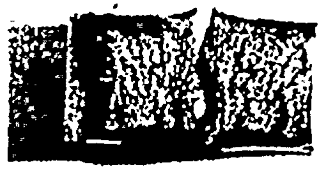

Specimen No.:	23L	227	23K
Test Temperature:	120°F	160°F	160°F

  

Specimen No.:	22B	22E	231
Test Temperature:	210°F	250°F	250°F

FIGURE V-38

FRACTURE SURFACES OF
CHARPY V-NOTCH IMPACT TEST SPECIMENS
BASE METAL (LONGITUDINAL)



Specimen No.:	12T	12A	114
Test Temperature:	0°F	40°F	60°F

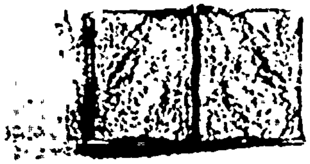
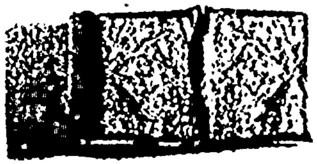
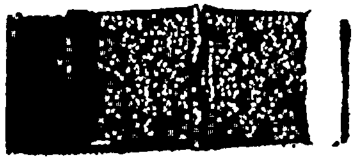

Specimen No.:	131	113	134
Test Temperature:	60°F	80°F	80°F



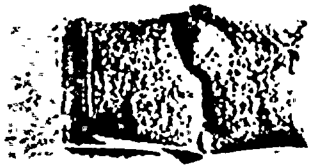

Specimen No.:	116	132	127
Test Temperature:	120°F	160°F	200°F

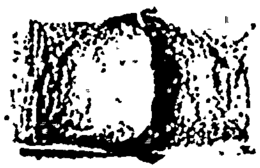

Specimen No.:	12U	115	12L
Test Temperature:	250°F	250°F	300°F

FIGURE V-39

FRACTURE SURFACES OF CHARPY V-NOTCH IMPACT TEST SPECIMENS WELD METAL

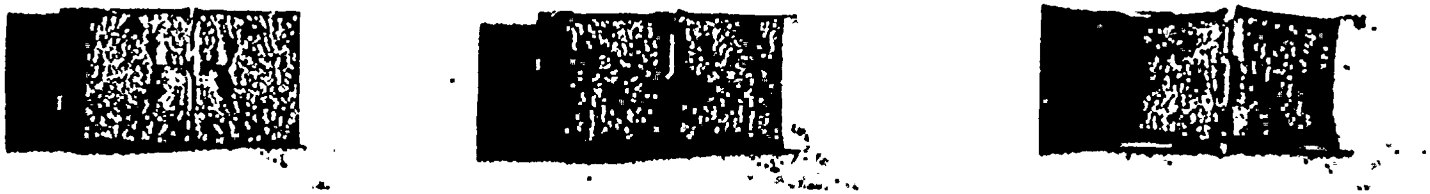

Specimen No.:	34C	36E	35B
Test Temperature:	-40^{o}F	0^{o}F	20^{o}F

Specimen No.:	33E	347	371
Test Temperature:	40^{o}F	40^{o}F	60^{o}F

Specimen No.:	36P	35P	341
Test Temperature:	60^{o}F	80^{o}F	120^{o}F

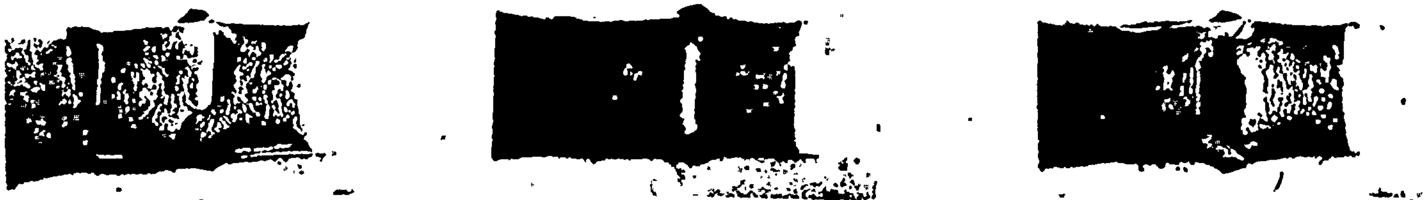

Specimen No.:	31A	323	33Y
Test Temperature:	160^{o}F	200^{o}F	200^{o}F

FIGURE V-40

FRACTURE SURFACES OF
CHARPY V-NOTCH IMPACT TEST SPECIMENS
HEAT-AFFECTED-ZONE

Specimen No.:	42D	42E	42B
Test Temperature:	-40°F	-20°F	-20°F

Specimen No.:	426	41Y	42P
Test Temperature:	0°F	40°F	40°F

Specimen No.:	42A	425	427
Test Temperature:	80°F	100°F	120°F

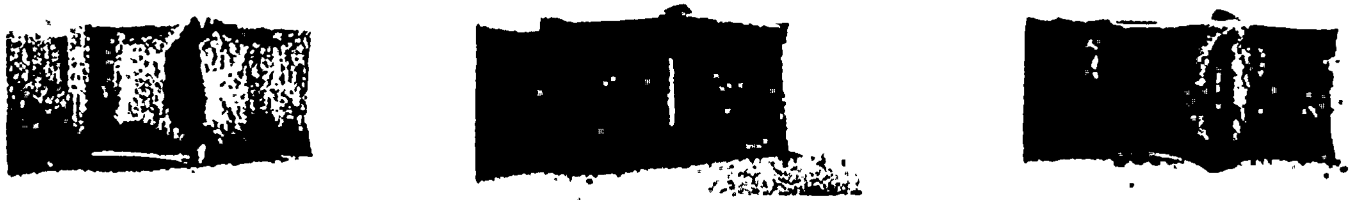

Specimen No.:	42C	41U	42T
Test Temperature:	160°F	210°F	210°F

VI. DATA ANALYSIS

A. Irradiation Exposure

The W-97 surveillance capsule was removed from the St. Lucie Unit 1 reactor vessel following plant shutdown on February 26, 1983. The surveillance specimens were irradiated at approximately 550^{0}F; the temperature variation along the length of the capsule was negligible based on the similarity in appearance of the three 558^{0}F monitors.

The surveillance capsule was exposed to a maximum neutron flux of 3.7×10^{10} n/cm^2-s (E >1.0 MeV). The highest flux was calculated for the middle compartment (7241). The neutron flux in the top compartment (7214) and bottom compartment (7273) was approximately 3.6×10^{10} n/cm^2-s and 3.5×10^{10} n/cm^2-s, respectively, indicating a total axial variation of 6%. The maximum surveillance capsule fluence after 4.67 effective full power years (EFPY) operation at 2700 Mwt was, therefore, 5.5×10^{18} n/cm^2 (E>1.0 MeV).

For the first five cycles, the average lead factors between the neutron fluence at the surveillance capsule and the maximum azimuthal position on the reactor vessel were calculated to be 1.41 at the vessel-clad interface, 2.62 at the quarter thickness location in the vessel, and 12.8 at the three-quarter thickness location.* The maximum neutron flux at the vessel-clad interface was, therefore, 2.7×10^{10} n/cm^2-s. The predicted end-of-life fluence at the vessel-clad interface is 3.5×10^{19} n/cm^2 ($\pm$30%); the Cycle 6 fuel management strategy was used as the basis for extrapolation beyond Cycle 5 to end-of-life for operation without the thermal shield.

*Lead factors subsequent to Cycle 5 will be lower due to a difference in fuel management strategy.

B. Chemical Analysis

X-ray fluorescence analysis of the irradiated base metal and weld metal Charpy specimens (Table V-8) demonstrated that the encapsulated surveillance specimens had the same chemical composition as that originally reported (Table III-4). The base metal chemistry was uniform throughout the surveillance plate. The weld metal chemistry, however, ranged from 0.22 to 0.32 w/o copper for the irradiated specimens and 0.20 to 0.44 w/o copper for the unirradiated specimens. From Figure V-14, the specimens exhibiting 0.32 w/o copper or greater (specimen numbers 31A and 323) came from one end of the surveillance weld, whereas the balance of the weld exhibited lower copper (0.20 to 0.22 w/o). None of the remaining six elements analyzed showed a significant variation indicating that the differences in copper content were a function of the weld wire copper coating thickness.

C. Uniaxial Tension Properties

Radiation induced changes in uniaxial tension properties of the St. Lucie Unit 1 surveillance materials were determined from a comparison of Tables V-9 and V-10. The yield strength and ultimate strength increased an average of 14% following irradiation to 5.5×10^{18} n/cm^2. Uniform and total elongation changed very little following irradiation, while reduction in area decreased about 7% (excluding HAZ material). Fracture stress (fracture load divided by final cross sectional area) was not changed significantly by irradiation. In general, property changes were similar for each of the materials despite the large difference in copper content between base metal and weld metal.

Post-irradiation room temperature yield strength values ranged from 78Ksi for the HAZ to 85Ksi for the weld metal. Total elongation of the irradiated materials ranged from 23% to 28%.

D. Charpy Impact Toughness Properties

The radiation induced changes in toughness of the St. Lucie Unit 1 surveillance materials are summarized in Table VI-1. Index temperature shifts were measured using the average curves at the 30 ft-lb level (Cv30), 50 ft-lb level (Cv50), and 35 mils lateral expansion level (Cv35). Upper shelf energy changes were based on the average impact energy for each set of test specimens exhibiting 100% shear fracture measured before and after irradiation. The unirradiated Charpy impact data were obtained from the baseline evaluation report.(2)

The base metal and weld metal exhibited similar shifts in the 30 ft-lb index temperature (68-74^{o}F). The shift for the heat-affected-zone material was significantly less (28F). The decrease in upper shelf energy was similar for the irradiated base and weld materials, ranging from 23 to 31%.

The St. Lucie Unit 1 design curve for prediction of transition temperature shift as a function of neutron fluence is given in Figure B3/4.4-1 of the Technical Specifications.(7) The design curve prediction for the surveillance capsule exposure of 5.5×10^{18} n/cm^2 is 137^{o}F, or 85% to 90% higher than the measured shifts for the base metal and the weld metal. In contrast, shifts predicted using NRC Regulatory Guide 1.99(8) based on measured copper and phosphorus content are 82^{o}F for the base metal (17% more than measured) and 159^{o}F for the weld metal (115% more than measured).

In order to provide an improved means of predicting transition temperature shift of the surveillance material for St. Lucie Unit 1, Figure VI-1 was developed. Figure VI-1 was developed based on the methodology of Regulatory Guide 1.99(8) using the measured value of shift at the 30 ft-lb level for the weld metal (74^{o}F) at 5.5×10^{18} n/cm^2. The shift versus neutron fluence relationship is as follows:

TABLE VI-1

SUMMARY OF TOUGHNESS PROPERTY CHANGES FOR ST. LUCIE UNIT 1

SURVEILLANCE MATERIALS (550F IRRADIATION, 5.5 x 10^{18} n/cm^2)

Material	Index Temperatures (^oF)						Upper Shelf Energy	
	Cv 30[a]	ΔCv 30	Cv 50[b]	ΔCv50	Cv 35[c]	ΔCv 35	Energy (ft-lb)	Change (%)
Base Metal (WR)	16[d]		40[d]		36[d]		103[d]	
	86	70	150	110	126	90	78	24
Base Metal (RW)	8[d]		43[d]		35[d]		139[d]	
	76	68	126	83	117	82	107	23
Weld Metal	-53[d]		-36[d]		-35[d]		144[d]	
	21	74	44	80	37	72	100	31
Heat-Affected Zone	-60[d]		-4[d]		-16[d]		133[d]	
	-32	28	0	4	7	23	114	14

a - 30 ft-lb Index Temperature

b - 50 ft-lb Index Temperature

c - 35 mils lateral expansion Index Temperature

d - Unirradiated values

FIGURE VI-1 PREDICTED TRANSITION TEMPERATURE SHIFT FOR THE ST. LUCIE UNIT 1 SURVEILLANCE MATERIALS

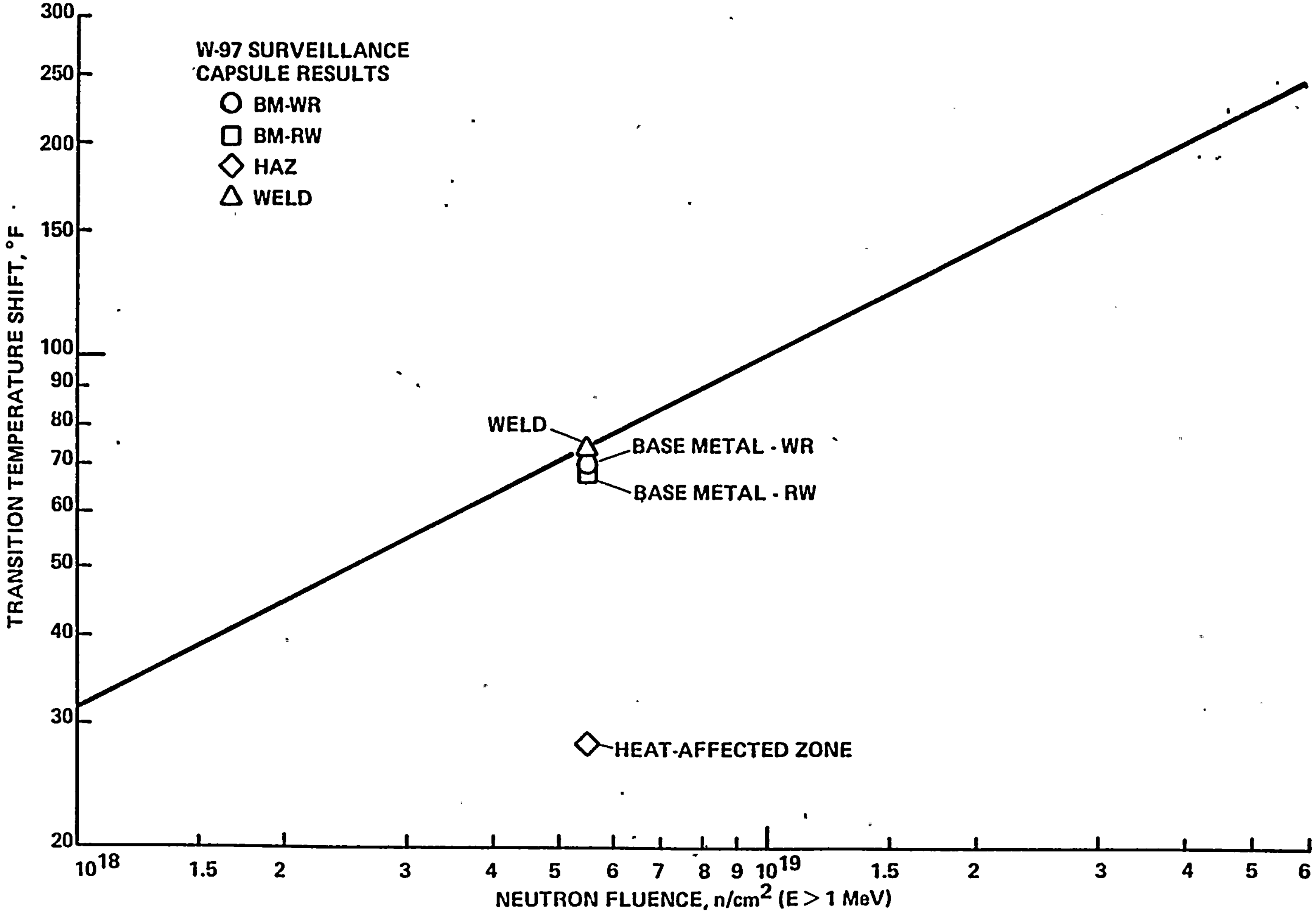

$$NDTT = 100 \left(\frac{\phi}{10^{19}}\right)^{0.5}$$

where ϕ = neutron fluence, E>1.0 MeV, and
ΔNDTT = transition temperature shift.

This relationship should be evaluated again once results are available from surveillance materials irradiated to a higher fluence.

The measured shift for the weld material was only 6% higher than that for the base metal material even though the copper content of the weld was significantly higher (0.23% Cu for the weld versus 0.15% Cu for the plate). The greater irradiation resistance of the weld is a result of the low nickel content (0.11%). Based on an empirical evaluation of weld metal irradiation sensitivity[9], low nickel weldments (e.g. less than 0.2% Ni) exhibited significantly smaller NDTT shifts than high nickel weldments. Similar results were observed with the Millstone Unit 2 surveillance weld.[10] Therefore, the low weld metal shift determined from the St. Lucie Unit 1 W-97 surveillance capsule evaluation is consistent with surveillance and experimental results. Furthermore, it is reasonable to expect that both the base metal and the weld metal will continue to exhibit similar shifts in subsequent analyses.

As noted in Section VIB, chemical analysis of the baseline and irradiated weld metal Charpy specimens indicated that a region of the weld contained higher copper (0.32 to 0.44 w/o Cu) than the balance of the weld (0.20 to 0.22 w/o Cu). The two irradiated specimens (31A and 323) identified as containing 0.32 w/o Cu exhibited Charpy impact properties consistent with the specimens containing lower copper. A third specimen (33E) which was not analyzed but which bordered on the higher copper region of the weld exhibited test results below the mean energy versus test temperature curve. However, the results were within the overall scatterband. Pending results from future surveillance capsules, it does not appear that the range of measured copper content has a significant effect on the radiation sensitivity of the surveillance weld.

Projected values of NDTT shift and adjusted RT_{NDT} are given in Table VI-2. Using the highest initial reference temperature ($20^{o}F$) for the surveillance materials (base metal transverse) and the revised shift prediction method and vessel fluence, the predicted adjusted RT_{NDT} (vessel inside surface) after 32 EFPY is $207^{o}F$. Similarly, the 1/4 t adjusted RT_{NDT} is projected to be $158^{o}F$. (Note that the revised shift prediction method applies to the specific plates and welds represented by the surveillance materials; i.e., it applies to the six beltline plates and to weld seams 9-203 and 2-203. It should not be applied to weld seams 3-203 or 8-203* because of the higher nickel content in these welds compared to the surveillance weld. Further information concerning shift prediction methodology for these welds is provided in separate report[11].)

*Weld seam 8-203 is the girth weld between the intermediate and upper shell course. It is located outside of the beltline as defined in 10CFR50, Appendix G.

TABLE VI-2

PROJECTED NDTT SHIFT AND ADJUSTED RTNDT FOR SURVEILLANCE MATERIAL

Vessel Location	Fluence[a]	END-OF-LIFE (32 EFPY) NDTT SHIFT	Adj. RTNDT[b] PLATE	Adj. RTNDT[b] WELD
Inside Surface	$3.5 \times 10^{19} n/cm^2$	187^0F	207^0F	127^0F
1/4 t	$1.9 \times 10^{19} n/cm^2$	138^0F	158^0F	78^0F
3/4 t	$3.9 \times 10^{18} n/cm^2$	62^0F	82^0F	2^0F

a - Projected fluence assuming same power level, coolant inlet temperature and fuel management strategy as for Cycle 6.

b - Adjusted RT_{NDT} = Initial RT_{NDT} plus NDTT shift, where initial RT_{NDT} is 20F for surveillance plate and -60F for surveillance weld.

The predicted decrease in upper shelf energy at end-of-life based on the method given in Regulatory Guide 1.99[8] is 41% for the weld and 32% for the plate at the one-quarter thickness location in the vessel. Using this conservative prediction, the upper shelf energy of the plates will remain above 70 ft-lb during the design life of the vessel. The upper shelf energy of the weld will remain above 85 ft-lb throughout vessel life. These projected values of upper shelf energy are well in excess of the 50 ft-lb value currently considered to provide a reasonable margin for continued safe operation.

Recommended changes to the surveillance capsule removal schedule are contained in Table VI-3. The schedule is designed based on 10CFR50, Appendix H and a time-averaged lead factor (capsule to vessel ID) of 1.25. (For example, the fourth capsule's exposure after 19 EFPY will be equivalent to that at the vessel inside surface after 24 EFPY). The 104^{o} and 284^{o} capsules are designated for standby purposes.

TABLE VI-3
PROPOSED NEW CAPSULE REMOVAL SCHEDULE FOR ST. LUCIE UNIT 1

Removal Sequence	Azimuthal Location	Alternate Location	Approximate Removal Time[a]
1	97^{o}	-	4.67 EFPY[b]
2	263^{o}	83^{o}, 277^{o}	7-9 EFPY
3	83^{o}	277^{o}	12-14 EFPY
4	277^{o}	-	17-20 EFPY
5	104^{o}	-	Standby
6	284^{o}	-	Standby

a) Time in effective full power years (EFPY) at 2700 Mwt.

b) Actual removal time.

VII. REFERENCES

1. "Program for Irradiation Surveillance of Hutchinson Island Plant Reactor Vessel Materials", Combustion Engineering, INC., F-NCM-007, September 15, 1970.

2. "Florida Power & Light Company, St. Lucie Unit No. 1, Evaluation of Baseline Specimens, Reactor Vessel Materials Irradiation Surveillance Program", TR-F-MCM-005, to be issued.

3. "SAND Neutron Flux Spectra Determination by Multiple Foil Activation - Iterative Method", CCC-112, Oak Ridge National Laboratory, Oak Ridge, Tenn.

4. "DOT-IV Version 4.3 Two Dimensional Transport Code System", CCC-429, Oak Ridge National Laboratory, Oak Ridge, Tenn.

5. "DOSDAM 81-82, Multigroup Cross-sections in SAND-II Format for Spectral, Integral and Damage Analysis", ORNL, DLC-97, Oak Ridge, Tenn.

6. C-E Drawing E-19367-165-111-02, "Weld Metal Test Specimens", January 28, 1972.

7. Florida Power & Light Company, St. Lucie Unit 1, Safety Technical Specifications, Docket 50-335.

8. Regulatory Guide 1.99, Revision 1, "Effects of Residual Elements on Predicted Radiation Damage to Reactor Vessel Materials", April 1977.

9. J. D. Varsik and S. T. Byrne, "An Empirical Evaluation of the Irradiation Sensitivity of Reactor Pressure Vessel Materials", Effects of Radiation on Structural Materials, ASTM STP 683, 1979.

10. "Northeast Utilities Service Company, Millstone Nuclear - Unit No. 2; Evaluation of Irradiation Capsule W-97", "TR-N-MCM-008, April 1982.

11. Florida Power & Light Company, St. Lucie Unit No. 1 (Thermal Shield Removal and Core Support Barrel Repair Evaluation Report), to be issued.

APPENDIX A

TENSION TESTS - DESCRIPTION AND EQUIPMENT

The tension tests were performed using a Riehle universal screw testing machine with a maximum capacity of 30,000 lb and separate scale ranges between 50 lb and 30,000 lb. The machine, shown in Figure A-1, is capable of constant cross head rate or constant strain rate operation. The tension testing was covered by the certificate of calibration which is included at the end of the Appendix A.

Elevated temperature tests were performed in a 2-1/2" ID x 18" long high temperature tension testing furnace with a temperature limit of 1800F. A Riehle high temperature, dual range extensometer was used for monitoring specimen elongation.

The tension specimen is depicted in Figure A-2. Figures A-3 through A-5 are isometric drawings showing the orientation and location of the tension specimens in the base metal, weld metal and heat-affected-zone, respectively.

Tension testing was conducted in accordance with ASTM Method E 8-82, "Tension Testing of Metallic Materials" and/or Recommended Practice E 21-79, "Elevated Temperature Tension Tests of Metallic Materials," except as modified by Section 2.1 of Recommended Practice E 184-79, "Effects of High-Energy Neutron Radiation on the Mechanical Properties of Metallic Materials." Implementation of the ASTM Test Methods to the testing of irradiated tension specimens is described in C-E Laboratory Procedure 00000-MCM-041, Revision 0, "Procedure for Tension Testing of Irradiated Metallic Materials," August 16, 1978.

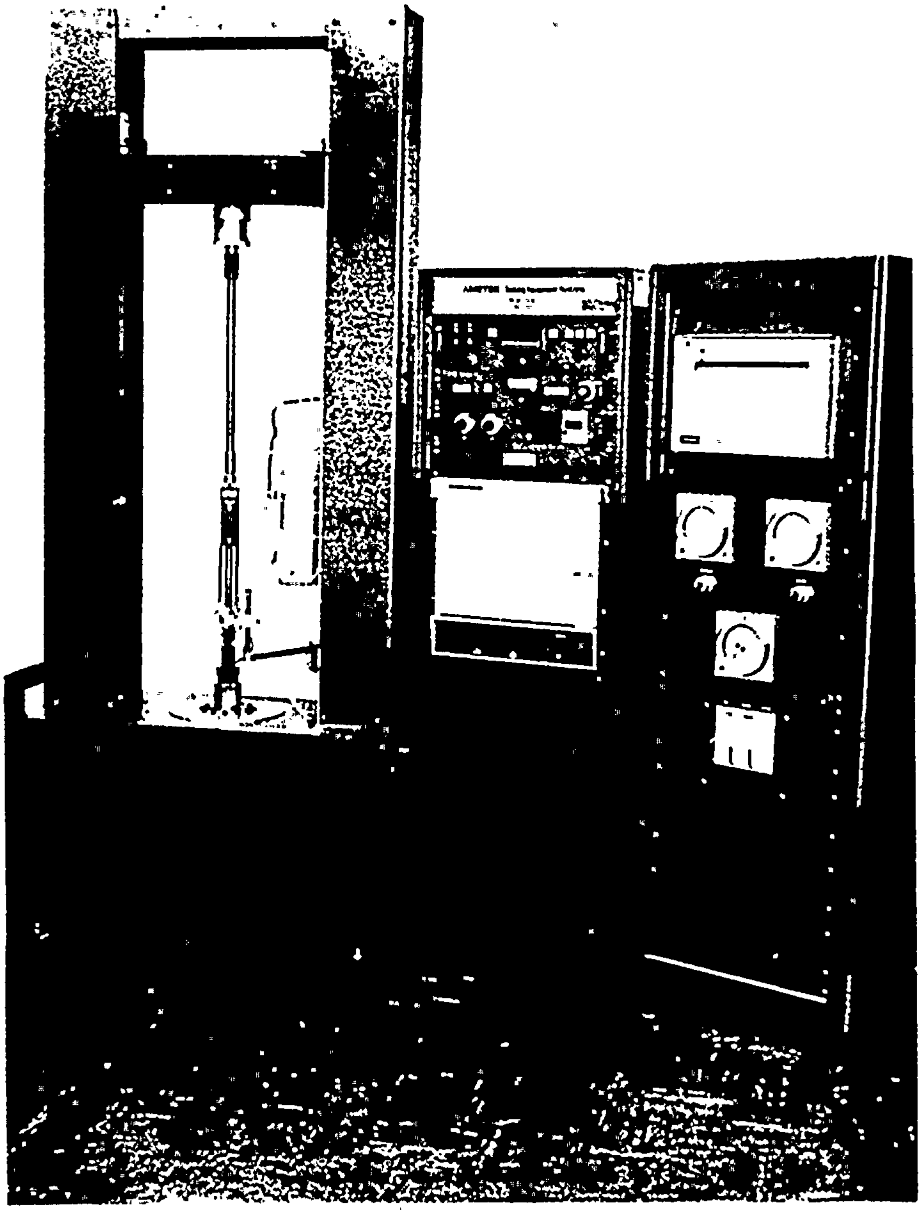

FIGURE A-1 TENSION TEST SYSTEM WITH CONTROL CONSOLE AND ELEVATED TEMPERATURE TESTING EQUIPMENT

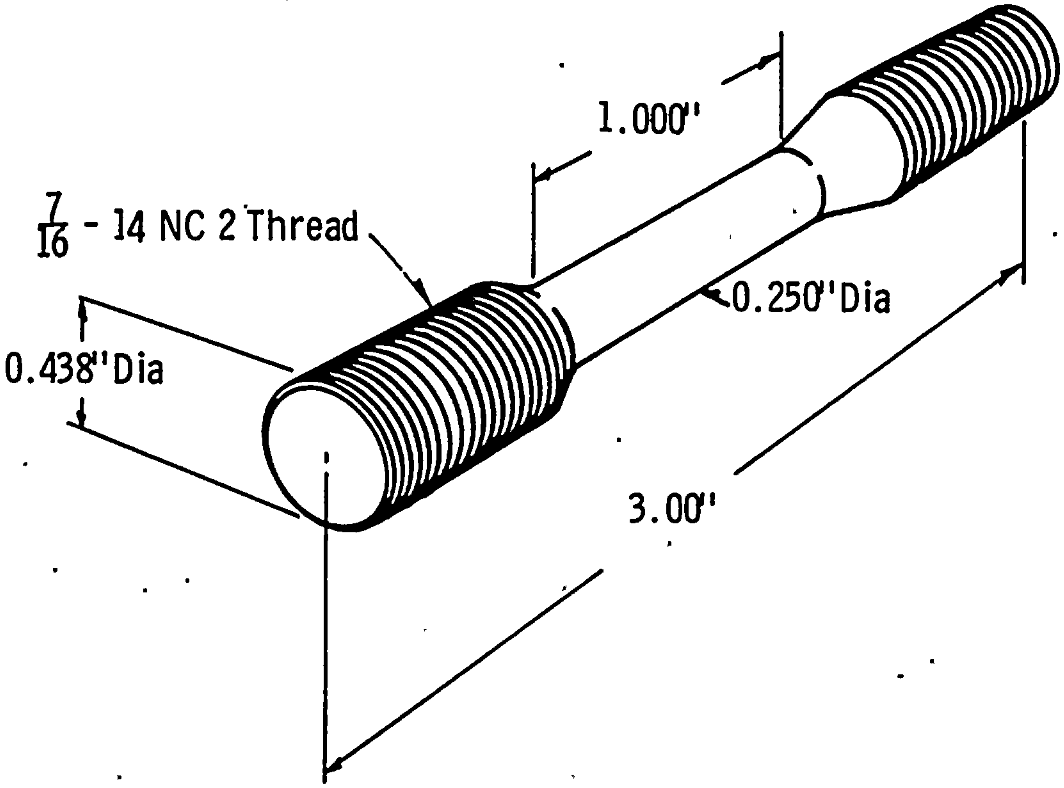

FIGURE A-2 TYPICAL TENSION SPECIMEN

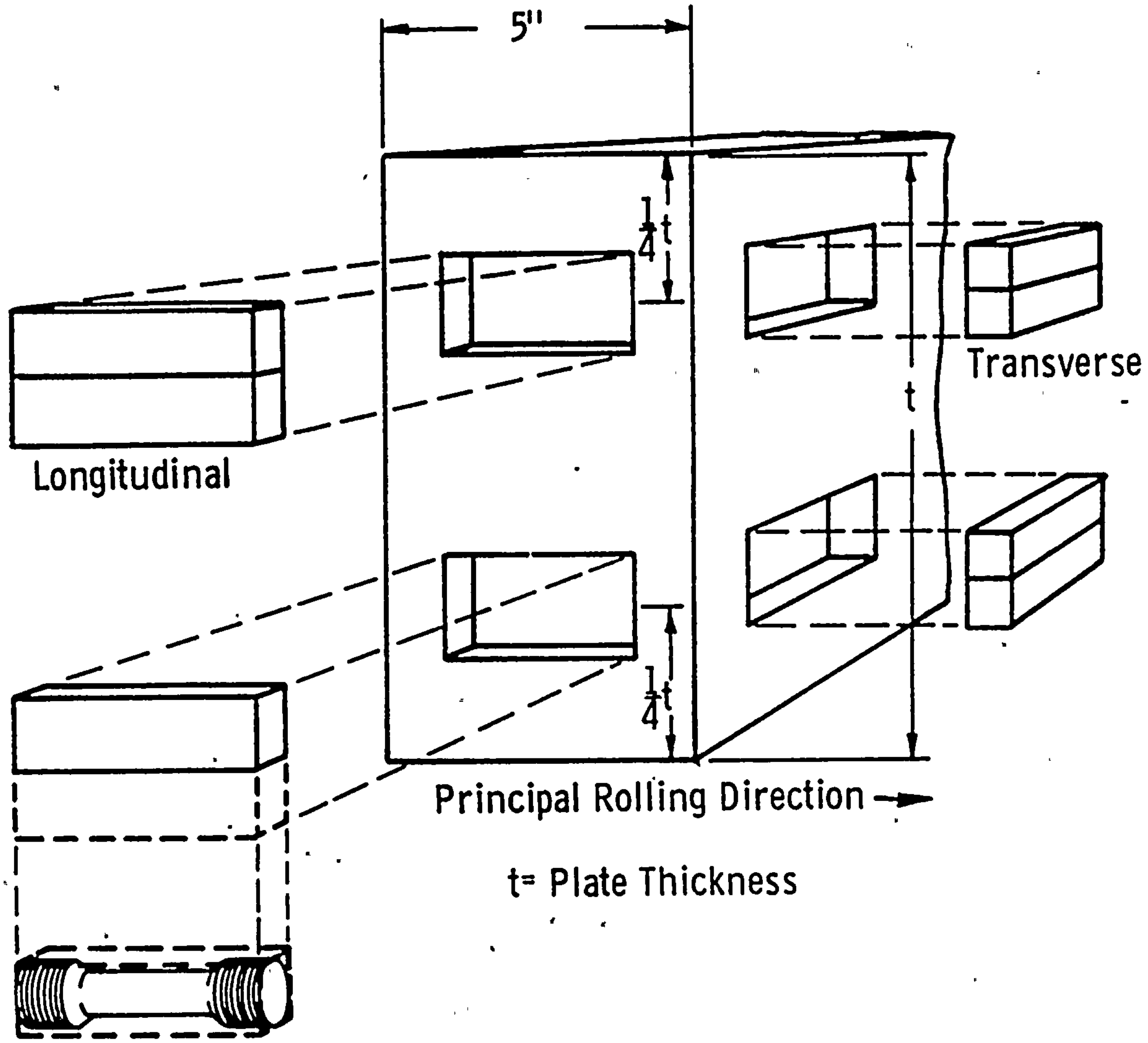

FIGURE A-3 LOCATION OF TENSION SPECIMENS WITHIN BASE METAL TEST MATERIAL

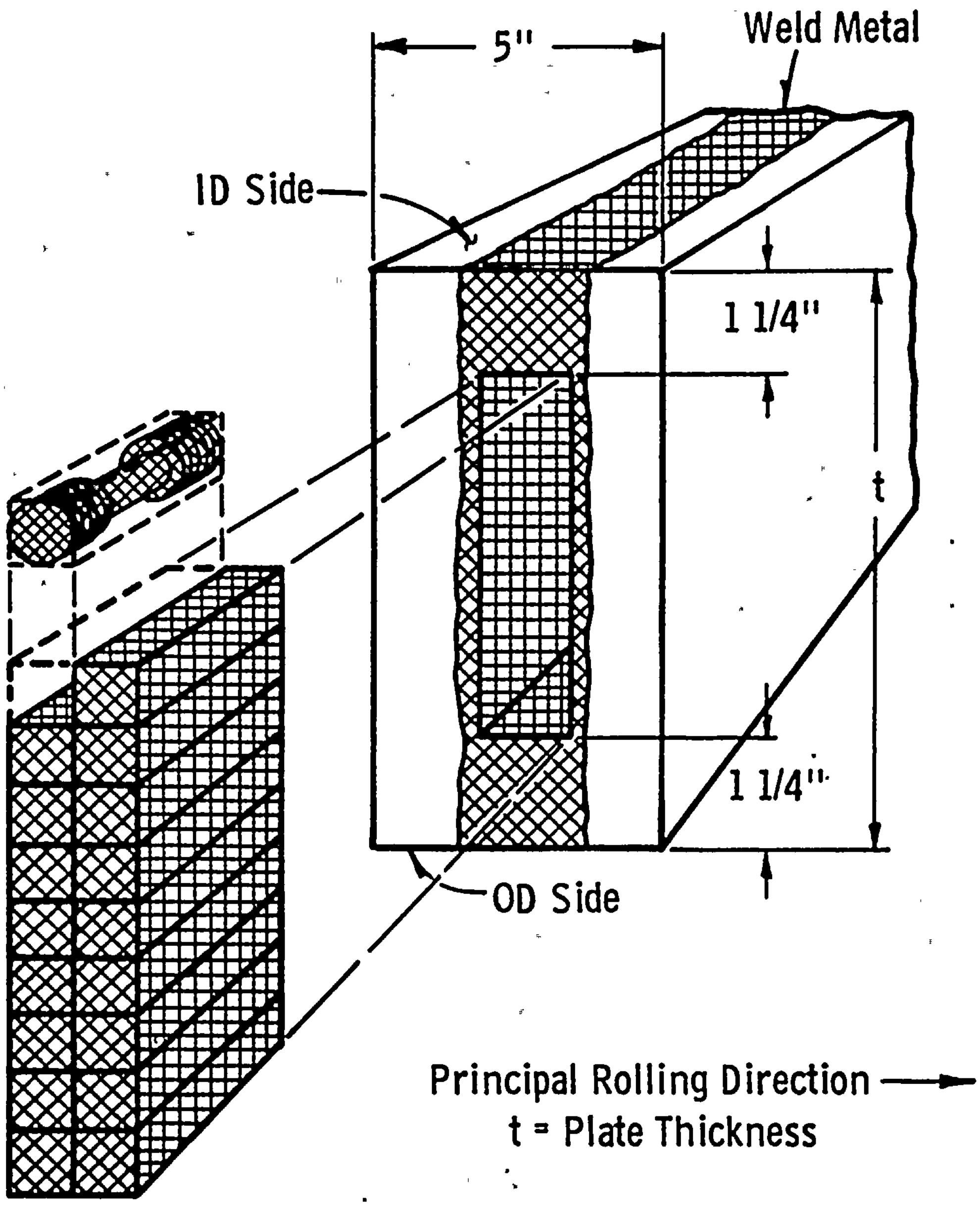

FIGURE A-4 LOCATION OF TENSION SPECIMENS WITHIN WELD METAL TEST MATERIAL

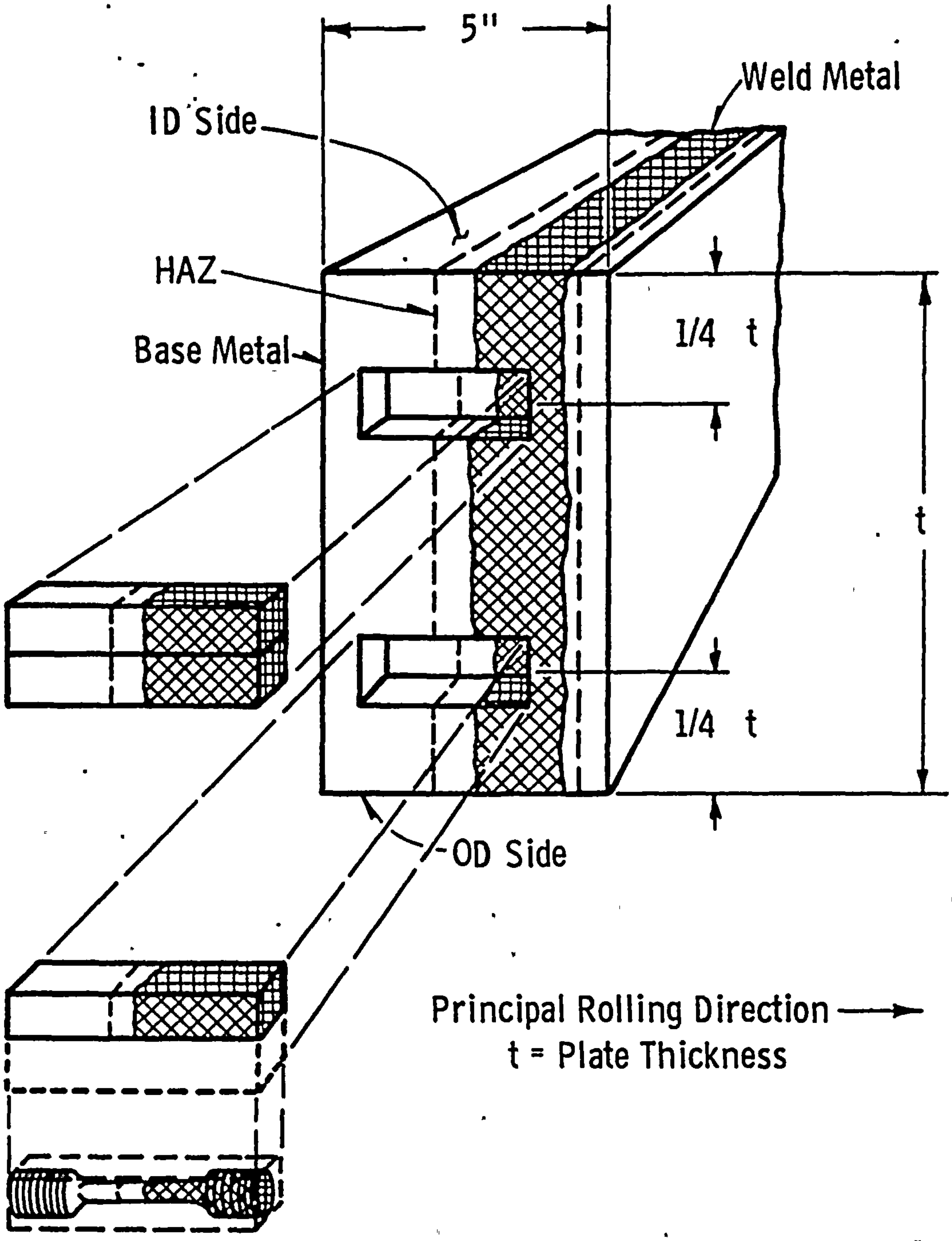

FIGURE A-5 LOCATION OF TENSION SPECIMENS WITHIN HEAT-AFFECTED-ZONE TEST MATERIAL

PAGE–WILSON
CORPORATION

MEASUREMENT SYSTEMS DIVISION
929 CONNECTICUT AVENUE, BOX 9021
BRIDGEPORT, CONNECTICUT 06602
(203) 335-2511 TELEX 96-4224

Certificate of Calibration

Riehle® Testing Machine

Calibration Date
3-16-83

Machine Description
Riehle DS. 30

Company
Combustion Engineering

Serial No.
GA 44372

Location
Bl 5 Windsor Conn.

Measurement Systems Division of Page-Wilson Corporation certifies that the machine described above has been calibrated to ASTM designation E4 using calibrated weights and/or elastic-calibration devices calibrated to National Bureau of Standards specification.

Tension

Machine Range 3000

Machine reading	% Error
600	+.333
1200	+.333
1800	+.277
2400	+.208
3000	+.167

Machine Range 15000

Machine reading	% Error
3000	0
6000	0
9000	−.111
12000	−.083
15000	−.033

Machine Range 6000

Machine reading	% Error
1200	0
2400	+.083
3600	+.056
4800	+.063
6000	+.067

Machine Range 30000

Machine reading	% Error
6000	−.333
12000	−.250
18000	−.111
24000	−.042
30000	−.033

Machine Range

Machine reading	% Error

Machine Range

Machine reading	% Error

R.C. Lepak
Calibration Engineer

Standards Manager

Calibrating apparatus used Riehle Load Cells

Capacity	Serial no.	Cal. date	Lab. no
50,000	1946	5/4/83	33T 01/102398
10,000	1101	5/5/83	" "
1,000	5724	5/2/83	" "

Form 18-33-005

PAGE–WILSON
CORPORATION

MEASUREMENT SYSTEMS DIVISION
29 CONNECTICUT AVENUE, BOX 9021
BRIDGEPORT, CONNECTICUT 06602
(203) 335-2511 TELEX 96-4224

Certificate of Calibration

Riehle® Testing Instrument

Calibration Date
8-16-83

Company
Combustion Engineering

Location
Bld.5
Windsor Conn.

Instrument Description
Riehle DND 10-20

Serial No.
DN-120007

Measurement Systems Division of Page-Wilson Corporation verifies that the attached graph is certification of calibration of the instrument described above. This instrument was calibrated to ASTM designation E83.

Riehle RD58 s/n R-67338
Riehle Master EM 528864
Equipment used in calibration

R.C. Lepak
Calibration Engineer

Robert J. Alkinson
Standards Manager

Job 18-00-0006 2M 382 RS Printed in U.S.A.

APPENDIX B

CHARPY IMPACT TESTS - DESCRIPTION AND EQUIPMENT

The standard impact tests and instrumented tests were performed on a calibrated instrumented impact testing system, shown in Figure B-1. C-E's instrumented impact test equipment provides for signal retention and the subsequent data analysis. The output signal from the instrumented tup is recorded by an oscilloscope. Permanent records were made of the load signal and integrated energy as it was displayed on the oscilloscope screen with a poloroid camera and with a computer printout.

The system consists of the following elements:

a. A Model SI-1 BLH Sonntag Universal Impact Machine with a specifically machined pendulum tup, instrumented with four resistance strain gages in full bridge circuit. This tup "load cell" is calibrated statically and dynamically to provide a given pounds/volt sensitivity for known settings of the balance and gain on the dynamic response system. The instrumented machine meets all impact test machine requirements of ASTM and is certified by AMMRC, the U.S. Army Materials and Mechanics Research Center (Watertown Arsenal). A copy of the certification papers is included in this Appendix.

b. A model 500 Dynatup dynamic response system which supplies regulated and constant dc excitation to strain gages on the pendulum tup, provides balancing, variable load sensitivity and calibration functions, and amplifies load-time signal to a ± 10 volt, ± 100 milliampere level while preserving kHz frequency response and 0.05 percent accuracy while simultaneously recording the area beneath the load-time trace.

c. A photoelectric triggering device and velocometer composed of a high intensity light directed through a grid mounted on the pendulum of the impact tester, and passed to a photosensor through fiber optics. A special circuit ensures accurate, reliable and fail safe triggering of the oscilloscope recorder plus an accurate display of the average velocity of the pendulum during impact.

d. A 5113 Dual Beam Tektronix Storage Oscilloscope with a No. 5A18N dual-trace amplifier plug-in unit and a No. 5B12N dual time base plug-in unit. Also included is a C-58 camera with mounting adapter. This device gives a display of each test trace for visual analysis of the load-time impulse recorded by the instrument.

The standard Charpy specimen is described in Figure B-2. Figures B-3 through B-5 are isometric drawings showing the orientation and location of the Charpy impact specimens in the base metal, weld metal and heat-affected-zone, respectively.

All Charpy impact tests were conducted in accordance with ASTM Method E 23-82, "Notched Bar Impact Testing of Metallic Materials." Implementation of ASTM E23 for the testing of irradiated Charpy specimens is described in C-E. Laboratory Procedure 00000-MCM-040, Revision 0, "Procedure for Instrumented Charpy Impact Testing of Irradiated Metallic Materials," July 31, 1978.

The constant temperature necessary for conducting the Charpy impact tests was obtained from a series of circulating liquid baths capable of maintaining stable temperature throughout the range of $-150^{o}F$ to $+250^{o}F$. For test above $250^{o}F$, specimens were heated in a controlled circulation furnace where temperature was maintained to an accuracy of $5^{o}F$. The temperature baths were composed of the following equipment:

Two Neslab Constant Temperature Circulating Baths - Model TEZ 10, with Model CT 150 Thermoregulators and Labline 11 inch diameter thermocups, Designated Baths 1 and 4.

Medium: Ethylene Glycol - room temperature to 250^oF.

One Neslab Constant Temperature Circulating Bath - Model TEZ 10 with a Model CT 59 Thermoregulator and a Labline 11 inch diameter thermocup. Designated Bath 2.

Medium: Isopropanol - room temperature to -10^oF. Neslab Portable Bath Cooler, Model PCB-2 connected.

One Low Temperature Stirred Bath, one 11 inch thermocup, one Honeywell Controller and Solenoid control valves to Flexi-Cool cooling system. Designated Bath 5.

Medium: Isopropanol - room temperature to -150^oF.
Coolant: Freon

One Grieve Industrial oven, controlled air circulation. Designated Bath 3.

Medium: Air, 100^oF to 800^oF.

All baths - Copper Constantan Thermocouple
Honeywell Six Point Temperature Chart Recorder
Digitec Themocouple Thermometer - Model 590 TF
Standard Mercury Column Thermometer
Bimetallic - spring Thermometer

The temperature instruments were calibrated in accordance with the ASME Boiler and Pressure Vessel Code, Section III, Paragraph 2360. Copies of the applicable certificates are provided at the end of this Appendix.

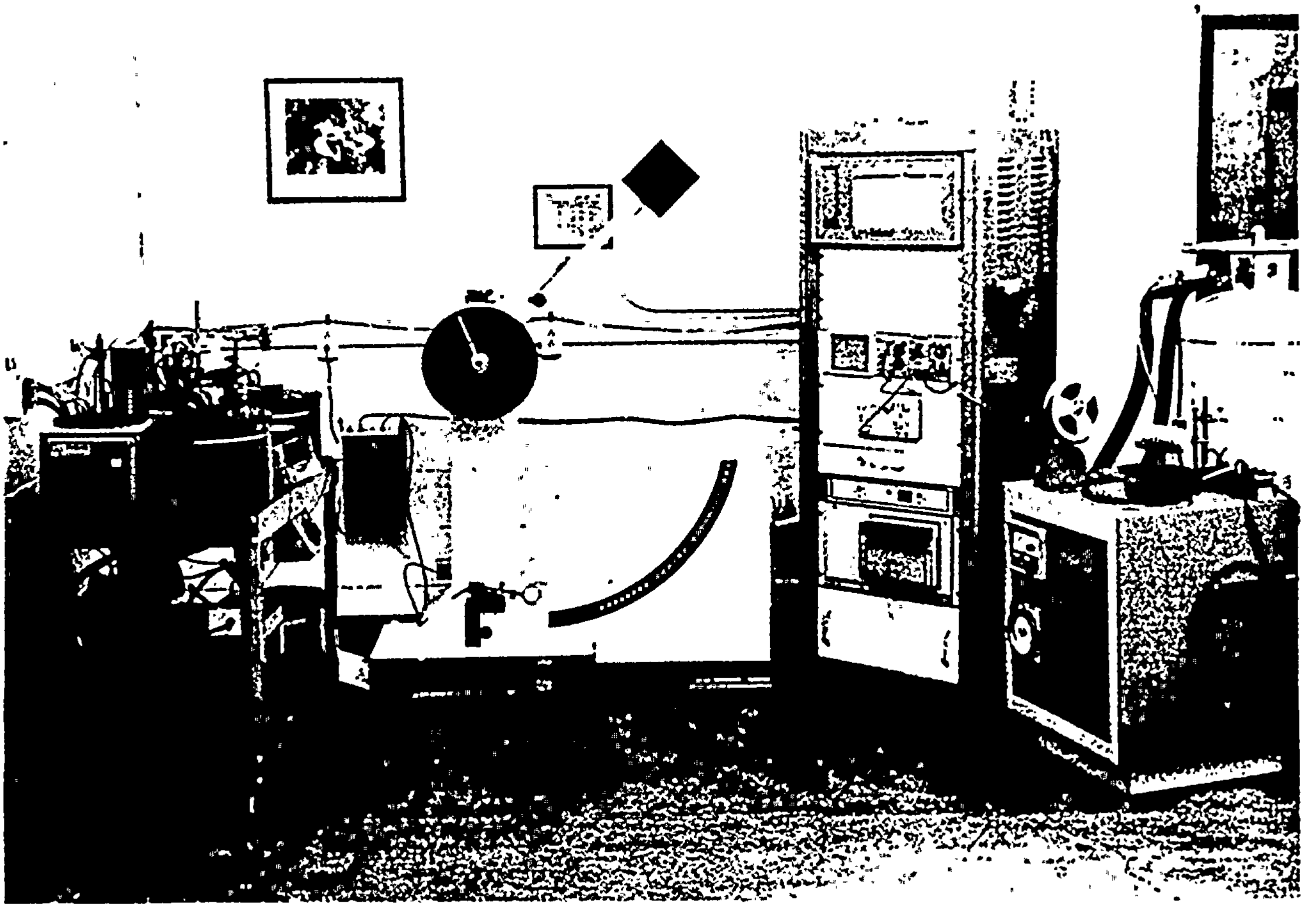

FIGURE B-1 CHARPY IMPACT TEST SYSTEM, ASSOCIATED CONSTANT TEMPERATURE BATHS AND INSTRUMENTED CHARPY IMPACT DATA PROCESSING EQUIPMENT

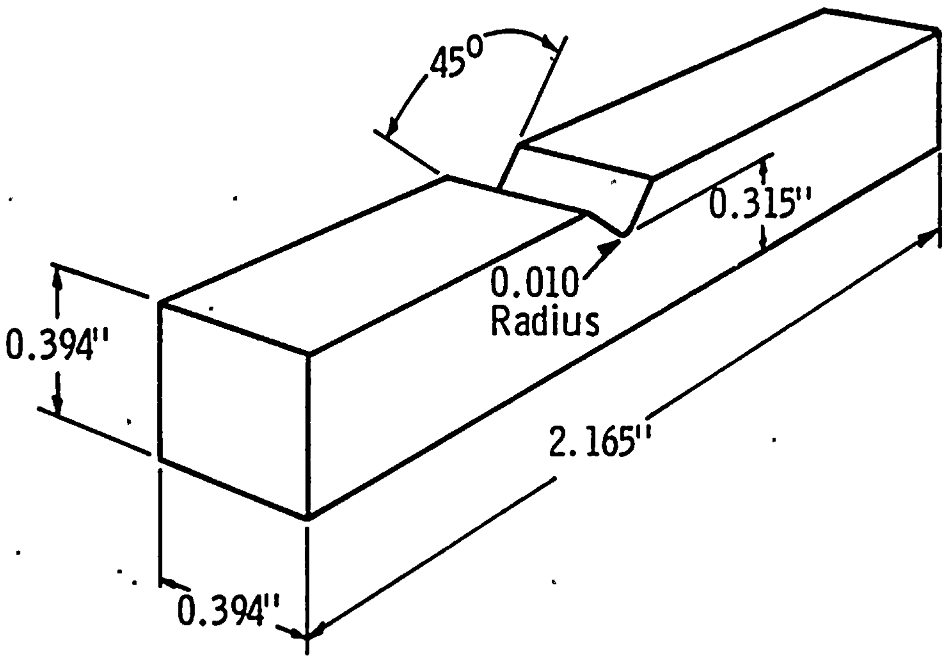

FIGURE B-2 TYPICAL CHARPY V-NOTCH IMPACT SPECIMEN

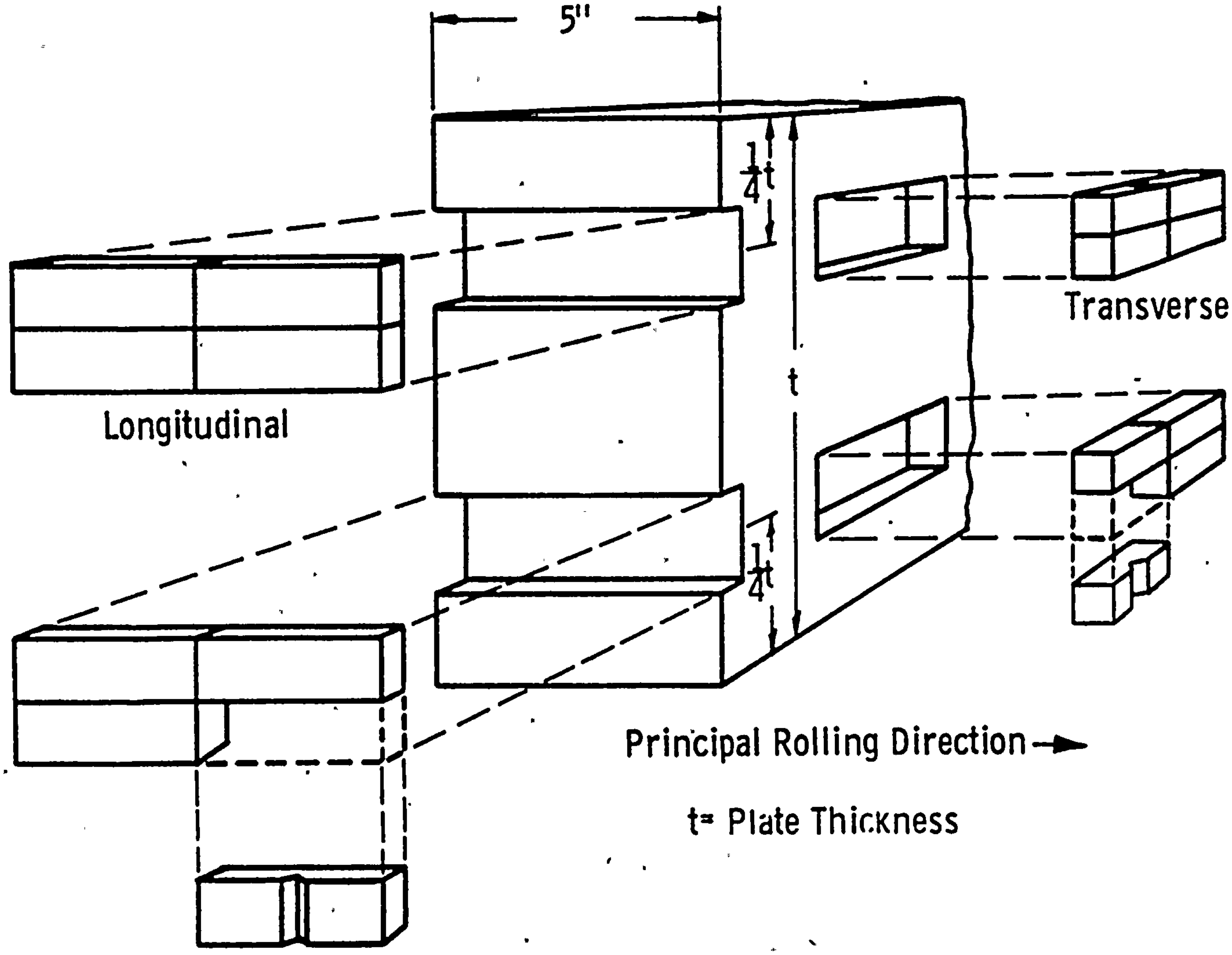

FIGURE B-3 LOCATION OF CHARPY IMPACT SPECIMENS WITHIN BASE METAL TEST MATERIAL

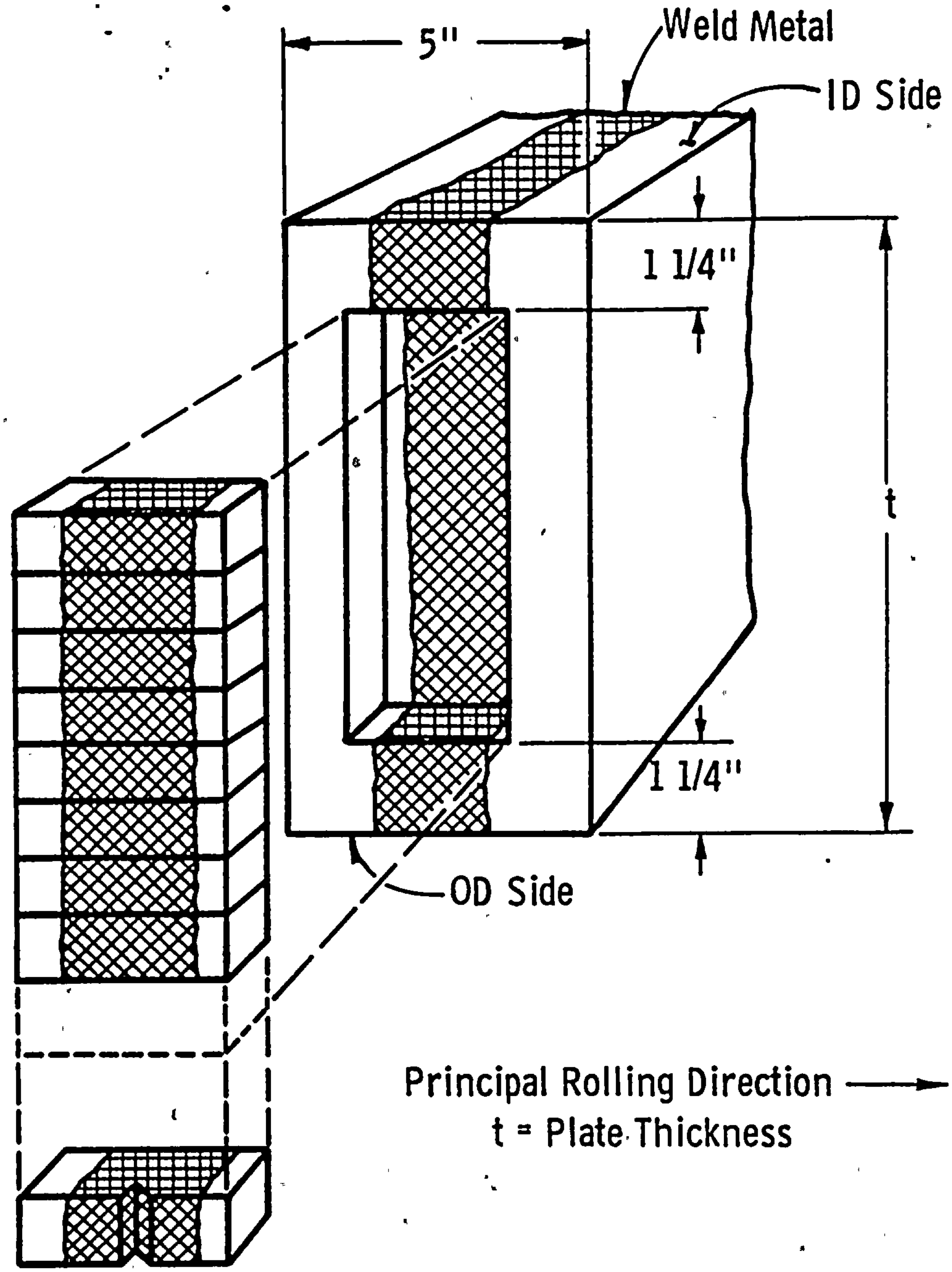

FIGURE B-4 LOCATION OF CHARPY IMPACT SPECIMENS WITHIN WELD METAL TEST MATERIAL

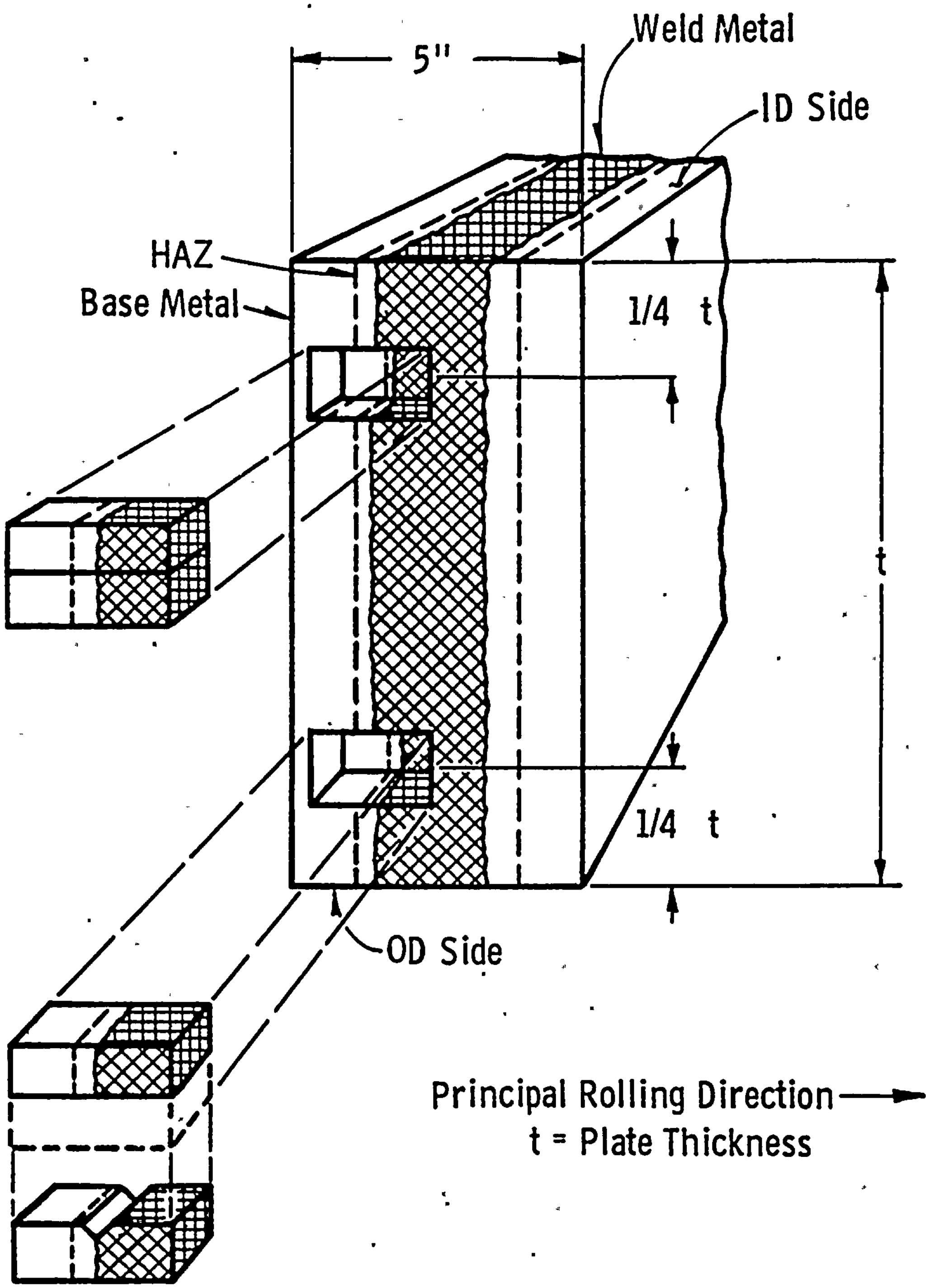

FIGURE B-5 LOCATION OF CHARPY IMPACT SPECIMENS WITHIN HEAT-AFFECTED-ZONE TEST MATERIAL

DEPARTMENT OF THE ARMY
ARMY MATERIALS AND MECHANICS RESEARCH CENTER
WATERTOWN, MASSACHUSETTS 02172

REPLY TO
ATTENTION OF

DRXMR-STM 5 July 1983

Combustion Engineering, Inc.
ATTN: Mr. R. J. Hurlburt
1000 Prospect Hill Road
P.O. Box 500
Windsor, CT 06095-0500

Dear Mr. Hurlburt:

A set of Charpy impact test specimens broken on the 240 ft-lb capacity Satec machine, Serial No. 1366 has been received for evaluation along with the completed questionnaire.

The results of the tests indicate the machine to be producing acceptable energy values at both energy levels (see inclosed table).

It is noted that one specimen has unusally sharp anvil marks. This could be caused by sharp radius or by not properly positioning the specimen against the anvil supports. The anvils' radii should be checked to assure that the radii are 0.039" $\pm$ 0.002". If the anvils are within limits, proper care should be taken when positioning the specimens against the anvils.

This machine satisfies the proof-test requirements of ASTM Standard E-23.

If this machine is moved or undergoes any major repairs or adjustments, this certification becomes invalid and the machine must be rechecked. Removal of the pendulum, replacement of anvils or adjusting the height of drop are examples of such major repairs or adjustments. It should be noted that if a specimen requires over 80% of the machine capacity to fracture, the machine should be checked to assure that the pendulum is straight, the anvils or striker have not been damaged and that all bolts are still tight. This certification is valid for one year from the date of the test.

Sincerely yours,

Roger M. Lamothe

ROGER M. LAMOTHE
Chief, Mechanical
Behavior & Testing Branch

1 Encl
Table

ARMY MATERIALS AND MECHANICS RESEARCH CENTER

Watertown, Massachusetts 02172

Date of Test: 4 June 1983

TABLE

COMPARISON TESTS ON CHARPY IMPACT MACHINES

Facility: Combustion Engineering, Inc.
1000 Prospect Hill Rd., P.O. Box 500, Windsor, CT 06095

Make of Machine: Satec Systems   Serial No. 1366

	AMMRC (ft-lb)	(ft-lb)	Variation Actual	Variation Allowed
High Energy	69.9	70.7	+1.1 %	±5.0%
Low Energy	11.6	11.9	+0.3 ft-lb	±1.0 ft-lb

XMR Form 105
Rev 1 Apr 81

COMBUSTION ENGINEERING, INC.
Nuclear Laboratories
INSTRUMENT CALIBRATION REQUIREMENT SHEET

DATE: 5/17/83

EQUIPMENT Digital Thermocouple Thermometer
EL-96

AREA Fracture Lab

INSTRUMENT		READABILITY		CALIBRATION		CHECKED
FUNCTION	TYPE	RANGE	MIN READABILITY	ACCURACY	FREQUENCY	BY
Thermometer	Digital	$-313^{0}F$ to $+752^{0}F$	$1^{0}F$	$\pm 1^{0}F$	3 mos.	

PREPARED BY Raymond J. Hurlbert

APPROVED BY S.T. Byrne

APPROVED BY

APPENDIX C

INSTRUMENTED CHARPY V-NOTCH DATA ANALYSIS

All baseline and irradiated Charpy impact tests in this program were performed on an instrumented test system. Instrumented impact testing provides more quantitative data from a Charpy specimen which enable a more detailed analysis of the surveillance material toughness behavior.

Photographs of the oscilloscope traces and computer printouts of load and energy versus time were taken for each test of the base plate (transverse and longitudinal orientation), weld, and heat-affected-zone. From each trace, the general yield load (PGY), maximum load (PM), and fracture load (PF) were determined, as shown in Tables C-1 through C-4. For each material, the loads were plotted against the corresponding test temperature to generate the irradiated load/temperature diagrams. The post-irradiation load/temperature results are shown in Figures C-1 to C-4.

Three index temperatures are of interest. T_B, the brittle transition temperature, corresponds to the onset of ductile fracture; below T_B the fracture is completely brittle. T_N, the ductility transition temperature, corresponds to the mid-transition region where the fracture has become predominantly ductile. T_D, the ductility temperature, corresponds to the onset of the upper shelf energy where fracture is completely ductile.

The radiation-induced toughness property changes of the surveillance materials are summarized in Table C-5. Standard Charpy impact data are included with the instrumented data since each method represents a unique material property. The standard Charpy test provides a measurement of the total energy to initiate and propagate a crack through to failure of the material. In contrast, analysis of the instrumented data enables characterization of the components of the dynamic load behavior prior to material failure. The shift in the brittle transition temperature, T_B, and the ductility transition temperature, T_N, are comparable to the shift in the 30 ft-lb Charpy index temperature, Cv_{30}. The radiation-induced changes in the instrumented data therefore tend to corroborate the changes determined from the standard Charpy impact data.

The third-parameter obtainable from the instrumented data is T_D, the ductility temperature, which is given in Table C-5. T_D corresponds closely with the onset of the upper shelf energy (minimum temperature for the material to exhibit 100% shear fracture). The agreement is seen to hold for both the unirradiated and irradiated data.

The instrumented Charpy analysis substantiates the results from the standard impact tests. In particular, this approach provides a more quantitative means of measuring radiation-induced property changes by analysis of the entire load record rather than using the single measurement of impact energy. As more experience is gained with this technique, it offers the potential of providing a more quantitative measurement of toughness property changes than is possible with current impact testing.

TABLE C-1

INSTRUMENTED CHARPY IMPACT

TEST, ST. LUCIE UNIT 1 IRRADIATED

BASE METAL (TRANSVERSE)

Specimen Identification	Test Temperature (^{o}F)	Yield Load, PGY (lb)	Maximum Load, PM (lb)	Fast Fracture Load, PF (lb)
22A	0	--	--	3800
23A	40	3400	4300	--
22D	60	3350	4000	--
237	60	3100	4200	--
232	80	3250	4300	--
22J	80	3000	4200	--
23T	120	3100	4300	--
227	160	3050	4250	4200
23K	160	2950	4200	4000
22B	210	2850	4100	3200
22E	250	2800	4000	3500
231	250	2900	4000	--

TABLE C-2
INSTRUMENTED CHARPY IMPACT
TEST, ST. LUCIE UNIT 1 IRRADIATED
BASE METAL (LONGITUDINAL)

Specimen Identification	Test Temperature (^{O}F)	Yield Load, PGY (lb)	Maximum Load, PM (lb)	Fast Fracture Load, PF (lb)
12T	0	3700	3900	--
12A	40	3350	4250	--
114	60	3200	4250	--
131	60	3200	4200	--
113	80	3150	4200	--
134	80	3200	4250	--
116	120	3100	4250	--
132	160	3050	4200	3800
127	200	2950	4200	--
12U	250	2900	4150	3300
115	250	2900	4150	--
12L	300	2850	4000	--

TABLE C-3
INSTRUMENTED CHARPY IMPACT
TEST, ST. LUCIE UNIT 1 IRRADIATED
WELD METAL

Specimen Identification	Test Temperature (^{o}F)	Yield Load, PGY (lb)	Maximum Load, PM (lb)	Fast Fracture Load, PF (lb)
34C	-40	3750	4250	--
36E	0	3400	3950	--
35B	20	3450	4300	--
33E	40	3300	4100	--
347	40	3400	4250	--
371	60	3300	4150	--
36P	60	3300	4100	3900
35P	80	3150	4050	3250
341	120	3050	4000	3250
31A	160	3050	4100	--
323	200	2850	3900	--
33Y	200	2900	3900	--

TABLE C-4
INSTRUMENTED CHARPY IMPACT
TEST, ST. LUCIE UNIT 1 IRRADIATED
HEAT-AFFECTED-ZONE

Specimen Identification	Test Temperature (^{o}F)	Yield Load, PGY (lb)	Maximum Load, PM (lb)	Fast Fracture Load, PF (lb)
42D	-40	4000	4400	--
42E	-20	3850	4350	--
42B	-20	3800	4500	--
426	0	3800	4600	--
41Y	40	3750	4600	4400
42P	40	3700	4650	4000
42A	80	3500	4400	4100
425	100	3300	4400	3900
427	120	3500	4500	3500
42C	160	3200	4400	3900
41U	210	3050	4200	--
42T	210	3000	4250	--

TABLE C-5

TOUGHNESS PROPERTY CHANGES BASED ON

INSTRUMENTED CHARPY IMPACT TEST

Material	T_B (°F)	ΔT_B (°F)	T_N (°F)	ΔT_N (°F)	ΔCv_{30} (°F)	ΔCv_{50}	T_D (°F)	Min. Temperature for 100% Shear Fracture (°F)
Base Metal (WR)								
unirrad	-52	--	32	--	--	--	114	110
irrad	5	57	140	108	70	110	221	250
Base Metal (RW)								
unirrad	-52	--	51	--	--	--	150	160
irrad	-4	48	130	79	68	83	280	260
Weld Metal								
unirrad	-96	--	-30	--	--	--	36	80
irrad	-59	43	40	70	74	80	135	160
Heat-Affected-Zone								
unirrad	-130	--	-8	--	--	--	62	120
irrad	-60	70	6	14	28	4	130	210

Figure C-1 INSTRUMENTED CHARPY LOAD - TEMPERATURE DIAGRAM, BASE METAL (TRANSVERSE)

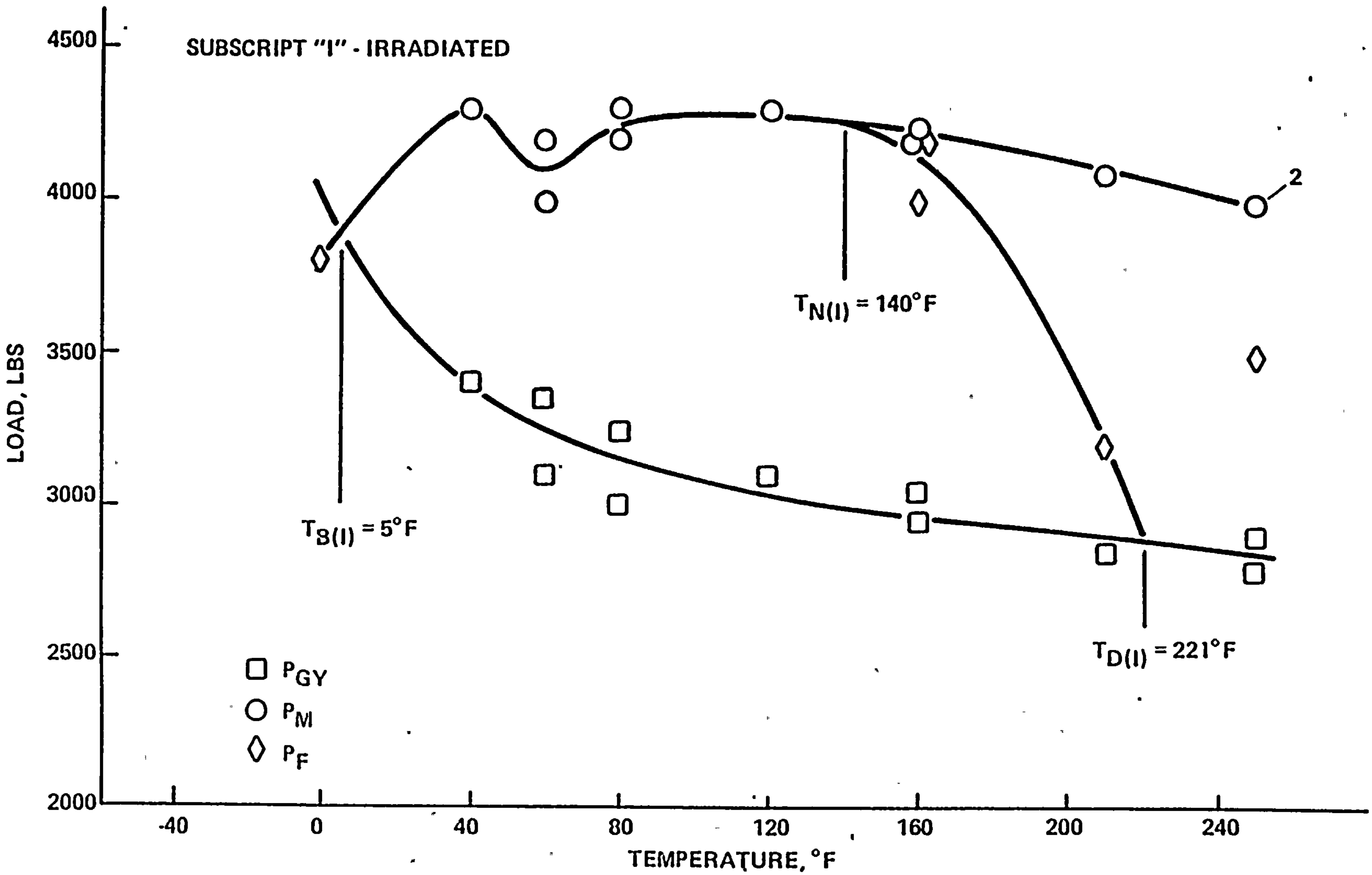

Figure C-2 INSTRUMENTED CHARPY LOAD - TEMPERATURE DIAGRAM, BASE METAL (LONGITUDINAL)

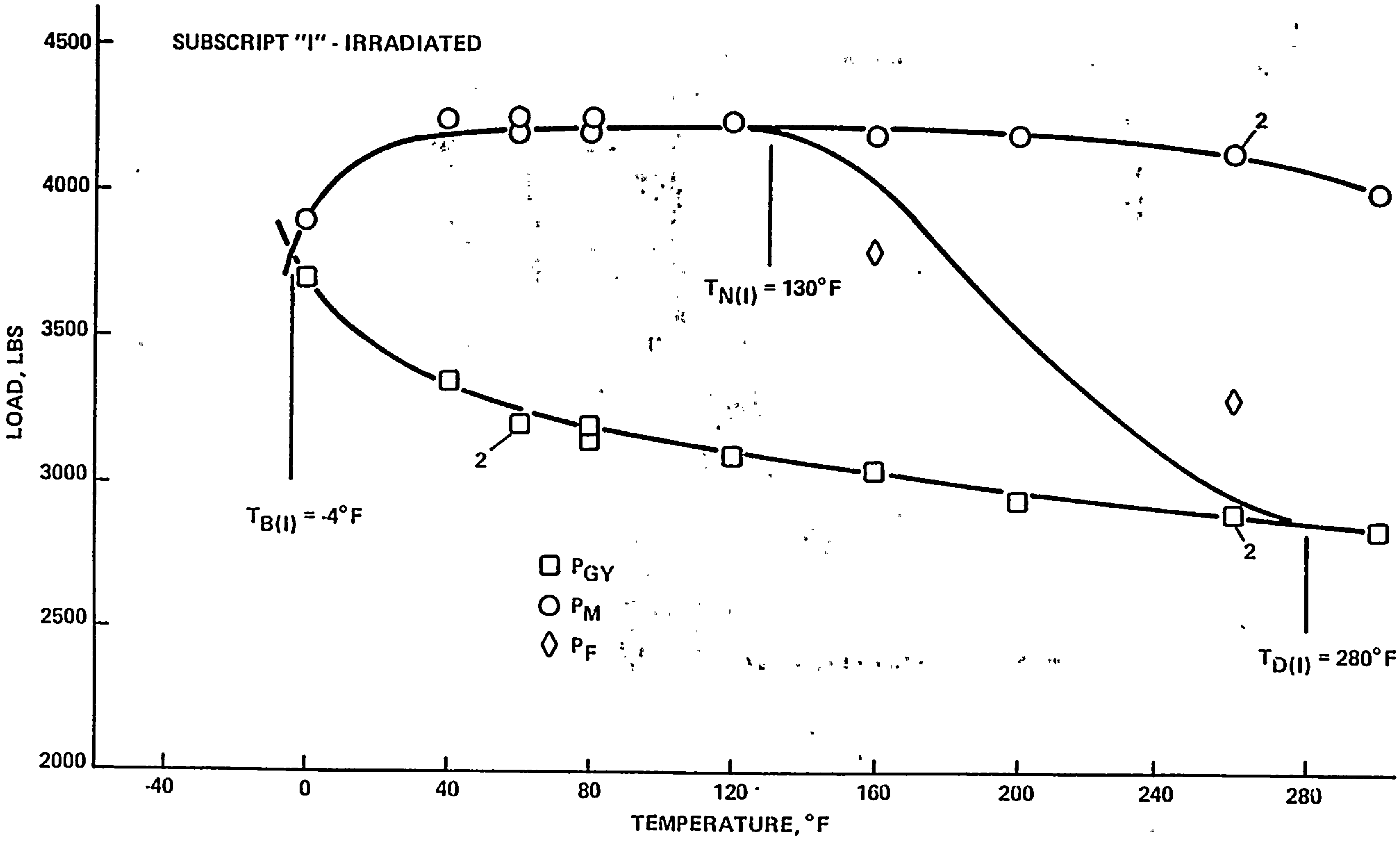

Figure C-3 INSTRUMENTED CHARPY LOAD - TEMPERATURE DIAGRAM, WELD METAL

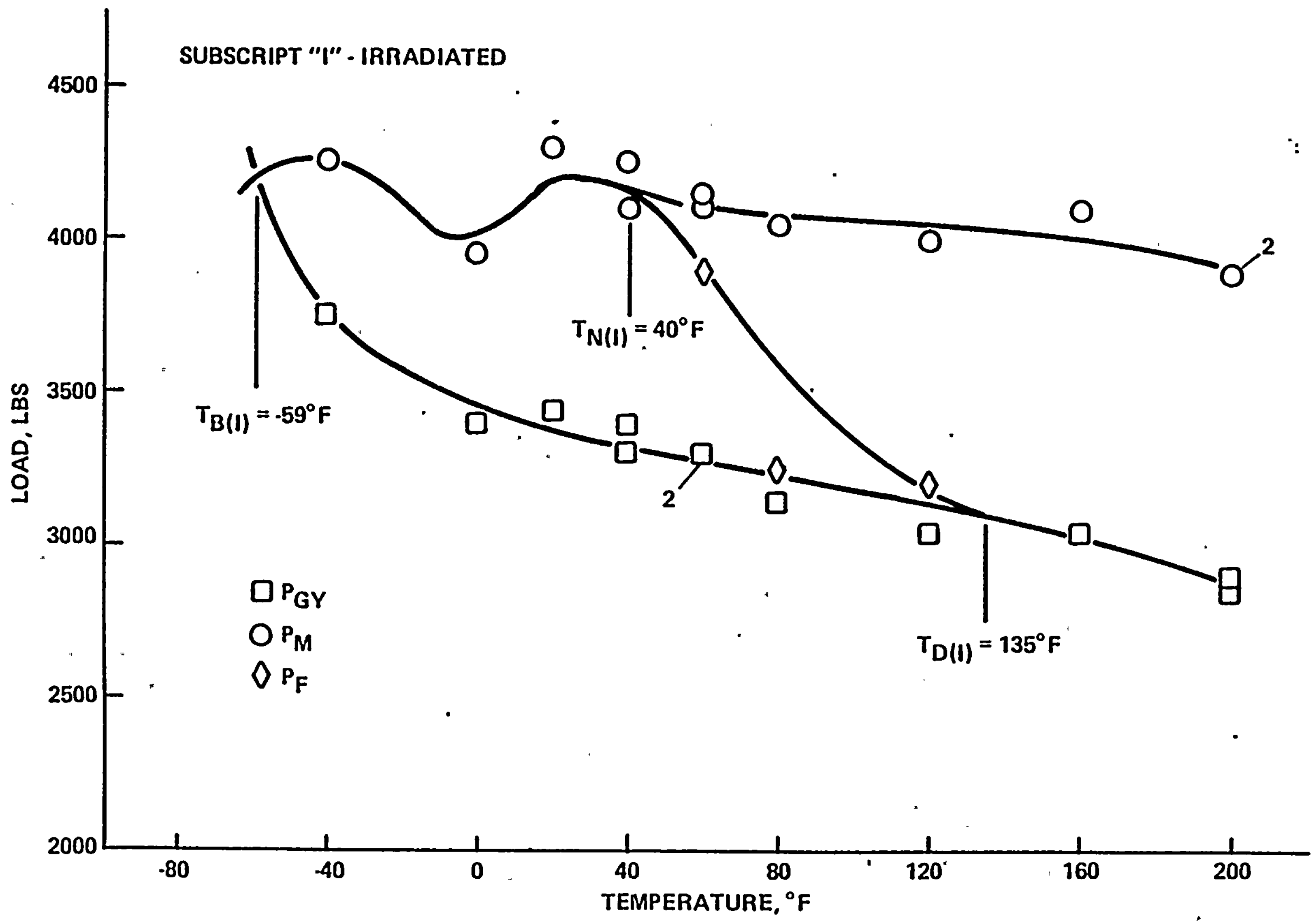

Figure C-4 INSTRUMENTED CHARPY LOAD - TEMPERATURE DIAGRAM, HEAT-AFFECTED ZONE